University of Stavanger

FACULTY OF SCIENCE AND TECHNOLOGY

MASTER'S THESIS

Study program: Computational Engineering	Spring semester, 2022 Open
Autor: Emre Baris Gocmen	
Program Coordinator: Emre Baris Gocmen Supervisor(s): Dan Sui	
Title of master's thesis: Trajectory Control via Reinforcement Learning with RSS Model	
Credits (ECTS): 30	
Keywords: - Rotary Steerable System - Optimization - Trajectory Control - Simulation - Reinforcement Learning - Artificial Intelligence	Number of pages: 56 + supplemental material/other: 34 Stavanger, 01.08.2022 date/year

Title page for master's thesis

Faculty of Science and Technology

Abstract

Various researchers proposed several types of methods, algorithms, and simulator to control bottom hole assembly (BHA) while drilling a deviated well. These works consist of drilling, control, mechanical and electrical engineering knowledge. The last year at University of Stavanger, Jerez established a work for this purpose. The aim of this work developing a physical method to control bit directions through the well path inside RSS simulator environment.

This study structured upon RSS simulator developed at University of Stavanger and propose a different perspective on trajectory control. After a serious struggle on RSS model to shape for reinforcement learning, managed to have a new environment for the trajectory control. This new environment cleaned all possible errors of RSS model. On the other hand, make possible to control path by weight on bit and rotational speed. Also, the observation parameters selected as coordinates, measured depth, and drilling time. Adding tool face angle and dog leg severity values to observation caused bad training for the agents.

Afterward, according to discrete observations and actions there was two RL agent options given by MATLAB reinforcement learning toolbox. The first one is proximity policy optimization agent, and the other one is deep q-network agent. After countless training sessions on J shape well, managed to create significant reward functions to test the environment on different well shapes.

First try made on J shape well with both RL agents offered by MATLAB and results were satisfactory. However, simulations attempt for S and complex shape wells were not precise and needs more development. Therefore, utilization of RL environment, reward function and optimization of time demand became crucial outputs of these attempts.

Acknowledgements

I would like to present my endless thanks to my advisor, Professor Dan Sui for her encouragement, guidance, advice, and support during my thesis. It was a great honour for us to work with her.

Also, I would like to thank for the support of PhD. Jie Cao, my friend Muhammad Usama, and my company eDrilling AS.

My special thanks are addressed to all other instructors of Computational Engineering department of University of Stavanger for their education and motivation.

In addition, I would like to say my gratitude to our beloved families for their guidance and support through my educational life.

Table Of Contents

List of Figures

List of Abbreviations

BHA	Bottom Hole Assembly
DL	Dogleg
DLS	Dogleg Severity
DQN	Deep Q-Network
HD	Horizontal Displacement
KOP	Kick-Off Point
MD	Measured Depth
PPO	Proximity Policy Optimization
PWP	Planned Well Path
RL	Reinforcement Learning
ROP	Rate of Penetration
RPM	Rotation per Minute
RSS	Rotary Steerable System
TVD	True Vertical Depth

1. Introduction

Drilling of an oil and gas well dramatically change over decades. Simple mining techniques replaced by state-of-the-art tools and techniques. Couple decades ago, main shape of wells was vertical, but recently almost all drilled wells are directional and complex. These advancements made available extended reach drilling, multiple target wells etc.

To be successful with this challenging operations industry developed complex tools such as Rotary Steerable System. However, complex drilling operations are very expensive and needs error-free calculations. In order to support this aim simulator became main helper for the engineers in the back office.

These simulators are mostly dependent on physical models and developed with complex mathematical equation and experiments. Year by year, simulator became more efficient and correct with the power of computation and investments. Simulators became a crucial element for the drilling industry to run the operations.

On the other hand, artificial intelligence and machine learning phenomenon changed everything in drilling simulation sector like any other sectors around the world. Engineers and scientist started to show interest to integrate AI and ML solutions for drilling industry. More and more research and application implemented on drilling industry to improve efficiency, cost, and time.

More importantly, the synthesis of modern tools like RSS and simulators increase the performance tremendously. However, this solution had some weakness about to estimate real conditions and uncertain cases. In order to fill this gap AI supported simulators can assist the tools and operations to boost efficiency, cost, and time. Even with this solution could make possible perfect simulations of real operations and could prevent major incidents and losses.

1.1. Background

Before drill a well, control of established trajectory is one of major issue of the todays drilling operations. Because of subsurface uncertainties, tool problems with other human and non-human factors make this control very problematic.

This study only considers configurations with RSS system which is the most modern and developed technology in directional drilling industry. However, the ability of this advance tool is limited until some points. The reason of this limitation is mainly because of formation and drilling parameters.

There is different application made my industry professionals to eliminate this handicap by optimizing RSS tool controls or manipulating drilling parameters for optimum path. However, there is very few applications have been done enhance this process by AI.

This study sees this empty spot, tries to optimize parameters by using Reinforcement Learning which is structured upon simulators developed at University of Stavanger 2021.

1.2. Literature Review

This thesis inspired and based upon the work named as Rotary Steerable Model. This model developed by Saramago (2020) and further developed by Jerez (2021) at University of Stavanger. This model consists

multiple complex parts. First of the method is establishment of planned well path by using Cubic Bezier Curves which inspired by the work of Sampaio (2016). This method makes available further construction of RSS model and RL environment.

On the other side, drilling simulation with RSS model structured upon various studies. However, skeleton of this module is ROP calculations for three dimensional directions. Over the years, numerous models have been developed to predict ROP from laboratory experiments. Examples include Bingham, Bourgoyne & Young, Hareland & Rampersad, and Motahhari, Hareland & James. In spite of this, advances in computational power and machine learning have allowed the development of data-driven ROP prediction models, such as Hegde & Gray (Hegde et al., 2018).

The sweet point of this study, reinforcement learning, which inspired by the work of Yu et al. (2021). This work is mainly in simulation environment is used to train an automated directional drilling agent using reinforcement learning. Their work was mainly training an agent inside the simulated environment which decides sliding and rotating of the bottom hole assembly.

At last, to establish the reward function, tool face angle calculations played important role. These calculations inspired by the work Liu (2014). The work offers very simple analytical calculation of tool face angle for spatial arc trajectories.

Especially, this project offers training of agents under RSS simulator environment and create a bright pathway for future research.

1.3. Objectives

The main motivation of this study is optimizing path created by RSS simulator by manipulating WOB and RPM. However, there is another couple objectives can be listed below:

- Is there any possibility to exhibit an excellent well path control from surface location to target hydrocarbon reservoir?
- What is the best way to implement reinforcement learning for trajectory control?
- How could increase the performance of RSS module further in terms of drilling speed?
- What is the confidence level for the reward function to train agents?
- Is it possible to perform a fully autonomous solution for this case?

1.4. Structure of Work

This study is constructed upon RSS simulator developed at University of Stavanger in 2021 and enhanced with Reinforcement Learning environment to utilize performance. The structure of this work briefly given below:

- Basics of drilling and directional drilling.
- Creation of Planned Well Path for simulation environments.
- Cleaning and discretization of RSS module.
- Establishment of Reinforcement Learning environment.
- Integration between RSS simulator and Reinforcement Learning environment.
- Determination of parameters for RL environment.
- Determination of reward function for RL agents.

2. Methodologies

This study consists multiple legs like octopus hold the body of this work. These parts are:

- Planned Well Path
- Rotary Steerable System Simulator
- Reinforcement Learning

Detailed explanation of the methods given in next sections. Before these methodologies, better to start understanding with basic drilling knowledge.

2.1. Basic Drilling Information and Systems

To begin with, it is best to understand and clarify the basics of drilling before diving into simulators and algorithms.

2.1.1. Directional Drilling

Directional drilling is primarily used to reach targets that are not accessible by vertical wells due to a variety of reasons (Farah, 2013). In other words, a well is considered a directional well if there is a specific deviation from the vertical line that has different rotation and inclination.

A directional drill can be used in a variety of situations, from optimizing future production to solving some blowouts. According to Adams and Charrier, directional drilling can be applied to the following purposes (Adams & Charrier, 1985):

- **Inaccessible locations:** In some cases, it is impossible to access the ideal rig site due to residential zones, riverbeds, mountains, or roads.

- **Multiple wells drilling from a single site:** Several directional wells can be drilled from a single well site at a lower cost.

- **Sidetracking:** This technique is used in the event of an obstruction in the well path, such as packoff, a trapped tool, or a collapse of the well.

- **Relief well drilling:** Creating a water and mud cross-section at the bottom of a near blowout well to alleviate the pressure associated with the blowout.

- **Multiple targets:** Drilling through one target then turning the direction to reach the next is necessary.

Furthermore, it is important to understand some technical terms in directional drilling engineering before discussing more detailed information. According to Farah, the following terms are commonly used in drilling engineering (Farah, 2013):

• **Azimuth:** Angle between the true North and the plane containing the vertical line from the wellhead and the vertical line through the target (Figure 2.1).

• **Build-up rate:** Angle from the kick-off point where the angle is steadily built up. Usually is measured in °/30 m.

• **Drop-off point:** The point since the inclination of the well begins to tend to vertical.

• **Horizontal Displacement (HD):** The horizontal distance between the vertical lines that pass through the wellhead and the target.

• **Inclination:** Angle between the tangential section of the hole with the vertical axis (Figure 2.1).

• **Kick-off point (KOP):** The depth at which the well deviates from the vertical.

• **Measured depth (MD):** The length of the well along the well path.

• **Tangential or hold section:** Section of a well where the inclination is maintained and the TVD and HD increase.

• **True vertical depth (TVD):** Vertical distance between the rotary table and the survey point. It is essential to mention that the TVD is considered positive when it increases the depth.

• **Well path:** The trajectory left by a directional well drilling in three dimensions.

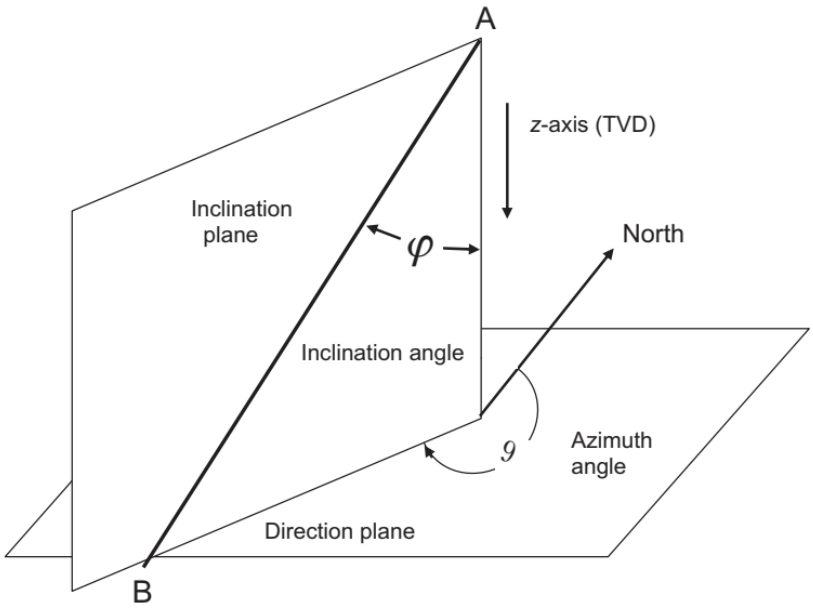

Figure 2.1: Inclination and Azimuth Angles (Mitchell et al., 2011)

2.1.1.1. Types of Well Trajectories

Depending on the steering system and DLS constraints, a directional well may follow a different trajectory. The purpose of a directional well and the formation problems that it may encounter in the formations it passes through will determine the type of trajectory it should follow. As described by Bourgoyne et al. (1991), the following types of well trajectory are the most common:

- **Build-and-hold (J type):** The wellbore penetrates the target at the same inclination angle as the hold section (Line A in **Error! Reference source not found.**2).

- **Build-hold-and-drop (S type):** The wellbore increases the inclination, then holds that inclination in the tangential section, and finally, it drops the inclination to enter the reservoir with a vertical section (Line C in Figure 2.2).

- **Build-hold-partial drop-hold (S special type):** Has the same principle as the S shape trajectory, but it penetrates the reservoir at some inclination angle less than the maximum inclination angle for the hold section (Line B in Figure 2.2).

- **Continuous build:** The inclination keeps incrementing right up or through the target (Line D in Figure 2.2).

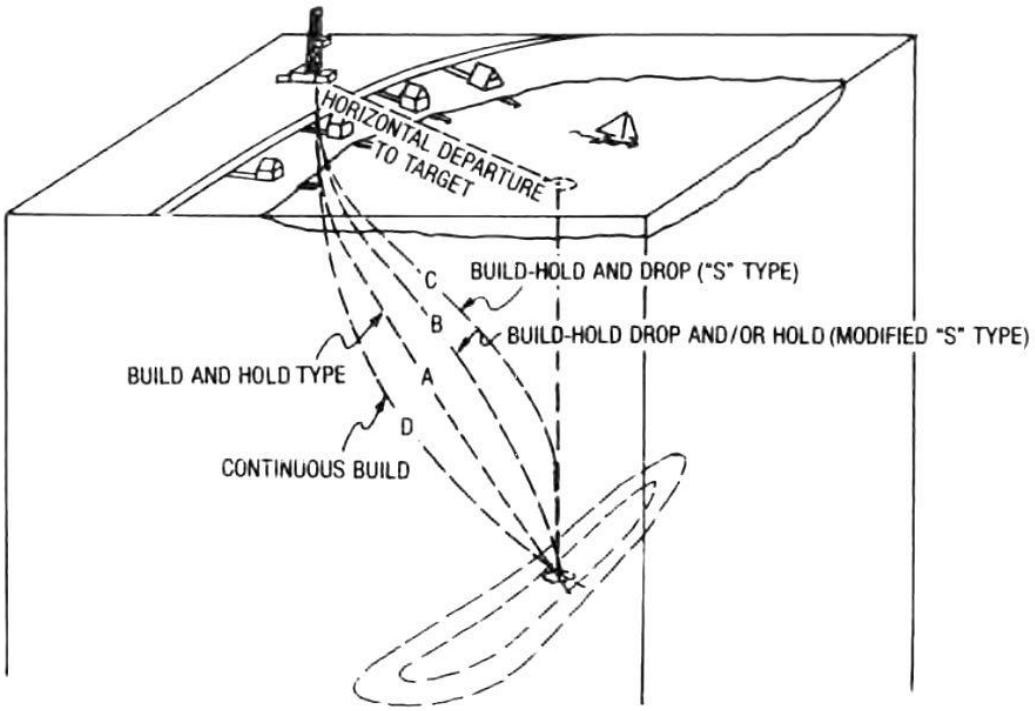

Figure 2.2: Different Directional Well Trajectories (Bourgoyne et al., 1991)

2.1.1.2. Survey Points Calculation

Survey points are locations at which certain measurements are recorded and sent to the surface to provide information regarding the inclination, azimuth, and depth of the bit. A survey point calculation model can only approximate the points between two survey points when the points between the two survey points are unknown (Mittal & Samuel, 2016).

There is plenty of survey calculation for directional wells. However, this study only focuses on the tangential method.

The tangential method involves connecting two survey points by a straight line, which represents the wellbore. There are some limitations to the method, and it can only be used when a limited amount of data is available (Farah, 2013). The equation of this method is seen in Figure 2.3.

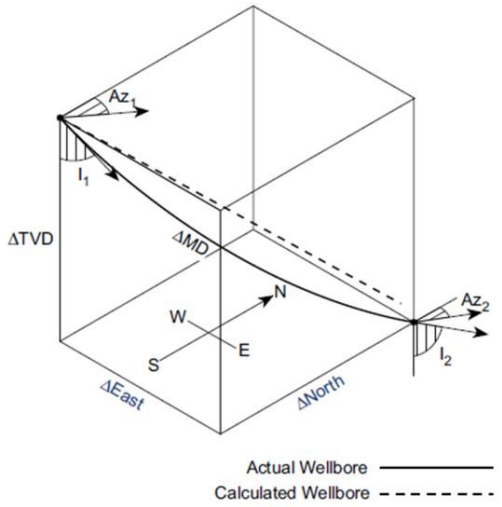

Figure 2.3: Tangential Method (Farah, 2013)

The equations for calculating the differences of the coordinates between both survey points are (Farah, 2013):

$$\Delta V = \Delta MD \cdot \cos \alpha_1 \tag{2.1}$$

$$\Delta N = \Delta MD \cdot \sin \alpha_1 \cdot \cos \varphi_1 \tag{2.2}$$

$$\Delta E = \Delta MD \cdot \sin \alpha_1 \cdot \sin \varphi_1 \tag{2.3}$$

Where:

- $\Delta V =$ vertical coordinate difference $[m]$
- $\Delta N =$ north coordinate difference $[m]$
- $\Delta E =$ east coordinate difference $[m]$

2.1.1.3. Dog Leg and Dog Leg Severity

In order to steer a wellbore, there is a build-up rate that needs to be carefully controlled to avoid creating a sharp dogleg (DL). As a result of the DL, the well trajectory rapidly changes, causing the tool to become stuck or the casings to become difficult to run down. This study will be based on the equation presented below (Liu & Samuel, 2016):

$$DL = \cos^{-1}(\cos \alpha_{i-1} \cdot \cos \alpha_i + \sin \alpha_{i-1} \cdot \sin \alpha_i \cdot \cos(\varphi_i - \varphi_{i-1})) \tag{2.4}$$

Where:

- $DL =$ dogleg calculated [°]

- $i =$ current survey station
- $i - 1 =$ last survey station (before the actual)
- $\alpha =$ inclination [°]
- $\varphi =$ azimuth [°]

The dogleg severity (DLS) is the wellbore curvature, and it is expressed in °/30 m or °/100 ft (Mitchell et al., 2011).

In addition, the information provided by the DLS can be utilized in order to estimate the following: stress fatigue in the drill pipe, casing wear, casing design loads, and stuck pipe situations. The consequences of a high DLS are as follows (Nkengele, 2019):

- The casing string could have some fitting issues in the curve section.
- Repeated abrasion of the drill string in the high DLS location.
- The casing cement may wear due to the higher contact forces.
- Increasing the likelihood of getting stuck or not reaching the target depth.

The DLS is calculated just dividing the Eq.(2.42.5) by the length between the survey points:

$$DLS = \frac{DL}{\Delta MD} \cdot 30 \tag{2.5}$$

Where:

- $DLS =$ dogleg severity calculated $\left[{}^{\circ}/_{30\ m}\right]$
- $\Delta MD =$ distance between 2 survey stations, where the DL has been calculated $[m]$

2.1.1.4. Tool Face Angle

Orientation and deflection capabilities of steerable drilling tools are generally determined by tool face angle and build-up rate, where the tool face angle represents working attitude, and the build-up rate represents deflection capability. As of now, tool face angle formulas only apply to borehole trajectory models based on spatial arcs. It is important to note that these rules do not apply to other models, such as the cylindrical helix model and the natural curve model. The spatial arc model is generally considered ideal for slide steering drilling, but not for rotary steering drilling, in the oil industry. Due to this, it is necessary to find methods of calculating tool face angle that are suitable for rotary steering as well as composite steering drilling in order to meet trajectory control requirements. Furthermore, the existing technologies focus on controlling the inclination and azimuth of the borehole trajectory. It is, however, difficult to monitor the consistency between actual and planned performance of steerable drilling tools due to the absence of technical methods for controlling orientation and deflection (Liu, 2017).

The tool face angle ω, which is the angle included between the tool face of steerable drilling tools and the borehole trajectory inclination plane, is used to characterize the working attitude of steerable drilling tools (Figure 2.4).

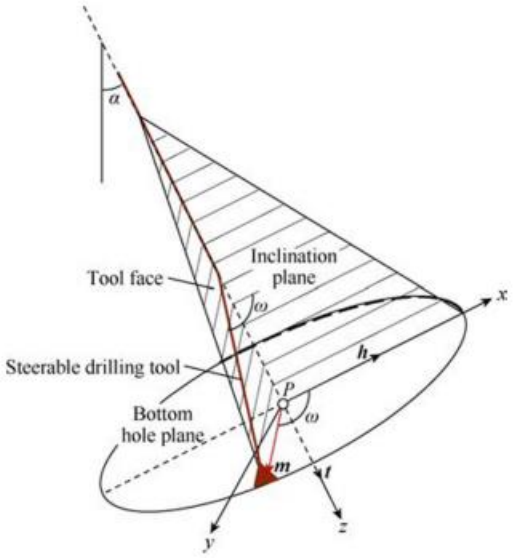

Figure 2.4: Borehole Coordinate System, all planes and directions (Liu, 2017)

The basic parameters characterizing the orientation and deflection performance of steerable drilling tool are build-up rate and tool face angle. Unit tangent vector, unit principal normal vector and unit binormal vector characterizing the bending and torsion of borehole trajectory can be expressed by inclination change rate, azimuth change rate, and borehole curvature, etc. (Liu, 2017)

According to the above statement equation for tool face angle is given below:

$$\omega = \tan^{-1}\left[\frac{\sin\theta_2 \sin(\emptyset_2 - \emptyset_1)}{\sin\theta_2 \cos\theta_1 \cos(\emptyset_2 - \emptyset_1) - \sin\theta_1 \cos\theta_2}\right] \quad (2.6)$$

Where:

- $\theta_1 =$ Inclination 1 [degree]
- $\theta_2 =$ Inclination 2 [degree]
- $\emptyset_1 =$ Azimuth 1 [degree]
- $\emptyset_1 =$ Azimuth 2 [degree]

2.1.2. Directional Drilling Steering Systems

BHA is responsible for steering the drill string. This curvature has been created using a controlled technique over time, as new technologies have become available each year.

First directional or divergent wells were made using whipstocks or jetting techniques. Typical whipstocks are wedge-shaped steel castings with a concave channel on one side that guides the bit against the wall to deflect the string. For the jetting technique in soft formations, a three-roller-cone bit with three nozzles is typically used. It should be noted, however, that one of the nozzles is larger than the others. The deviation begins washing or eroding the rock due to the fluid pressure at the bottom of the hole, and erosion is the result of the fluid momentum at the bottom of the hole (Mitchell et al., 2011). Nowadays, steerable mud motors and rotary steerable systems are the most widely used techniques.

2.1.2.1. Steerable Mud Motors

In 1985, steerable mud motors were introduced to the drilling industry, enabling the industry to drill more complex and longer wells. Most directional wells are now drilled using this technology (Kuznetcov, 2016).

By applying hydraulic pressure to the drill bit and bending the sub, the mud motors create a side force that changes the direction of drilling (Wiktorski et al., 2017).

In order to create a deviation in the bottom of the well, the bend sub is configured in the surface at the required angle. While it is not necessary to create an angle at this point, the drill string rotates as a whole.

After the bit is positioned in accordance with the bend sub and rotation stops, the angle is constructed by sliding the bit. By pumping fluid through a rotor and stator inside the tool, hydraulic power is generated to make the bit rotate. Kuznetcov (2016) explains that the drill string does not rotate except for the bit, which begins to create the build-up section.

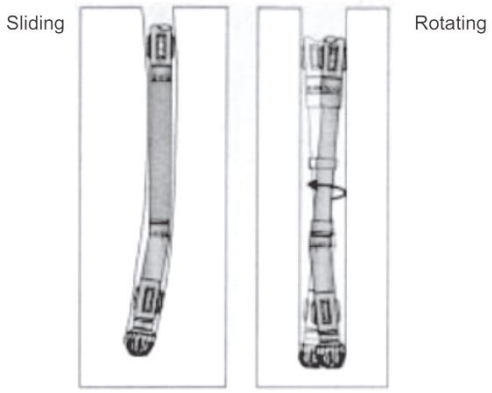

Figure 2.5: Steerable Mud Motor Modes (Mitchell et al., 2011)

2.1.2.2. Rotary Steerable Systems

There has been a significant evolution in the rotary steerable system (RSS) over the past few years, but the basic principle remains the same: generate a side force in one of the wellbore walls in order to direct the bit in the opposite direction of the push-the-bit force (Jerez, 2021).

According to Wang et al. (2017), a mechanical RSS is equipped with three steering pads that extend to the borehole wall and generate an opposite force that pushes the drill string to the other side, resulting in reaction forces in the stabilizer and bit.

There are two main components of RSS guide systems: the control platform and biasing mechanism. A control platform controls the direction of the bias mechanism, which is considered the "brain" of the system. Lastly, there is an "actuator" that executes the extension of the pads in accordance with the correspondent side in order to apply force (Li et al., 2020).

It should also be noted that pads are activated only when they are approaching the face wall of the borehole; once they have passed this point, the pads are inactivated and return to a closed position.

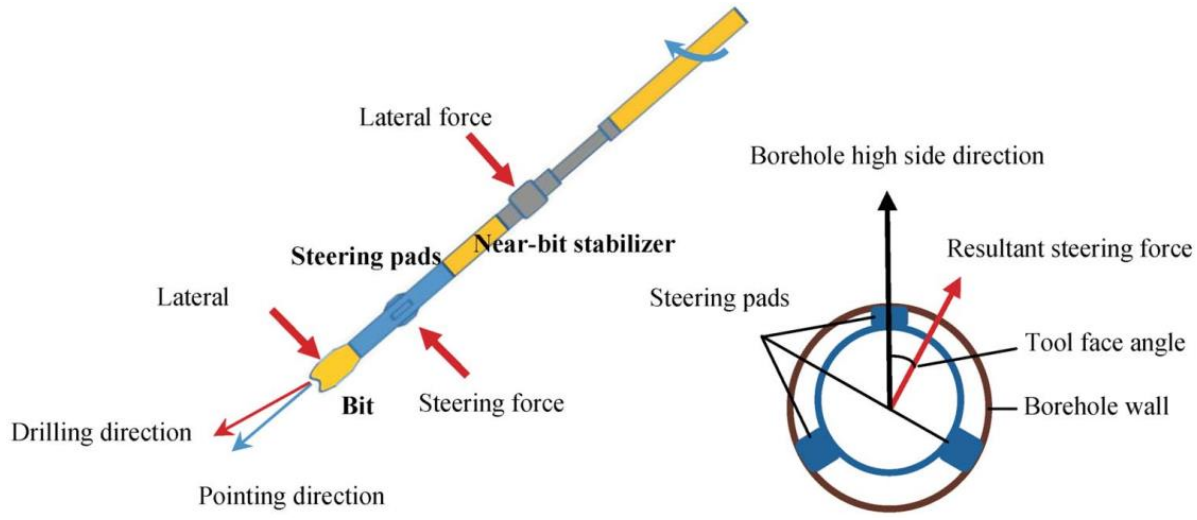

Figure 2.6: Rotary Steerable System (RSS) Tool (Wang et al., 2017)

Depending on the rotary steering device, it can be accomplished through gravity-based orientation or by flexing internal driveshafts or applying forces from pads against the borehole walls (Ruszka, 2003).

2.2. RSS Simulator Environment

The Rotary Steerable System Simulator (RSS Simulator) is developed by Saramago and enhanced by Jerez at the University of Stavanger which is core environment for this study.

RSS simulator is a unique environment to mimic or simulate real directional drilling cases. This simulator models the drill string movement with respect to the triaxial ROP calculations with resultant forces. The RSS function is structured based upon the OrientXpress RSS developed by Canrig Norway as the actuator of the BHA that creates the angle deviations.

The RSS simulator environment consists of various elements. However, couple of them are the core of this environment which are:

- Generation of Planned Well Path
- Automatically regulate the BHA tool offset based on the inclination, azimuth, and measured depth.
- Suitable for integrating with other models used in Drillbotics Student Competition.

This environment has ability to simulate all 2D or 3D well trajectories based on given survey data from the user end. For result, simulator can provide Planned Well Path (PWP) and drilling simulation results.

2.2.1. Main modules of simulator environment

As indicated in the previous section this simulator environment has two different modules:

- Planned Well Path (PWP) function
- Rotary Steerable System (RSS) simulator

All modules working in Python coding environments under sufficient requirements. According to the input from user end, results with simulated results for virtual drilling environments.

The connection between modules is shown in Figure 2.7. The figure represents the base case structure for this study. In later phases, these modules will connect with Reinforcement Learning environment.

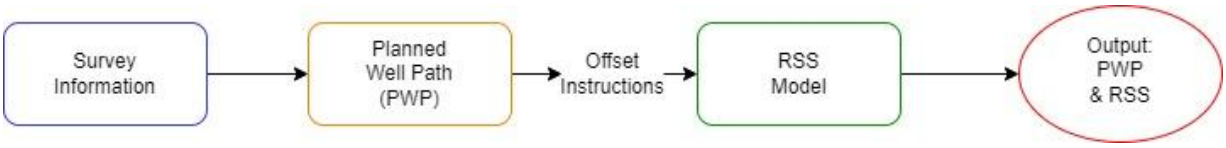

Figure 2.7: Modules Involved in the RSS Simulator Environment

The process starts with the survey information input set by user in the beginning of process. It is important to note that some constraints will be used as conditions to achieve specific drilling objectives among the parameters set by the user.

The PWP function analyzes the survey points given by user in terms North, East and Vertical. According to some constraints defined by user, creates best hold and curvature sections of trajectory. The final well path built by main function is planned well path points. These points will be main structure or trajectory for consecutive processes.

When the planned well path defined, offset instructions sent to RSS module in terms of inclination and azimuth. Offset function inside the RSS module, calculates the offset values according to inclinations and azimuth values between two survey points in PWP array. This value activates the actuator on RSS tool which will affect the progression of bit through simulation.

Ultimately, the RSS model calculates the next bit position according to the inputs, current bit position, offset instructions, force on the bit calculate, and results from the 3D ROP equations.

Every step till the target point, RSS model takes next points from PWP and if it is necessary executes the process according to measured depth.

2.2.1.1. Simulator Flowchart

The modules used in modules mentioned above are processed as code in Python environment using the flow process given in Figure 2.8. This flowchart is representation of Python code, which consists of more details.

The flowchart starts with data input which consists of survey point, parameters for PWP and RSS and some other actions. Also, this data updated for every given survey point.

In order to create a planned well path, the PWP module analyzes the input data and creates points based on the input data. There is a primary condition that must be met in order to stop the entire simulation. As the path is composed of a series of survey stations, they are structured in the form of a matrix whose number of rows determines how many times the program is iterated.

When the simulator iterates through all points in the matrix, simulator executes model and exports outputs.

There is important thing RSS module, which is input from reference path. This input consists of inclination, azimuth, and measure depth of reference path. These three parameters trigger offset controller in RSS controller. RSS simulators consider these parameters as target information.

Inside the RSS module, there are two main conditions, one after the other, where the algorithm decides if the next point will still simulate the next bit position using the current target inclination and azimuth or if a new target inclination and azimuth, coming from the PWP (Jerez, 2021).

The "next survey" phrase that appears in many conditionals refers to the next MD that will simulate a survey point analysis. This variable is determined with an initial MD equal to 0 that will be updated with the delta MD chosen by the user (Jerez, 2021).

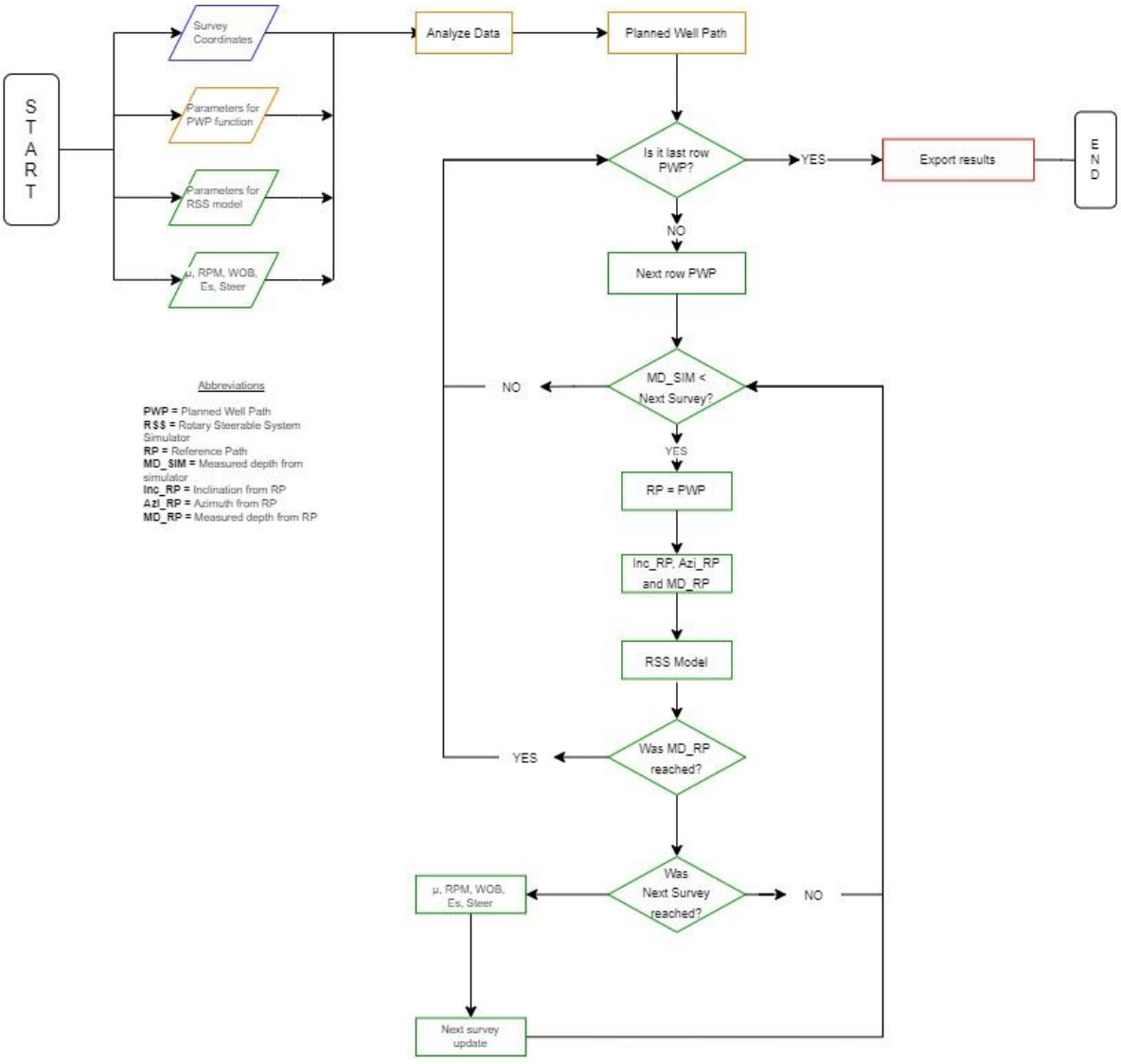

Figure 2.8: RSS simulator environment flowchart (modified Jerez, 2021)

2.2.2. Trajectory Design and Optimization with PWP module

First step of creating environment is establishing smooth path by using given survey points. This trajectory called as Planned Well Path (PWP) in this work. PWP will be main skeleton of this research, and all modules will be constructed over this trajectory. Specifically, PWP limits the number of iterations, target information's of each survey point, etc.

Process through PWP module starts with analyzing points to determine whether in hold section or curve section. If points are inside curve section established a curve in 3D space. Ultimately, module merge all section in shortest and smoothest way.

Output trajectory is overline of given survey points and exported in matrix format. The parameters of matrix are given in Table 2.5. Each row of the matrix is the survey point of newly created PWP.

Detailed explanation of this module will be shown in next sections to understand the calculations and natures.

2.2.2.1. Cubic Beziér Curves

To construct the curve sections inside the PWP, main source of calculations and modelling is Cubic Beziér Curves. The Cubic Beziér Curves are one of the Beziér Curves' variants, which starts from the linear form until unlimited order. Moreover, the Bezier curves have been implemented in many industries, but also some authors have also adapted this methodology to the drilling industry (Jerez, 2021).

The construction of this part totally obtained from work of Sampaio which is "Designing 3D Directional Well Trajectories Using Beziér Curves" (Sampaio, 2016). An adaptation of the typical Bezier implementation has been made by the author in order to apply the method to the 2D and 3D directional well curves.

In computer graphics, Beziér curves are often used to model smooth curves using parametric curves. Pierre Beziér invented them in 1962 for use in the design of automobiles (Joshi & Samuel, 2017)

A first order Beziér curve consists of only the points S and E at the ends of the line, which is the simplest Beziér curve. The second order Beziér curve uses three points: S, E, and C. The last point is the control point, which is not collinear with the other two points. Beziér's third order curve uses four points, the start and end points S and E, as well as two control points C1 and C2. (Sampaio, 2016). One of the control points will be related to the start point, while the other to the end point. As a result, they will be called start control point or attractor C_S and end control point or attractor C_E.

All the Beziér curves have a dimensionless parameter u that goes from 0 to 1, and it will represent the step for the interpolation point B that goes from the start point until the end point. The trajectory that takes the point B will define the Beziér curve, as can be seen in Figure 2.9 (Jerez, 2021).

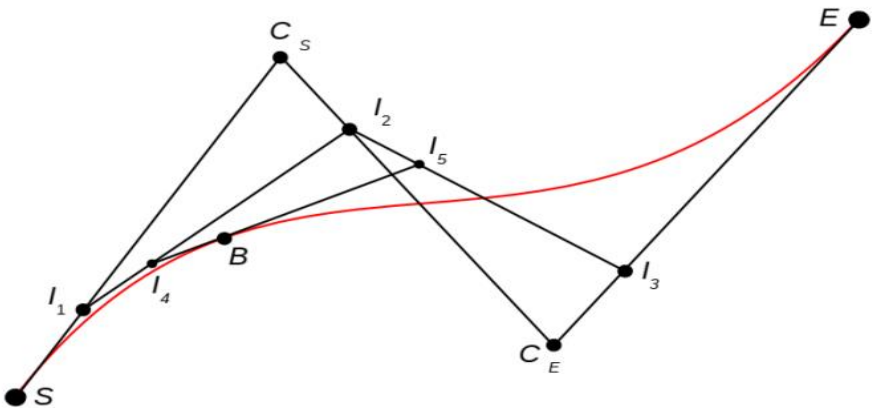

Figure 2.9: Third-order or Cubic Beziér Curve (Sampaio, 2016)

In this case, the number of nested interpolations is the same as the order of the Beziér curve. In the same way, the position of the attractor points with respect to the start or end points determines the shape of the Beziér curve. In the Sampaio method, either the C_S or C_E attractor points follow the direction of the tangential line from the start or end point. Fig. 4.2 shows both the case where the end attractor point C_E is fixed (case a) and the case where the start attractor point C_S is fixed (case b) (Jerez, 2021).

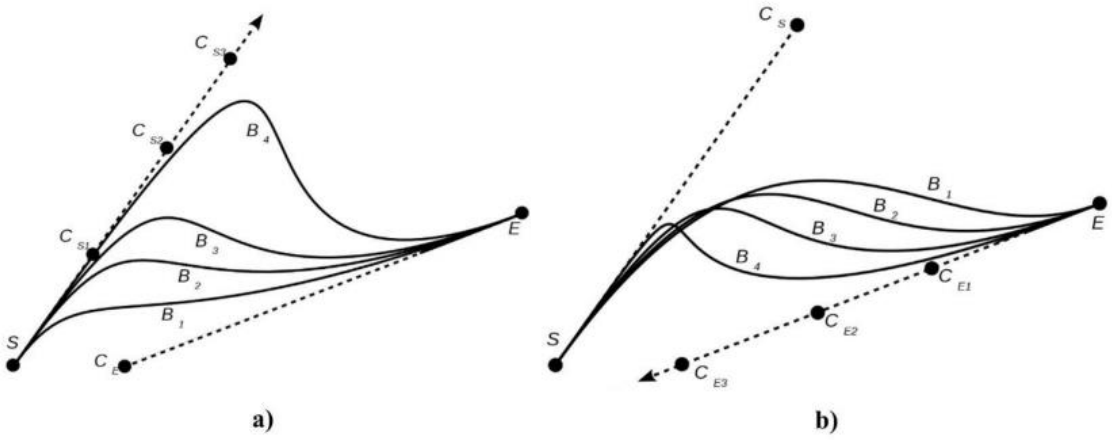

Figure 2.10: Fixed Beziér Attractor Points Alternatives (Sampaio, 2016)

The tangent lines in the last Figure 2.10 can be skew lines (with no intersections but are not parallel) which means that the resulting Beziér curve is a 3D curve that is non-planar (Sampaio, 2016).

The PWP function starts the calculation of the Beziér curve with two initial fixed values for initial distance to starting attractor and end distance to ending attractor. While attempting to create a low DLS and short path, it will search for the best combination.

2.2.2.2. Close view to Planned Well Path module

Planned Well Path function structured upon Cubic Beziér curves and tangential method which is survey calculation method for trajectory. In the environment of this work PWP module runs in the beginning of sequence and briefly illustrated in Figure 2.11.

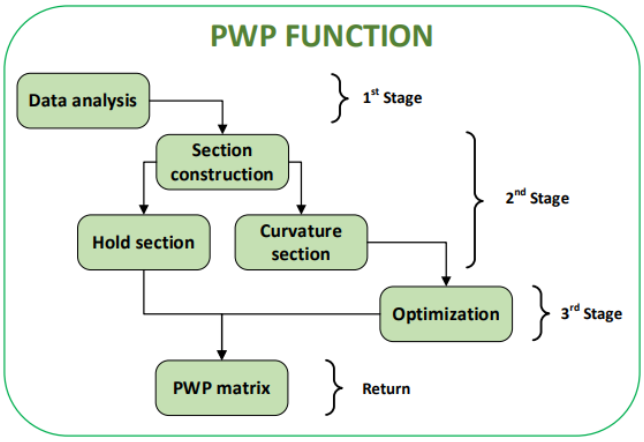

Figure 2.11: PWP Function Stages (Jerez, 2021)

2.2.2.3. Analysis of Survey Points

The purpose of this function under PWP module is to determine the curve and hold sections with respect to survey points. To proceed in module, this function is detrimental to stability of planned well path. If anything went wrong with creation of curve or hold sections, rest of module creates deceptive results for RSS simulator and ultimately for this work.

At the beginning of the run, the user sets a tolerance value and imports the data. As shown in Figure 2.12, once the survey points are saved, the PWP function will place them in their corresponding positions in 3D space.

In Figure 2.13, an imaginary straight line is drawn between each two survey stations. This imaginary line is used as the basis for calculating the inclination and azimuth using the tangential method equations, Eq. (2.1) and (2.2). In Figure 2.13, the last curve section from Figure 2.12 is zoomed in so that the inclination angles between the two survey stations can be better understood. In the figure, stations are identified by the letter P and their respective station numbers. Furthermore, the following equations are used to approximate inclination and azimuth:

$$\Delta MD_i = \sqrt{(V_i - V_{i-1})^2 + (N_i - N_{i-1})^2 + (E_i - E_{i-1})^2} \tag{2.7}$$

$$\alpha_i = \cos^{-1}\left(\frac{V_i - V_{i-1}}{\Delta MD}\right) \tag{2.8}$$

$$\varphi_i = \cos^{-1}\left(\frac{N_i - N_{i-1}}{\Delta MD \cdot \sin\alpha}\right) \tag{2.9}$$

Based on the inclination and azimuth of all intermediate lines between the points, the analysis calculates the difference between the inclinations and azimuths of adjacent lines. Differences between the tolerance value and the difference are compared, resulting in two possible outcomes:

- If the tolerance value is bigger than the difference, then the line belongs to a hold section.
- If the tolerance value is lower than the difference, then the line belongs to a curvature section.

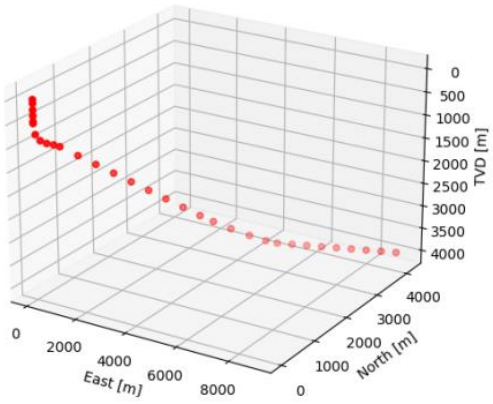

Figure 2.12: Given Data Survey Points Example (Jerez, 2021)

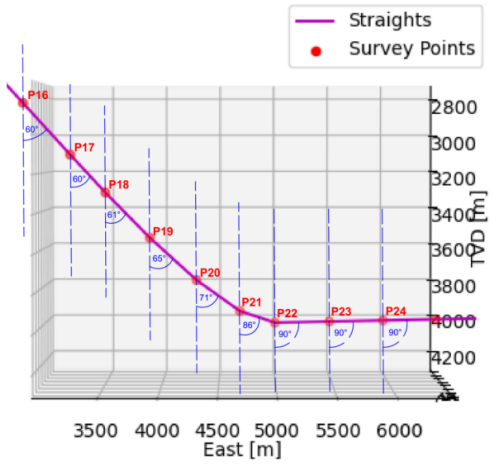

Figure 2.13: Process for Classification of the Sections of the Well (Jerez, 2021)

2.2.2.4. Construction of Hold and Curvature Sections

As shown in Figure 2.13, section construction divides two part which are hold section and curve section construction. Hold section function creates number of points between start and end survey points of hold. Besides, curvature section function establishes build-up or drop in refence of three survey points by assistance of Cubic Beziér Curves.

For the hold section, the first step is to determine where the start and end points are, and for the curvature section, the start, middle, and end points should be determined. As the PWP survey stations are set much

more easily in hold sections than in curvature sections, the following description will begin with hold sections.

2.2.3. Drilling Simulation with the RSS Model

This model used in this work structured and modified upon RSS model developed by Jerez in University Stavanger in 2021. The main aim to use RSS Model is it potential and uniqueness. However, the model has not perfected for real time situations and open for development and further discussions.

For this work, there some modifications and error analysis made but the model still open for further improvements after all. Especially, to decrease the time expensiveness of model could be shrink down more to increase performance(speed) of Reinforcement Learning simulations.

In addition, the main iteration conditional was very basic, and it was based on the maximum number of iterations instead of a drilling parameter such as MD or time. The reason for this was that the maximum number of iterations had already been reached, and it was not possible to stop once the target zone was reached. This chapter will provide an overview of the RSS Model explained by Jerez in his work. To learn more about the idea of the model, the reader should consult Jerez's thesis. Besides, the chapter will show the principal upgrades made during the adaptation of the Reinforcement Learning application with the RSS Model function.

2.2.3.1. RSS Model Structure

In order to simulate bit movement and position when drilling with the OrientXpress® RSS tool, Saramago has developed the RSS model. Based on the weight on the bit (WOB) and the bending of the RSS system, the model determines the forces acting on the bit. By using these forces, the model can decompose the traditional ROP definition into two or three ROP values that correspond to 2D and 3D modelling, respectively (Saramago, 2020).

A number of mathematical models have been developed to study the relationship between the rate of penetration (ROP), several variables that can be controlled during drilling, such as the rotary speed of the drill string (RPM), the weight of the bit (WOB), the weight of the mud, the pump pressure, and the flow rate of the pump (Esmaeili et al., 2012).

Bingham, Bourgoyne & Young, Hareland & Rampersad, and Motahhari, Hareland & James all developed deterministic models to predict the ROP based on laboratory experiments. In spite of this, increased computing power and machine learning have allowed the development of robust data-driven ROP prediction models, which are purely based on data statistics (Hegde et al., 2018).

In order for the RSS Model function (Figure 2.14) to operate, some organised steps must be executed in an organized order each time the function is called. Although the RSS Model originally had two variants, one in 2D, and another in 3D, this article will focus on the 3D variant since the RSS Simulator is a 3D application.

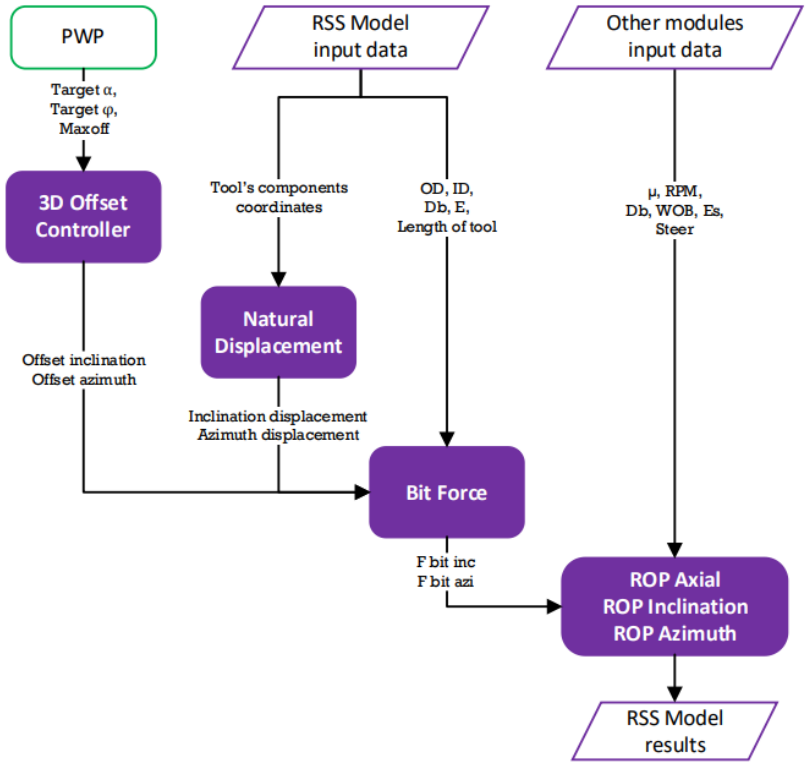

Figure 2.14: RSS Model Process (Jerez, 2021)

2.2.3.2. 3D Offset Controller

For 3D, the offset controller directs the inclination and azimuth goals to be reached or approximated in the next drilling simulation. The instructions, or target inclination and azimuth, are based on the PWP.

With the offset controller, the inclination and azimuth values of the target are transformed into offsets or actuator displacement lengths. Based on the offset length, the OrientXpress® RSS tool will move more or less intensely to one side of the borehole, as shown in Figure 2.15 (Jerez, 2021).

On the basis of Saramago's information, the maximum displacement in the tool may be as high as 6 mm, since accurate information regarding the tool's limitations will be provided by Canrig Norway (Saramago, 2020). This will result in the tool's action remaining unchanged and its behavior remaining unchanged. Offset controllers may be used in three different situations:

- Fully activate the actuator according to the maximum opening offset percentage ($maxoff$).
- Deactivate the actuator gradually
- Entirely deactivate the actuator

In order to ensure a soft entanglement, the offset controller gradually decreases the opening value when the bit inclination and azimuth are nearing their target values. In the final stage, when the hold section has been reached, with the correct inclination and azimuth, the offset controller deactivates the opening and keeps it at 0% until another section of curvature is being drilled or the trajectory needs to be corrected (Jerez, 2021).

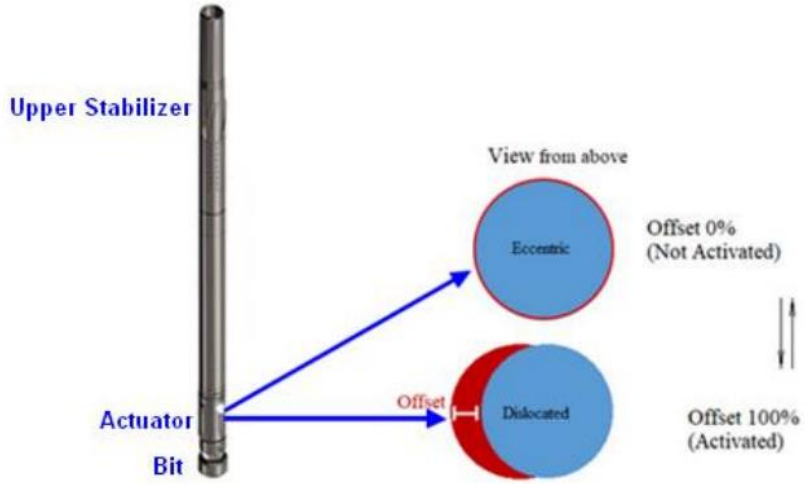

Figure 2.15: Offset Displacement Operation (Saramago, 2020) and (Nabors Industries Ltd., 2021)

2.2.3.3. Natural Displacement

A BHA tool will cause the drill string to bend in the desired direction due to the displacement or offset caused by the tool. From the profile plane of the displacement, as shown in Figure 2.16, two straight lines can be formed. There are two lines connecting the middle point of the bit to the upper stabilizer. The longest line is called the "Long line". From the middle point of the bit until the actuator of the BHA tool is connected by the "Short line" (Jerez, 2021).

A displacement occurs between the two lines every time the inclination and azimuth change, and the tool offset is activated (green vector in Figure 2.16). As a result, the natural displacement will determine the magnitude of the force acting on the wellbore walls from the BHA actuator (Jerez,2021).

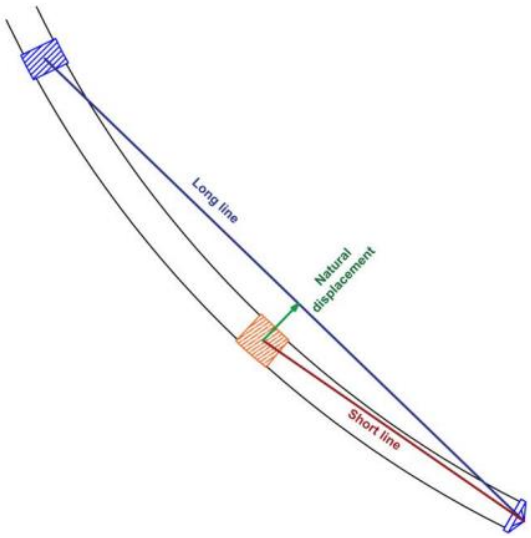

Figure 2.16: Natural Displacement Concept (Jerez, 2021)

2.2.3.4. Bit Force Estimation

In turn, trajectory path depends significantly on the forces acting on the bit. In other words, they are the physical magnitude that is applied to the borehole wall. Therefore, it is necessary to develop a reliable model for estimating them.

Using a beam bending model applied to a steel pipe, Saramago represents the forces acting on the drill string as a balance between force and momentum (Saramago, 2020). Figure 2.17 illustrates the beam bending scenario, in which the W_b and W_a represent the reaction forces to the punctual load applied to the steel pipe along its length.

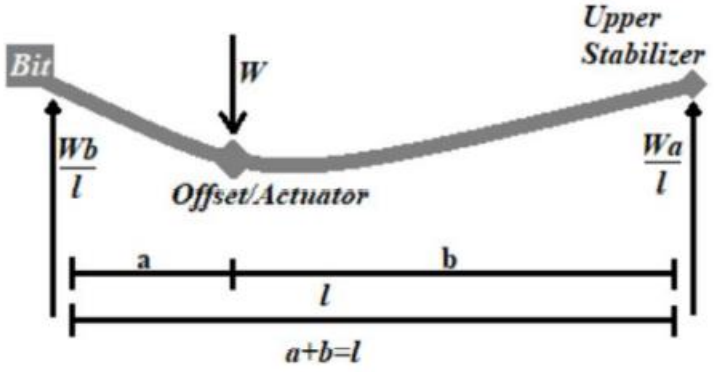

Figure 2.17: Beam Bending Scenario to Model the Drill String Forces (Saramago, 2020)

The details of the derivation of the calculation of the bit forces are in Saramago's work, but the relevant equations for the RSS Model implementation are the following (Saramago, 2020):

$$F_{ND_{azi}} = \frac{3 \cdot ND_{azi} \cdot E \cdot I}{a^2 \cdot b} \tag{2.10}$$

$$F_{ND_{inc}} = \frac{3 \cdot ND_{inc} \cdot E \cdot I}{a^2 \cdot b} \tag{2.11}$$

$$F_{Offset_{azi}} = \frac{3 \cdot Offset_{azi} \cdot E \cdot I}{a^2 \cdot b} \tag{2.12}$$

$$F_{Offset_{inc}} = \frac{3 \cdot Offset_{inc} \cdot E \cdot I}{a^2 \cdot b} \tag{2.13}$$

Where:

- $F_{ND_{azi}}$ = force on the bit due to azimuth natural displacement $[N]$
- $F_{ND_{inc}}$ = force on the bit due to inclination natural displacement $[N]$
- $F_{Offset_{azi}}$ = force on the bit due to azimuth offset $[N]$
- $F_{Offset_{inc}}$ = force on the bit due to inclination offset $[N]$
- ND_{azi} = natural displacement caused by the azimuth change $[m]$
- ND_{inc} = natural displacement caused by the inclination change $[m]$
- $Offset_{azi}$ = offset used in the BHA actuator to reach the target azimuth change $[m]$
- $Offset_{inc}$ = offset used in the BHA actuator to reach the target inclination change $[m]$

- $E =$ elasticity modulus of a steel pipe $[Pa]$
- $I =$ inertia moment $[m^4]$
- $a =$ distance from the bit to the actuator $[m]$. Assumed 0.5 m.
- $b =$ distance from the bit to the upper stabilizer $[m]$. Assumed 2.7 m.

According to the last set of equations, there are two types of forces acting over the bit (each with an inclination and azimuth component). As a result of the natural displacement, the bit is being pushed in the opposite direction by the reaction force of the formation contact. Second, the offset opening produces a reaction force that will be transferred to the bit. A clearer understanding of the forces and directions of the reaction forces can be seen in Figure 2.18 (Jerez, 2021).

The relevant bit force equations given below:

$$F_{bit\ azi} = F_{ND_{azi}} + F_{Offset_{azi}} \tag{2.14}$$

$$F_{bit\ inc} = F_{ND_{inc}} + F_{Offset_{inc}} \tag{2.15}$$

Where:

- $F_{bit\ azi} =$ total force on the bit for the azimuth component $[N]$
- $F_{bit\ inc} =$ total force on the bit for the inclination component $[N]$

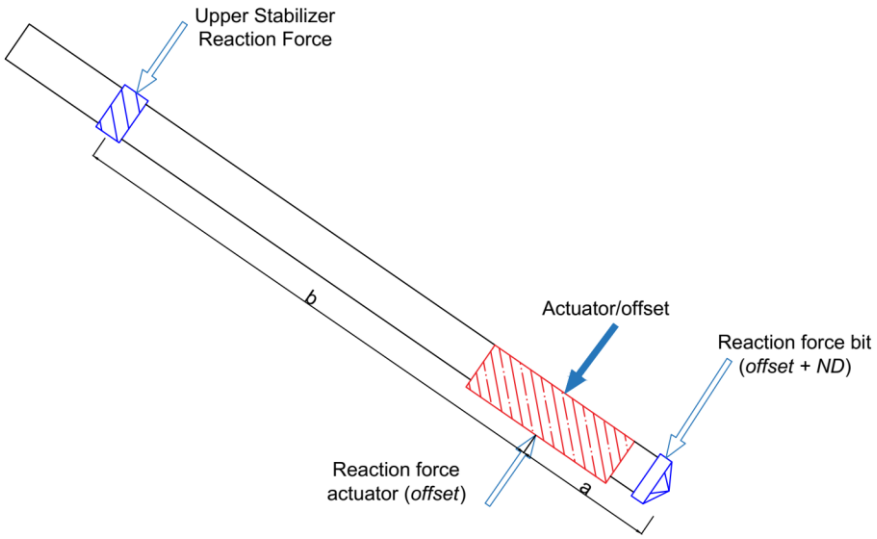

Figure 2.18: Acting Forces on the Bit (Jerez,2021)

2.2.3.5. ROPs Calculations

Among the distinctive features of the RSS Model are the ROPs calculations, which provide a novel method for calculating bit movement, including its inclination, azimuth, and DLS. During the calculation, three types of ROPs are utilized in a three-dimensional space (see Figure 2.19), where blue represents the bit and red represents the remainder of the BHA).

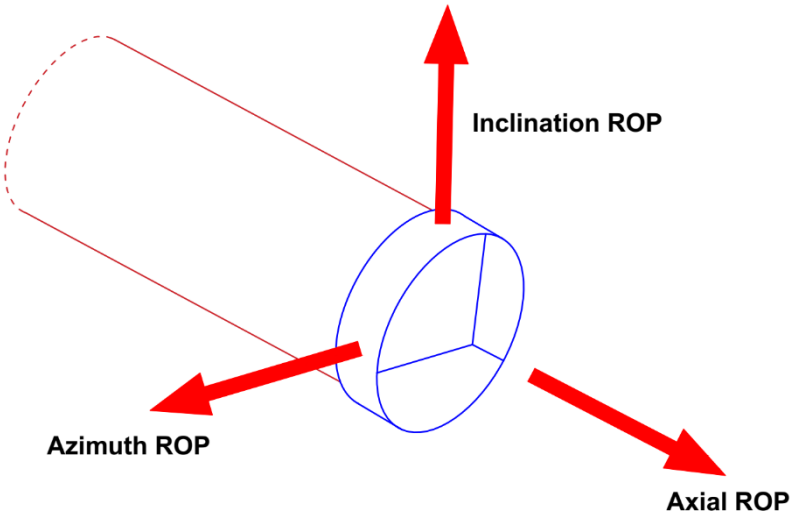

Figure 2.19: 3D ROPs Acting on the Drill Bit (Jerez,2021)

Each ROP represents the bit's movement over time based on the measurement unit of the ROP (distance over time). In 1965, Teale proposed ROP equations in which the rock mechanics depend on the rock's energy (Teale, 1965).

The Saramago equation of ROP was adapted by converting the original WOBs into F_{bits} and decomposing the common ROP into an axial ROP, an inclination ROP, and an azimuth ROP. To overcome the reaction force imposed on the bit during directional drilling, ROPs are applied to generate some displacement in the opposite direction of the reaction force (described above)(Jerez, 2021).

The third concept is illustrated in Figure 2.20, which illustrates both offsets and natural displacements as well as the ROPs that result from the frontal plane of the bit.

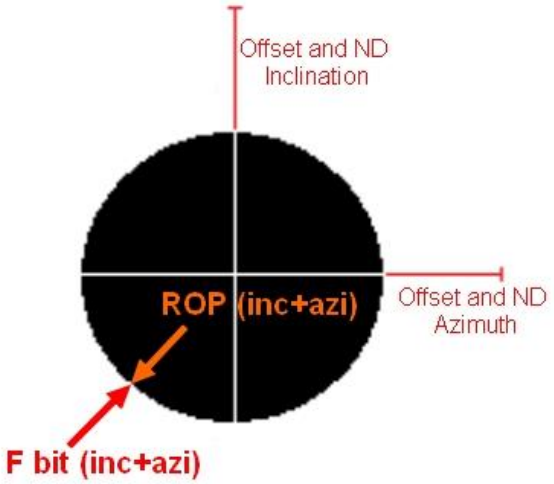

Figure 2.20: Resultant ROP Pushing the Bit Against the Reaction Force on the Bit (Jerez,2021)

ROP equations (Saramago, 2020):

$$ROP_{axial} = \frac{13.33 \cdot \mu \cdot N}{D\left(\frac{Es}{WOB} - \frac{1}{Ab}\right)} \cdot 0.3048 \tag{2.16}$$

$$ROP_{azi} = \frac{13.33 \cdot \mu \cdot N \cdot steer}{D\left(\frac{Es}{F_{bit\ azi}} - \frac{1}{Ab}\right)} \cdot 0.3048 \tag{2.17}$$

$$ROP_{inc} = \frac{13.33 \cdot \mu \cdot N \cdot steer}{D\left(\frac{Es}{F_{bit\ inc}} - \frac{1}{Ab}\right)} \cdot 0.3048 \tag{2.18}$$

Where:

- ROP_{axial} = ROP in the axial direction $[m/hr]$
- ROP_{azi} = ROP in the azimuth direction $[m/hr]$
- ROP_{inc} = ROP in the inclination direction $[m/hr]$
- Ab = transversal area of the borehole $[in^2]$

These equations can be used to calculate the next bit position or next bit survey in the RSS Model (Saramago, 2020):

$$MD_{(t)} = MD_{(t-1)} + \sqrt{{ROP_{azi_{(t)}}}^2 + {ROP_{inc_{(t)}}}^2 + {ROP_{axial_{(t)}}}^2} \cdot \frac{\Delta t}{3600} \tag{2.19}$$

$$Inc_{(t)} = Inc_{(t-1)} + \tan^{-1}\left(\frac{ROP_{inc_{(t)}}}{ROP_{axial_{(t)}}}\right) \cdot \frac{\Delta t}{3600} \tag{2.20}$$

$$Azi_{(t)} = Azi_{(t-1)} + \tan^{-1}\left(\frac{ROP_{azi_{(t)}}}{ROP_{axial_{(t)}}}\right) \cdot \frac{\Delta t}{3600} \tag{2.21}$$

$$HD_{(t)} = HD_{(t-1)} + \sin\left(Inc_{(t)}\right)\sqrt{{ROP_{inc_{(t)}}}^2 + {ROP_{axial_{(t)}}}^2} \cdot \frac{\Delta t}{3600} \tag{2.22}$$

$$TVD_{(t)} = TVD_{(t-1)} + \cos\left(Inc_{(t)}\right)\sqrt{{ROP_{inc_{(t)}}}^2 + {ROP_{axial_{(t)}}}^2} \cdot \frac{\Delta t}{3600} \tag{2.23}$$

$$East_{(t)} = East_{(t-1)} + \sin\left(Azi_{(t)}\right)\left(HD_{(t)} - HD_{(t-1)}\right) \tag{2.24}$$

$$North_{(t)} = North_{(t-1)} + \cos\left(Azi_{(t)}\right)\left(HD_{(t)} - HD_{(t-1)}\right) \tag{2.25}$$

$$DLS_{(t)} = \frac{\cos^{-1}\left[\cos\left(Inc_{(t)}\right)\cos\left(Inc_{(t-1)}\right) + \sin\left(Inc_{(t)}\right)\sin\left(Inc_{(t-1)}\right)\cos\left(Azi_{(t)} - Azi_{(t-1)}\right)\right]}{MD_{(t)} - MD_{(t-1)}} \tag{2.26}$$

Where:

- $t =$ Current iteration position
- $t - 1 =$ Last iterated position

2.3. Reinforcement Learning Basics

In a simple way, Reinforcement Learning (RL) is a successfully trained computer algorithms which plays game better than any human players. The programs designed for the game, finds the best action among the very large action space with respect to state space. During this process, the programs handle imperfect world information, and uncertainty of environment space.

In real life cases, engineers encounter similar challenges when they design controller for real life systems. Is there any possibility to solve complex problems from drilling industry by reinforcement learning? This work will show deeper explanations for this question.

The goal of reinforcement learning is to maximize a numerical reward signal by learning what to do-how to map situations to actions. Instead of being instructed on which actions to take, learners must determine which actions will yield the greatest reward by trying them out for themselves (Sutton and Barto, 2018)

As a rule, a control system determines which inputs (actions) should be applied to a system in order to generate the desired behaviour as shown in Figure 2.21. In feedback control systems, state observations are used to improve performance as well as to correct for random errors and disturbances. This feedback is used by engineers to design the controller in accordance with the system requirements, along with a model of the plant and its environment. When the system is hard to model, highly nonlinear, or has a large state space and action area, this concept can quickly become difficult to achieve (MATLAB, 2022).

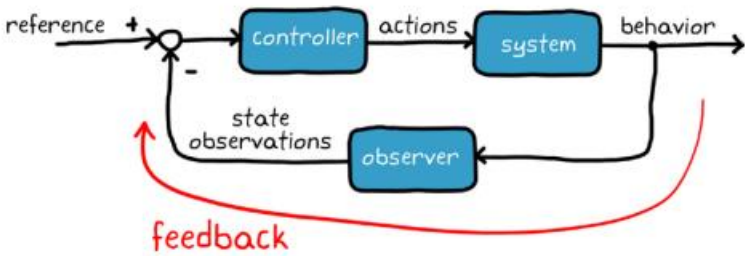

Figure 2.21: Basic Structure of Reinforcement Learning (MATLAB, 2022)

If the observations were gathered directly from the users, instead of having each of these components designed separately, imagine squeezing everything into a single function that would output low-level actions directly based on the observations. Reinforcement learning may appear more challenging than developing a control system composed of piecewise subcomponents; however, this is an area where it can be utilized effectively as can be seen in Figure 2.22.

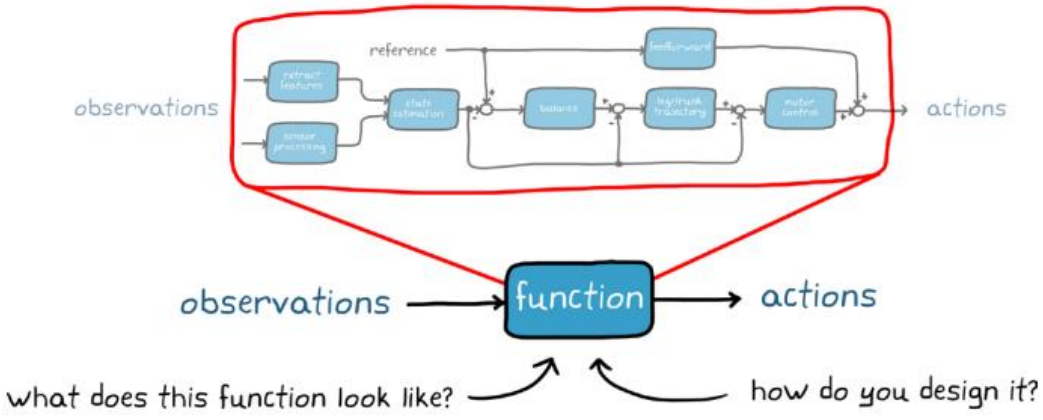

Figure 2.22: Example of Chunk Function Instead of Having Multiple Components (MATLAB, 2022)

Reinforcement learning is a part of machine learning, but this work does not cover supervised and unsupervised learning as shown in below Figure 2.23.

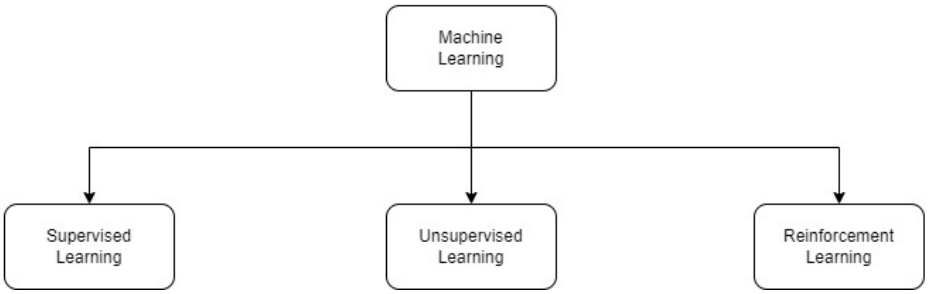

Figure 2.23: Types of Machine Learning

Reinforcement learning may appear more challenging than developing a control system composed of piecewise subcomponents; however, this is an area where it can be utilized effectively (Figure 2.24).

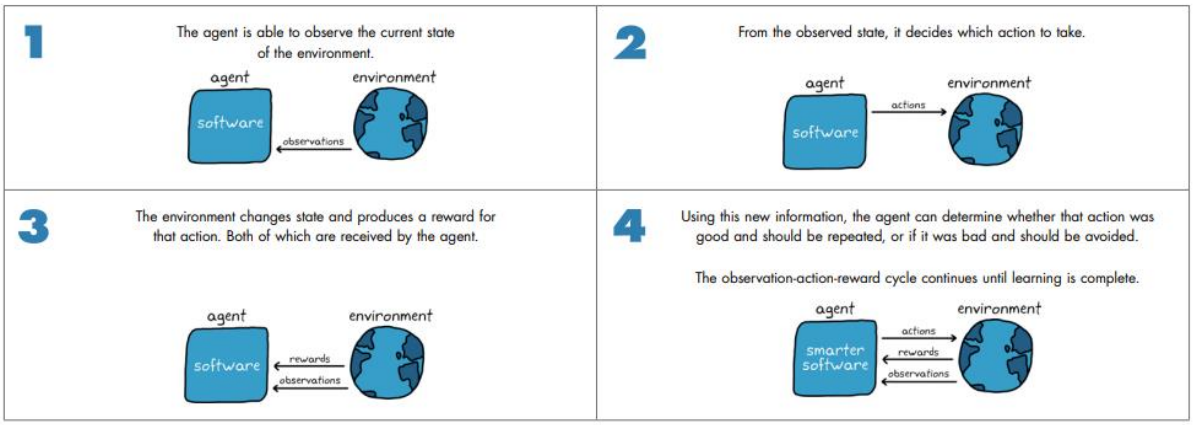

Figure 2.24: Simple Process of Reinforcement Learning (MATLAB, 2022)

A function is contained within an agent that maps state observations (inputs) to actions (outputs). This single function will replace all of the individual components of your control system. According to the RL nomenclature, this function is known as a policy. The aim of a policy is to determine what actions should be taken in response to a series of observations (MATLAB, 2022).

The detailed graphical illustration given in Figure 2.25 below, which will cover more detailly in next sections.

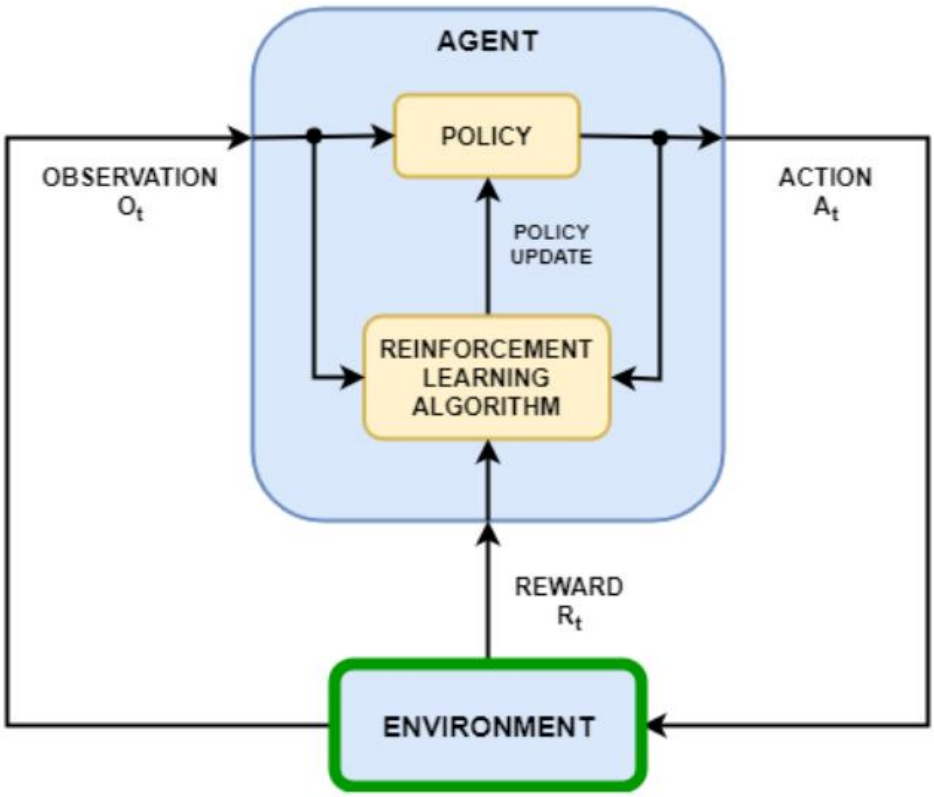

Figure 2.25: Flowchart of Reinforcement Learning Organization (MATLAB Reinforcement Learning Toolbox, 2022)

The design of a policy will be complete once you have designed a policy that commands the appropriate actuators based on the observed state. It would be difficult to achieve this in most cases. A static mapping would not be optimal over time, regardless of finding the perfect policy. A reinforcement learning algorithm is the next step in this process. The policy is modified as a result of actions taken, observations made from the environment, as well as rewards collected. Based on reinforcement learning algorithms, agents are able to determine the best policy as they interact with the environment in order to take the most advantageous action, given any given state, for the longest period of time.

The process of systematically adjusting these parameters to reach the optimal policy is known as learning. By doing so, you will be able to focus on setting up an appropriate policy structure without having to manually tune the function to obtain the right parameters. In the future we will discuss how to let the computer learn the parameters on its own, but for now you may think of it as fancy trial and error (MATLAB, 2022).

2.3.1. Reinforcement Learning Workflow

Reinforcement Learning divides into five different stages in terms of environment, reward, policy, training, and deployment as can be seen below.

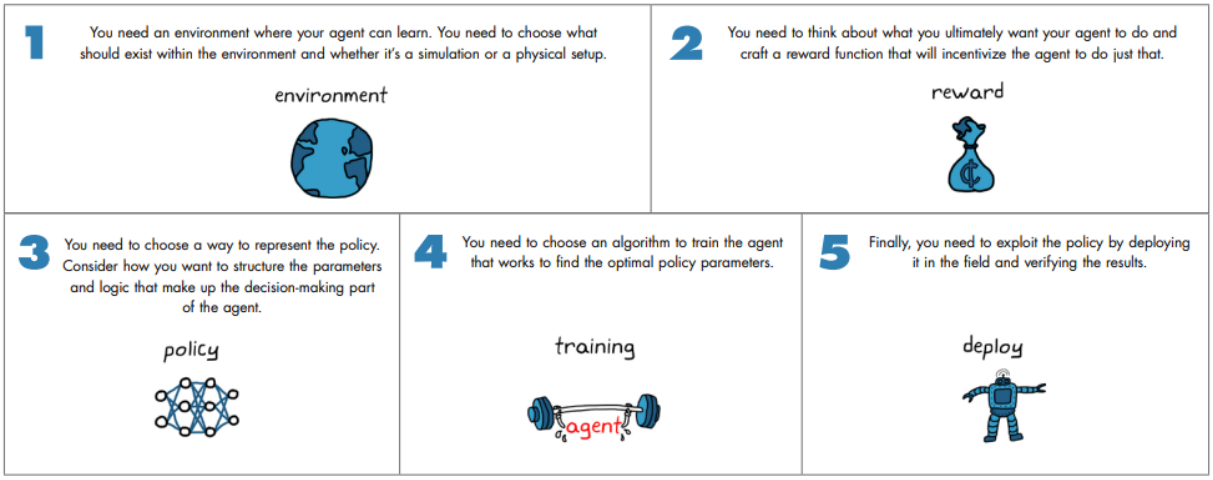

Figure 2.26: Steps of Reinforcement Learning (MATLAB ,2022)

2.3.1.1. Environment

The Reinforcement Learning environment which consists everything outside of RL agent. Agent sends action and receive rewards and observation (Figure 2.27). Besides, the environment is everything except agent. In detail, it consists of functions of system dynamics. For example, for our case RSS simulator. The agent is just kind of software generating actions and updating the policy through training.

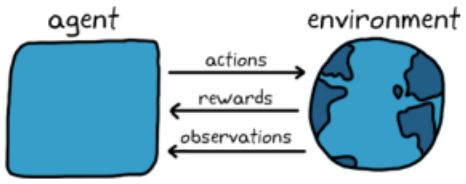

Figure 2.27: Agent and Environment Relation (MATLAB, 2022)

The strength of reinforcement learning lies in the fact that the agent does not need to have any prior knowledge of the environment in order to learn. However, it is still possible for it to learn how to interact with it. A walking robot, for instance, does not require the agent to be knowledgeable about its dynamics or kinematics. Even though it doesn't know how the joints move or how long the appendages are, it still determines how to collect more rewards. In reinforcement learning, this is referred to as model-free reinforcement learning. You can integrate RL-equipped agents into any system and have them learn the optimal policy through model-free reinforcement learning (MATLAB, 2022).

Providing the agent with the ability to interact with the environment is essential to ensuring that the agent learns through interaction with it. Depending on the circumstances, a simulation or a real physical environment may be recommended.

The most common method of training an agent is through the use of simulated environments. Having a good model of the system and environment is a nice benefit when dealing with control problems. Traditional control design normally requires such models. It is important to understand that learning is a process that requires a great deal of sampling: trials, errors, and corrections. Consequently, it is extremely inefficient in this respect since it can take thousands or millions of episodes to reach a conclusion that is optimal. Simulations can be run in parallel to generate a model of the environment that runs faster than real time. Learning can be accelerated by both approaches (MATLAB, 2022).

2.3.1.2. Reward

Once the environment has been established, it is time to consider what you would like your agent to do and how you will reward it for achieving your goals. The learning algorithm must be able to understand" when the policy is getting better and ultimately converge on the desired result (MATLAB, 2022)

As the name suggests, reward is a formula that produces a scalar number that represents how "good" it is for an agent to be in a particular state and to take a certain action.

$$reward = function(state, action) \tag{2.7}$$

Introducing domain-specific knowledge into an agent through engineering. The agent can be rewarded for maintaining the robot's trunk at a walking height. You want the robot to walk rather than crawl along the ground as shown in Figure 2.28. It is also possible to reward someone who has a low actuator effort. It spends more time on its feet and doesn't stray from its path. There are several challenges associated with reinforcement learning, including finding the right reward function; this does not imply that it is an easy task. Until your agent has failed to produce the desired results after spending considerable time training it, it may not be obvious that your reward function is poorly designed. Nevertheless, with this general overview, you can better understand some of the things you'll need to keep in mind while crafting the reward function (MATLAB, 2022).

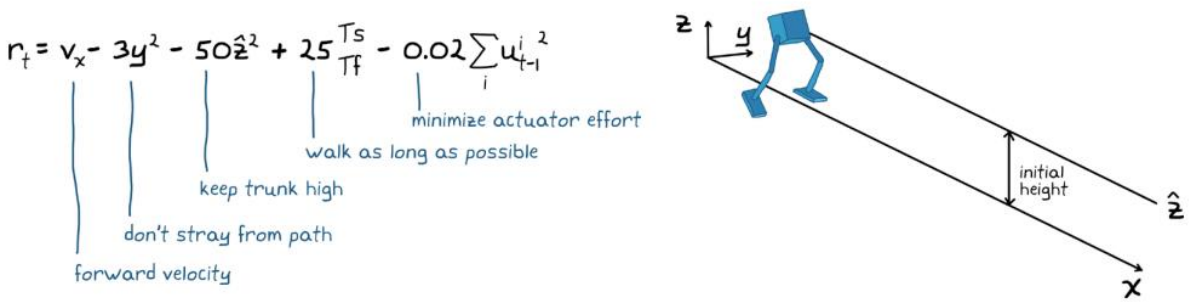

Figure 2.28: Example Structure for Reward Function (MATLAB, 2022)

2.3.1.3. Policy

An agent is composed of two components: a policy and a learning algorithm. By optimizing the function which maps observations to actions, learning algorithms determine the optimal policy. In its most fundamental form, a policy is a function that takes in state observations and generates actions in response (MATLAB, 2022)

$$Policy \rightarrow actions = function\ (state\ observations) \tag{2.8}$$

Here, we do not discuss in detail the mathematics of neural networks. Nevertheless, it is important to highlight a few points in order to better understand some of the decisions that will be made once the policies are set up. According to Figure 2.29, the input nodes are located on the left, one for each input to the function, while the output nodes are located on the right. A hidden layer is a column of nodes located in between the visible layers. The network has two inputs, two outputs, and two hidden layers of three nodes each. Each input node is connected to each node in the next layer, and then from these nodes to the next layer, and again until the output nodes are connected (MATLAB, 2022).

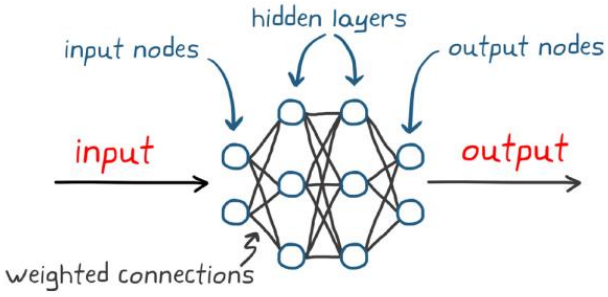

Figure 2.29: Policy Functions as Neural Network (MATLAB, 2022)

2.3.1.4. Training

Reinforcement learning (RL) algorithms utilize neural networks to represent policy in the agent. It is impossible to structure a policy without also selecting an algorithm for reinforcement learning. A learning algorithm based on policy functions trains a neural network that receives observations about the state and produces actions based on those observations. A policy function-based algorithm is a neural network that embodies the entire policy. As a result of its direct influence on the agent's actions, the neural network is called the actor (Figure 2.30).

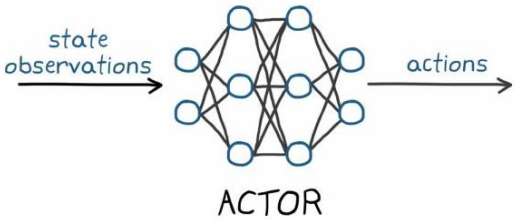

Figure 2.30: Policy Function-Based Learning (MATLAB, 2022)

2.3.1.5. Deployment

Even if most of the learning is carried out offline in a simulated environment, it may be necessary to continue learning with the actual hardware after deployment. Due to the fact that some environments may be difficult to model accurately, this is the case. In light of this, a policy that is optimal in a model may not be optimal in a real-life scenario. A further consideration is that the agent may have to continue to learn periodically as the environment gradually changes over time. As a result, both the static policy and the learning algorithms are deployed to the target.

There is a complementary relationship between learning in a simulated environment and learning in a real environment. With simulation, you can learn a sufficiently optimal policy relatively quickly and safely -- one that maintains the safety of the hardware while getting close to the desired behavior, even if it is not perfect. Using the physical hardware and online learning, the policy can be tweaked to tailor it to the environment (MATLAB, 2022).

Initially, you may believe that you can setup an environment, place an RL agent in it, and then let the computer solve your problem while you go to the store for a cup of coffee. There are, however, many disadvantages to this approach, regardless of whether the agent and environment are perfect and the learning algorithm converges on a solution. (MATLAB, 2022).

2.3.2. Agents

As indicated in Figure 2.25 agent consists of two parts which are policy and reinforcement learning algorithm. In this work, because of practicality picked in place agents in Reinforcement Learning Toolbox of MATLAB. In this study only two agent is available for sparse action and state space. These are Proximity Policy Optimization and Deep Q-network RL agents.

2.3.2.1. Proximity Policy Optimization (PPO) RL Agent

PPO is an on-policy, proximal policy gradient reinforcement learning method that is model-free, online, and on-policy. As a type of policy gradient training, this algorithm alternates between sampling data through environmental interaction and optimizing a clipped surrogate objective function using stochastic gradient descent. By limiting the size of the policy change at each step, the clipped surrogate objective function enhances training stability (MATLAB RL Toolbox, 2022).

During training, a PPO agent (MATLAB RL Toolbox, 2022):

- Estimates probabilities of taking each action in the action space and randomly selects actions based on the probability distribution.
- Interacts with the environment for multiple steps using the current policy before using mini-batches to update the actor and critic properties over multiple epochs.

2.3.2.2. Deep Q-network (DQN) RL Agent

DQN (deep Q-network) algorithms are model-free, online, off-policy reinforcement learning algorithms. As a value-based reinforcement learning agent, DQN agents train critics to estimate future rewards. Q-learning is a variant of DQN.

During training, the agent (MATLAB RL Toolbox,2022):

- Updates the critic properties at each time step during learning.
- Explores the action space using epsilon-greedy exploration. During each control interval, the agent either selects a random action with probability ϵ or selects an action greedily with respect to the value function with probability 1-ϵ. This greedy action is the action for which the value function is greatest.
- Stores past experiences using a circular experience buffer. The agent updates the critic based on a mini-batch of experiences randomly sampled from the buffer.

2.3.3. The Future of Reinforcement Learning

Using reinforcement learning to solve difficult problems can be very effective. As we discussed, there are some challenges associated with understanding the solution and confirming that it will work. However, you have a few options at your disposal right now to overcome those difficulties. Despite the fact that reinforcement learning has yet to reach its full potential, it may not be long until it becomes the design method of choice for all complex control systems. (MATLAB, 2022)

3. Trajectory Control via Reinforcement Learning

Having established the planned well path, controlling the trajectory of the well is an important and challenging task. Previously, Jerez developed trajectory control algorithms using vectors and ellipses of uncertainty. However, this study aims to optimize the weight on bit and rotational speed of a control trajectory using Reinforcement Learning.

Figure 3.1 illustrates the structure of this work, and later sections provide a detailed explanation. A unique synthesis of RSS simulator and Reinforcement Learning is presented in this study and contributes to utilizing trajectory control. RSS simulator modified and differentiated small functions in Python Programming Language, enabling it to operate in any environment. On the other hand, the reinforcement learning environment is structured within MATLAB and is integrated with Python functions. A planned well path and ellipses of uncertainty are also created as external files and can be imported into MATLAB. The reward calculations were made in Python and recalled in the main MATLAB environment.

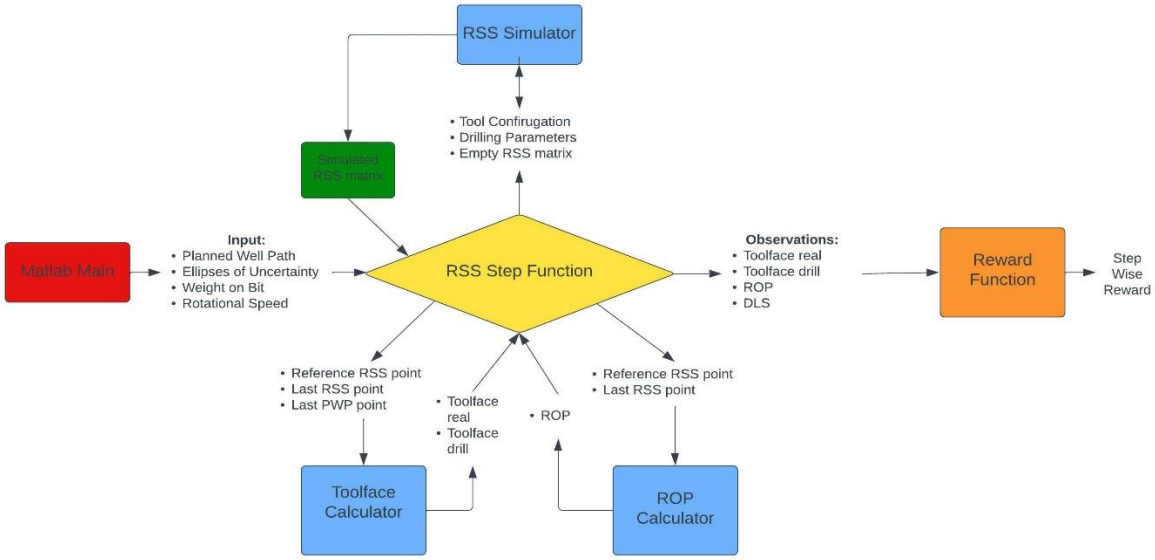

Figure 3.1: Summary of Integration between MATLAB and Python Environment

3.1. RSS Simulator in Python Environment

In 2021, the University of Stavanger's in-house simulator for RSS was not suitable for integration with other environments and was not criticized for its efficiency. In order to carry out this study, the first step will be to clean and restructure the RSS simulator code into appropriate parts that can be used in other environments.

In RSS simulator as shown in Figure 3.1, the main loop is stripped from trajectory control algorithms and referred to as RSS Step Function. Due to various variables sent by the MATLAB environment, this function cleaned and corrected for possible errors. The function holds RSS matrix elements indicated in Table 2.6, some drilling parameters indicated in Table 2.3, and some tool configuration variables indicated in Table 2.2. This function is intended to send the necessary inputs and to call the RSS Simulator, ROP Calculator, and Tool face Calculator functions. The output side of this function transmits RSS matrix to MATLAB

environment for the next phase, as well as tool face angles, ROP values and DLS values to the reward function.

3.2. MATLAB Reinforcement Learning Environment

This study is based on Reinforcement Learning Environment in MATLAB, which is the core of the study. Basically, this is a chunk of code that consists of some functions and is connected to Python as well as a base for RL agents. An overview of the procedure is shown in Figure 3.2.

As part of this environment, necessary variables are defined as properties of subsequent operations in the simulator. Reinforcement Learning simulations are based on RSS matrices and observation values selected precisely. Under the state matrix, observation values and timesteps are merged. Additionally, there is an action matrix that consists of step WOB and RPM values. These actions are automatically controlled by the agent in terms of observation and reward. In this study, action and observation spaces are defined as discrete spaces.

As soon as the properties have been generated, the main function runs and calls the Python environment functions, which return the RSS matrix with the reward. The process is repeated at each survey point in the PWP until the target point is reached. Upon reaching the target point, the simulation stops, the agents analyse the observations and rewards and generate new actions for the next episode.

State variables should also be reset by a reset function within the environment after every episode. This allows the simulator to start from the initial point of the well path.

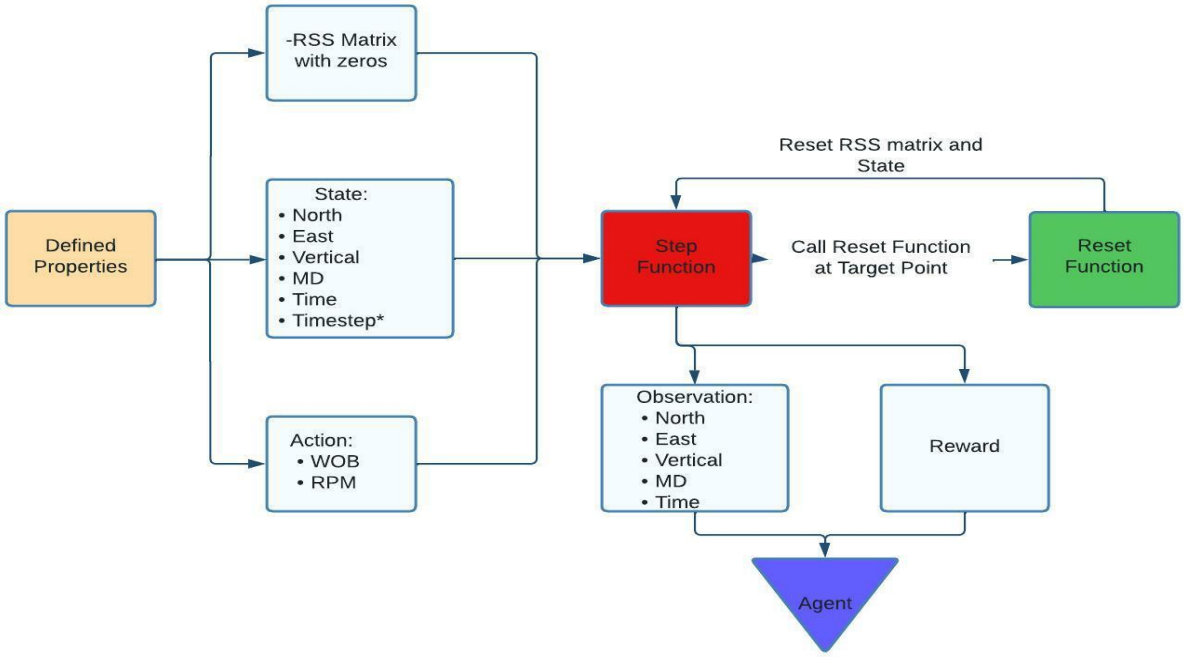

Figure 3.2: MATLAB Reinforcement Learning Environment for This Study

3.3. Reward Function

Reward function is main way to manipulate the agent through simulation. This function should balanced between penalty and reward outputs to maximize efficiency of simulator with cooperative work with agent.

Previously indicated in section for reward in Chapter 2, walking robot reward function based upon different elements. For our study, the reward function structured upon toolface angle, ROP, DLS, and position with respect to ellipse.

Firstly, toolface angles are calculated for simulated point and desired point. The first angle is between survey point and next generated point by RSS simulator and the second one is between survey point and next survey point. After the calculation of two angles, part of reward structure based on difference of these angles. If the angle difference is higher, reward is likely lower and increases with low difference.

ROP is directly difference of measured depth two survey points divided by time spend between these survey points. DLS is taken from RSS matrix without any manipulation and shouldn't be higher than given value inside code.

The last part of this reward function is determination of bit inside or outside predefined ellipse. The ellipse is defined by user in this study, but it could be determined by ellipses of uncertainty calculations. Visually ellipses are shown in Figure 3.3. If bit position is not inside of ellipse, this gives penalty to cumulative reward.

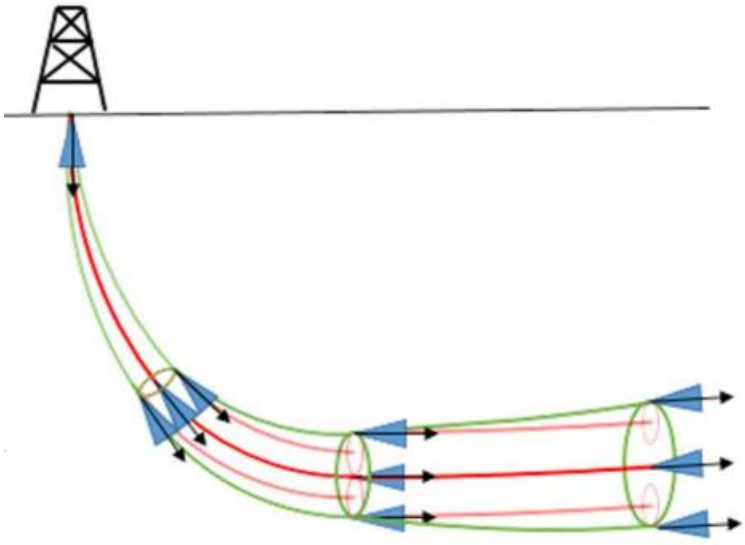

Figure 3.3: Simple Illustration for Ellipses Around Survey Points Through Well Path (Willerth, 2016)

3.4. Discussion and Assumptions

As explained in this section all parts of this work are quite complex and demands precise preparing. The system is connected to each method to find the optimum output after a drilling simulation. In order to achieve that some assumptions have been made as indicated below.

- Planned Well Path created as a file from output of PWP function. This file used as an input file for MATLAB RL environment.
- Also, decided to use ellipses with selected values like starting with 1 m radius and 0.2 m increase. The reason behind that, ellipses of uncertainty algorithm create very narrow ellipses for each survey point before kick of point and that cause negative reward during this section.
- Observation space is automatically picked discrete by RL environment. However, action space selected discrete intentionally. Because continuous action space doesn't allow user to limit the action intervals, and this causes illogical results with inputs.

4. Case Study

For the purpose of verifying the RSS Simulator with Reinforcement Learning environment, various trainings and simulations have been conducted with respect to a variety of reward functions, reinforcement learning agents, and hyperparameters. After establishing different results with different conditions, it can be determined what the best condition is by applying different trajectory types. The following sections provide a detailed discussion of each of these results.

The following visual illustrations were used to proof the work:

- 3D visualization of RSS simulator matrix vs PWP matrix
- Vertical comparison of main parameters like WOB, RPM, ROP, Tool face angles, DLS and Reward.
- Training statistics.

The action space is discrete and determined between intervals given below. Some exceptions indicated individually.

- WOB: 60000 N to 180000 N every 500 N
- RPM : 70 to 180 every 1

4.1. Different Cases to Optimize Simulator

4.1.1. Tests with Reward Function Type-1

This test has been made only show the results of reward function type-1 shown below. Only DQN agent used for this case. The shape of well used for this case is simple J shaped. Also, ellipse around each survey points starts with 5m for each direction increases 0.5 m for every survey point on the PWP. The detailed table of PWP matrix and Ellipse matrix shared in appendix C.

$$r(\Delta Toolface, DLS) = \begin{cases} \frac{r_1}{10} + r_2(ROP)^2 + r_3 + r_4 & \Delta\text{abs}(Toolface) < 0.1 \\ \frac{r_1}{(Toolface\_calc)^2} + r_2(ROP)^2 + r_3 + r_4 & DLS < DLS_m \&\& \Delta r < R \\ p_1 + p_2 & DLS \geq DLS_m \\ p_2 & \Delta r \geq R \end{cases}$$

$$\Delta Toolface = Toolface\ between\ two\ survey\ points - Toolface\ between\ model\ point\ and\ survey\ point$$

$$\text{Toolface\_calc} = \frac{r_1}{abs(\Delta Toolface) * (abs(toolface_{real})^{0.5} + abs(toolface_{rss})^{0.5})^5}$$

Where:

- r1 = 20, reward for tool face angle
- r2 = 1, reward for ROP
- r3 = 0.2, reward for DLS

- r4 = 0.1, reward for ellipse
- p1 = -5, penalty for DLS
- p2 = -2, penalty for out of ellipse
- DLS_m= 15 degree

4.1.1.1. DQN Agent with 10k Episodes

This simulation gave partially good results in terms of path matching as shown in Figure 4.1. Furthermore, drilling speed has expected behavior (Figure 4.2). However, the agent does not prefer much to variate WOB and RPM values through simulation.

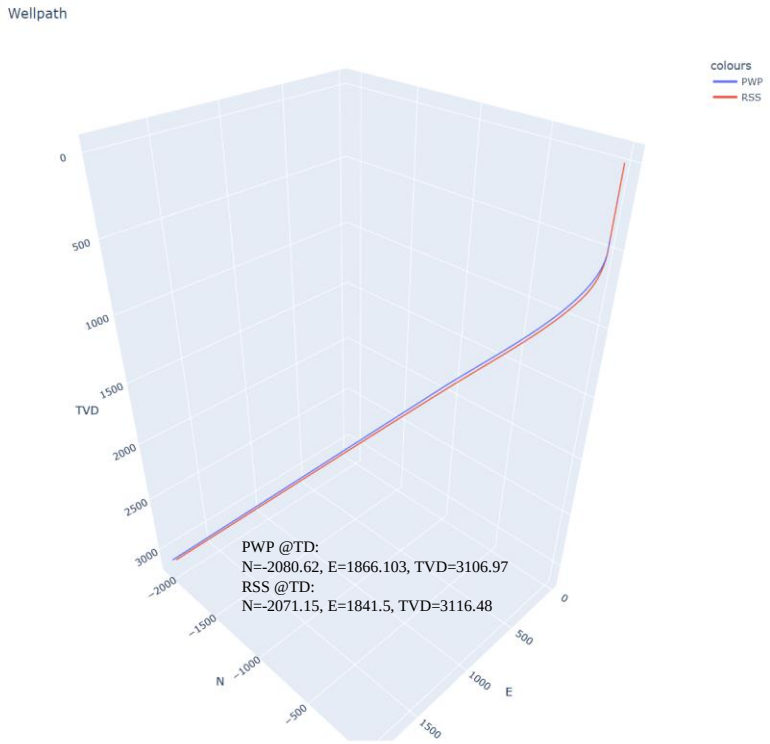

Figure 4.1: 3D View of Planned Well Path vs Path by RSS Simulator.

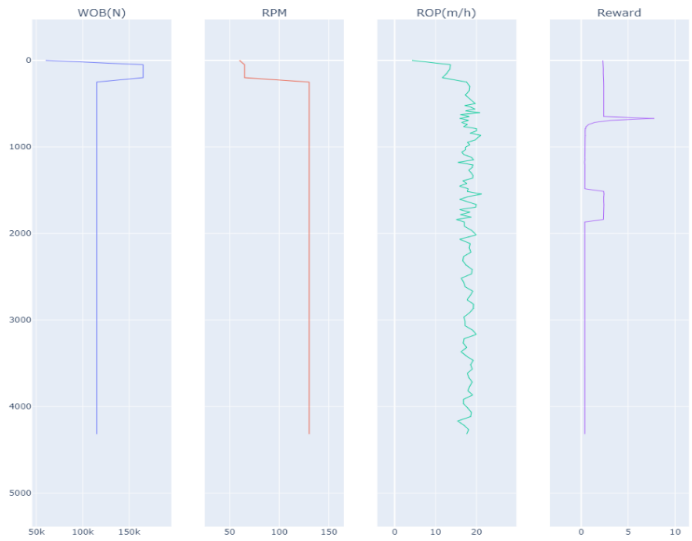

Figure 4.2: DQN Agent WOB, RPM, ROP, and Reward Outputs with Respect to Depth.

4.1.1.2. DQN Agent Changed Hyperparameters with 10k Episodes

In this simulation, some hyperparameters are changed related to policy learning rate and critics learning rate but it affected results badly (Figure 4.3 & 4.4). Especially, the path is deviated from the original path. Because of complexity and scarce time hyperparameters left at default for all other cases.

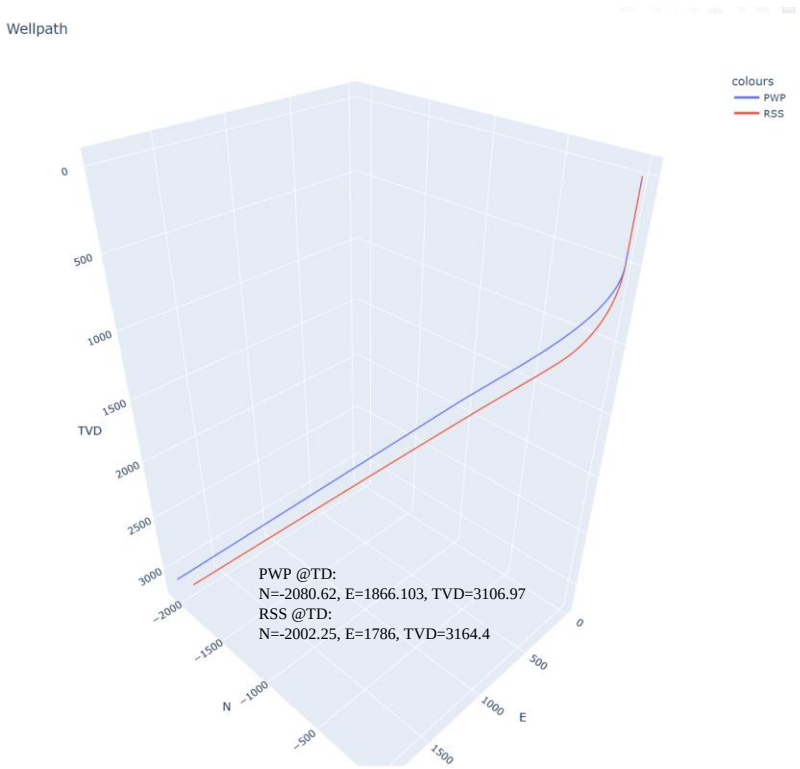

Figure 4.3: 3D View of Planned Well Path vs Path by RSS Simulator for Altered Hyperparameters.

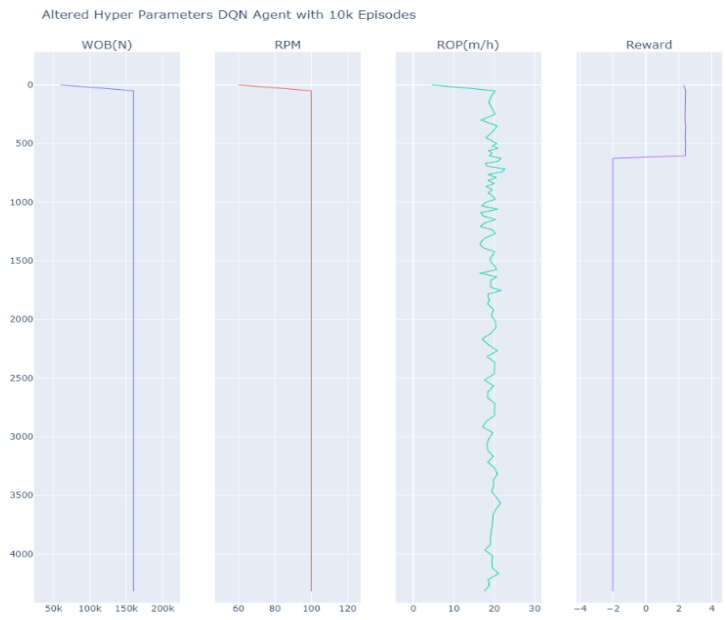

Figure 4.4: DQN Agent With Altered Hyper Parameters; WOB, RPM, ROP, And Reward Outputs with Respect to Depth.

4.1.2. Tests with Reward Function Type-2

This test has been made only show the results of reward function type-2 shown below. There are two different agents used case. The shape of well used for this case is simple J shaped. Also, ellipse around each survey points starts with 5m for each direction increases 0.5 m for every survey point on the PWP. The detailed table of PWP matrix and Ellipse matrix shared in appendix C.

$$r(\Delta Toolface, DLS) = \begin{cases} \dfrac{r_1}{10} + r_2(ROP)^2 + r_3 + r_4 & \Delta \text{abs}(Toolface) < 0.1 \\ \dfrac{r_1}{(Toolface\_calc)^2} + r_2(ROP)^2 + r_3 + r_4 & DLS < DLS_m \&\& \Delta r < R \\ p_1 + p_2 & DLS \geq DLS_m \\ p_2 & \Delta r \geq R \end{cases}$$

$$\Delta Toolface = Toolface\ between\ two\ survey\ points - Toolface\ between\ model\ point\ and\ survey\ point$$

$$\text{Toolface\_calc} = \frac{r_1}{abs(\Delta Toolface) * (abs(toolface_{real})^{0.5} + abs(toolface_{rss})^{0.5})^5}$$

Where:

- r1 = 20, reward for tool face angle
- r2 = 2.2, reward for ROP
- r3 = 1, reward for DLS
- r4 = 0.5, reward for ellipse
- p1 = -1000, penalty for DLS

- p2 = -100, penalty for out of ellipse
- DLS limit= 15 degree

4.1.2.1. DQN Agent with 10k Episodes

With changing reward there is improvement for trajectory matching but ROP trend shows similar results (Figure 4.5 & 4.6).

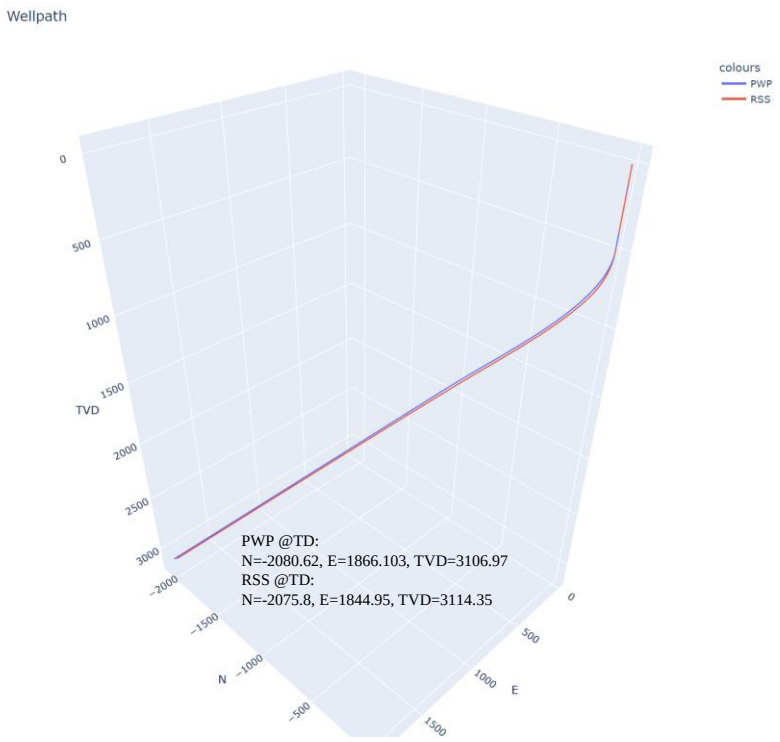

Figure 4.5: 3D view of Planned Well Path vs Path by RSS Simulator for DQN Agent.

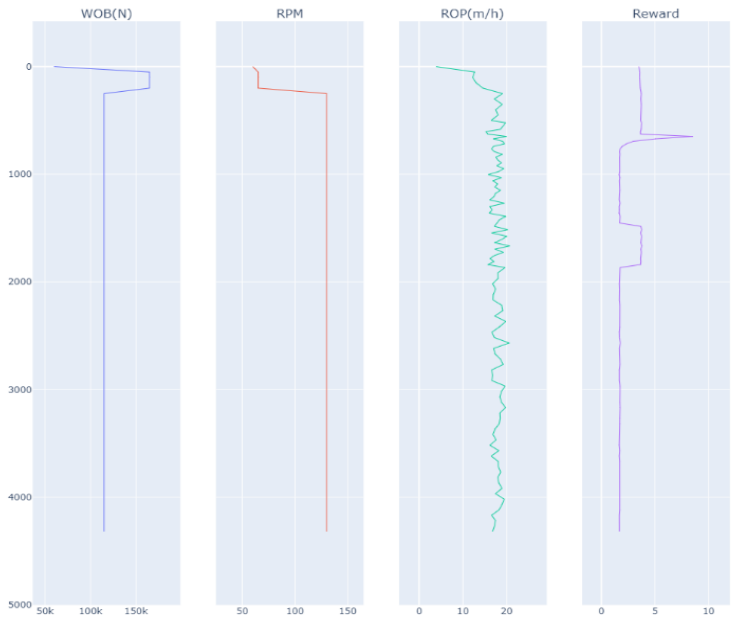

Figure 4.6: DQN agent WOB, RPM, ROP, and Reward Outputs with Respect to Depth.

4.1.2.2. PPO Agent with 30k Episodes

For this try trajectory matching almost perfect (Figure 4.8) but ROP decreased dramatically in parallel to WOB and RPM decrease (Figure 4.9). Despite DQN agent, PPO agent is preferring to stay consistent with action values during training. Training result is given in below.

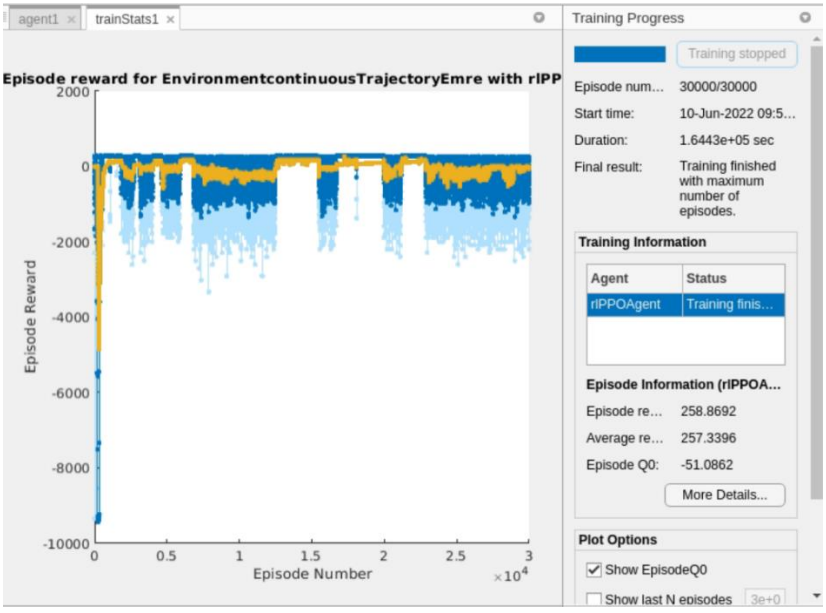

Figure 4.9: Train Statistics for PPO Agent.

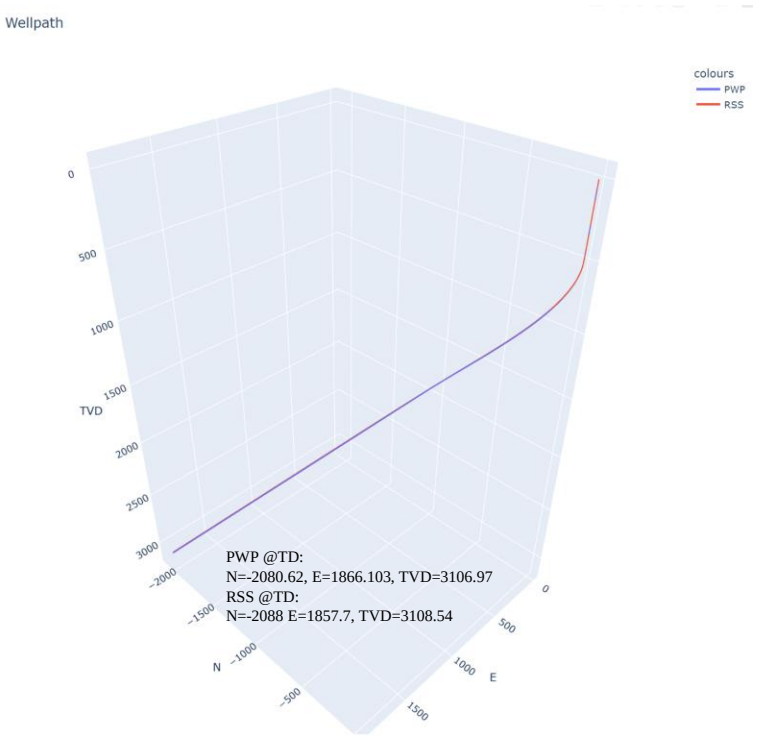

Figure 4.8: 3D View of Planned Well Path Vs Path by RSS Simulator for PPO Agent.

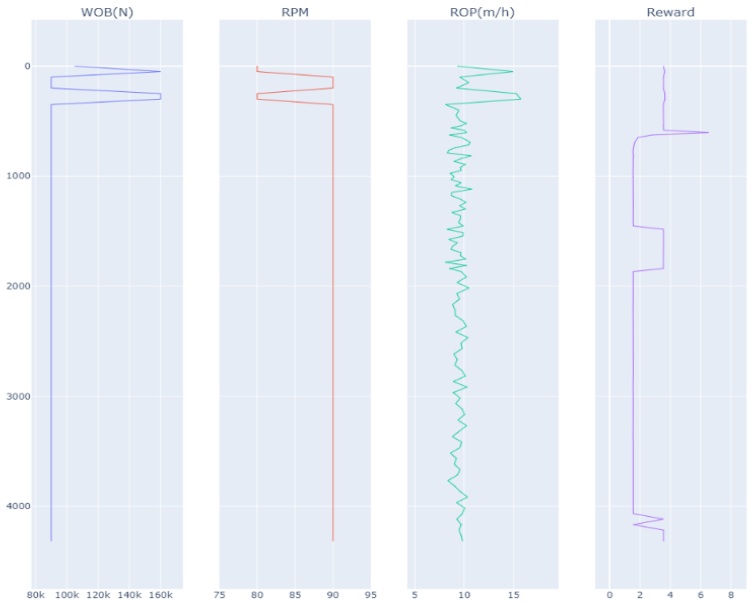

Figure 4.9: PPO Agent WOB, RPM, ROP, and Reward Outputs with Respect to Depth.

4.1.2.3.DQN Agent with 5k Episodes with Modification

As can be seen in Figure 4.7 there is significant oscillation even for same actions because of noise factor from the RSS simulator in place noise behavior. In order to detect to effect of the noise, new tests are made without noise. On the other hand, to see consistency of reward according to same action. Furthermore, tool

face angles and DLS values are added to observation to see are they correctly calculated. The consistency of path is high but ROP is quite low (Figure 4.10 & 4.11)

- WOB: 80000 N to 100000 N every 500N
- RPM: 100 to 120 every 1

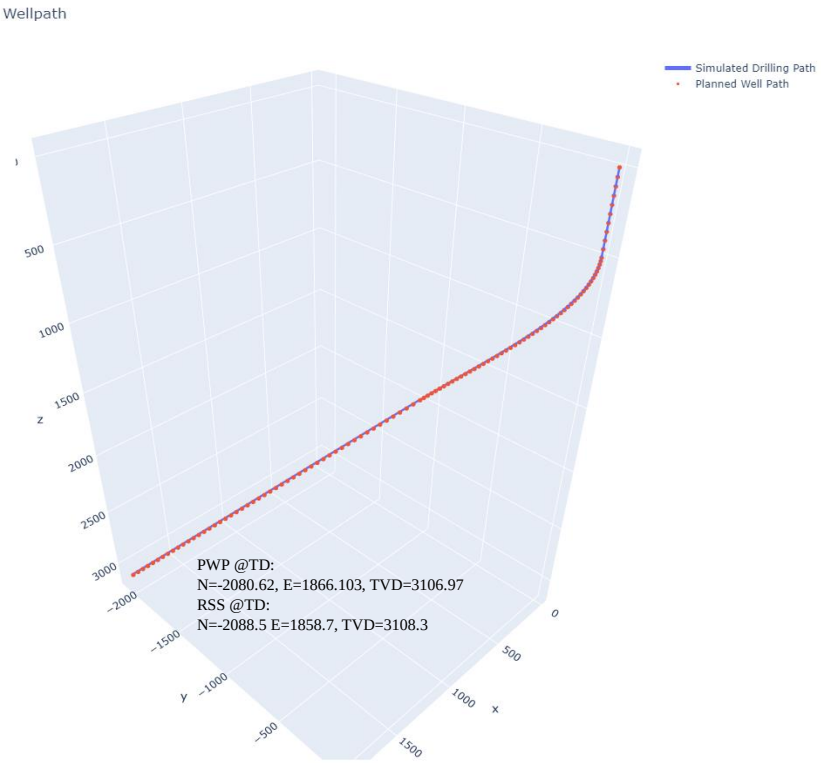

Figure 4.10: 3D view of Planned Well Path vs Path by RSS Simulator for DQN Agent.

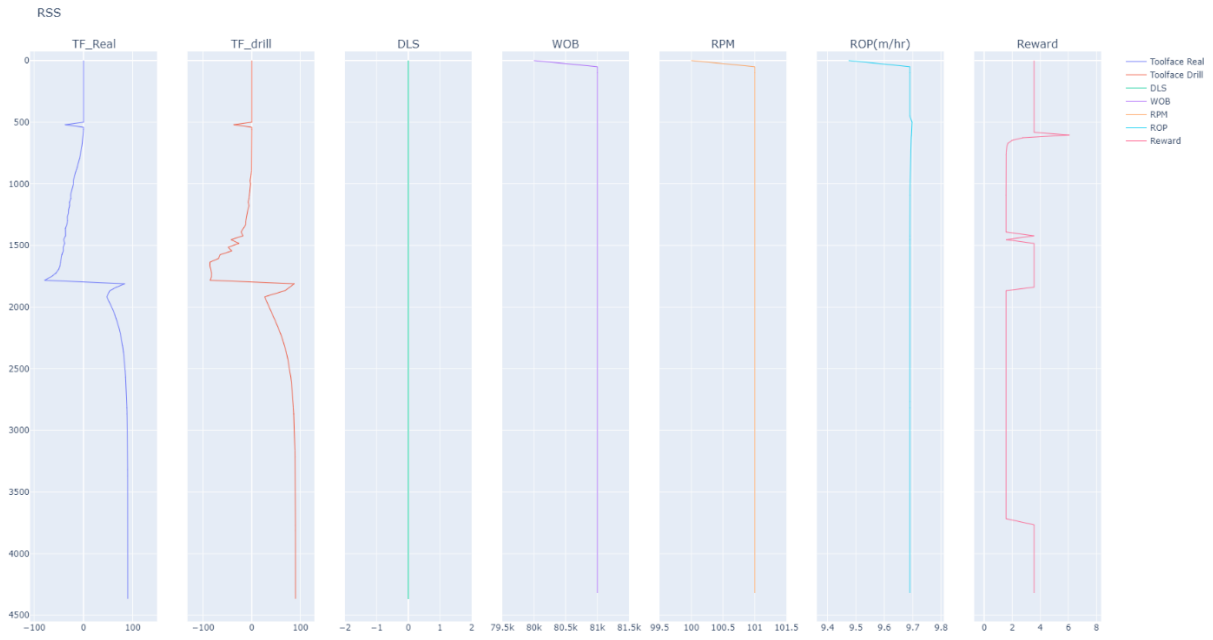

Figure 4.11: DQN agent observation and outputs with respect to depth.

4.1.3. Verification of DLS Penalty

Generally, paths, tools and parameters used RSS simulator doesn't allow DLS deviation too much. To verify it inside reward function illogical WOB and RPM values are assigned to simulator and results are shown in Table 4.1.

Table 4.1. DLS variation with respect to WOB and RPM.

DLS	WOB(N)	RPM	Reward
0	8000	1022	3.556224
86.13309	6500	1022	-1100
81.44226	6500	1022	-1100
23.44268	8000	1022	-1100
88.02671	8000	1022	-1100
83.84739	8000	1022	-1100
81.92438	8000	1022	-1100

4.2. Main Reward Function and Test with Different Well Shape

After countless try and different reward functions, most optimum package for simulation was picked with details given below.

Ellipse radii start with 1m radius for every direction and increases 0.2 m for every survey station. Detailed tables of three different shape in PWP and ellipse radius are given in appendix C.

The action space is discrete and determined between intervals given below.

- WOB: 60000 N to 180000 N every 500 N
- RPM : 70 to 180 every 1

The main reward function:

$$r(\Delta Toolface, DLS) = \begin{cases} r_2\text{ROP} & \text{abs}(toolface_{real}) + \text{abs}(toolface_{rss}) = 0.1 \\ p_t\text{Toolface\_calc} + r_2\text{ROP} & DLS < DLS_m \&\& \Delta r < R \\ p_1 + p_2 & DLS \geq DLS_m \\ p_2 & \Delta r \geq R \end{cases}$$

$$\Delta Toolface = Toolface\ between\ two\ survey\ points - Toolface\ between\ model\ point\ and\ survey\ point$$

$$\text{Toolface\_calc} = abs(\Delta Toolface) * ((abs(toolface_{real}) + abs(toolface_{rss}))^{0.2})$$

Where:

- p_t = -0.1 penalty for Tool Face angle deviation
- r_2 = 50 reward for ROP
- p_1 = -100 penalty for out of ellipse
- p_2 = -1000 penalty for DLS deviation

4.2.1. "J" Shape Well with both PPO and DQN Agent

This shape well is main type to train agents and used as reference to simulate for other two shape wells. Before start analysing, unfortunately this study could not find the perfect reward function for RSS simulator. Training given in Figure 4.12 and 4.13 shows the result of training agent according to the best possible reward function indicated in previous section. The number of episodes is limited to 50000 because of computational expense is very high. Especially, DQN agent is almost double computationally expensive in compared to PPO agent 10 days vs 5 days subsequently. During the training of PPO agent, it picks more consistent value inside an episode and prefers to change action after episode ends. However, DQN agents picks varying actions for almost every step which makes it computationally expensive. Also, this policy causes need of more episode to train DQN agent, but this study does not have enough time to test it.

For the J shape well, results are pretty expected according to previous attempts indicated in previous sections. Drilling paths established by two different agents are almost similar, but DQN agent showed better performance especially for target point. Main reason behind of this result could be slight variation of WOB and RPM by DQN agent (Figure 4.14 & 4.15)

However, the performance of ROP by PPO agent is much better in compared to DQN agent simulation. DQN agent showed good ROP performance before kick off point with high WOB and RPM, but decided to behave more conservative with low WOB and RPM. It seems that, PPO agent reacted for ROP reward in compared to DQN agent which caused this difference. However, as mentioned before this doesn't cause obvious deviation from the planned path (Figure 4.16 & 4.17)

Inspection of reward behaviour in Figure 4.16 and 4.17 shows crucial indicators. For DQN agent, conservative action starts just after subsequent penalty during high ROP. On the other hand, PPO agent has more consistent reward pattern.

Detailed table of Figure 4.16 & 4.17 given in appendix D.

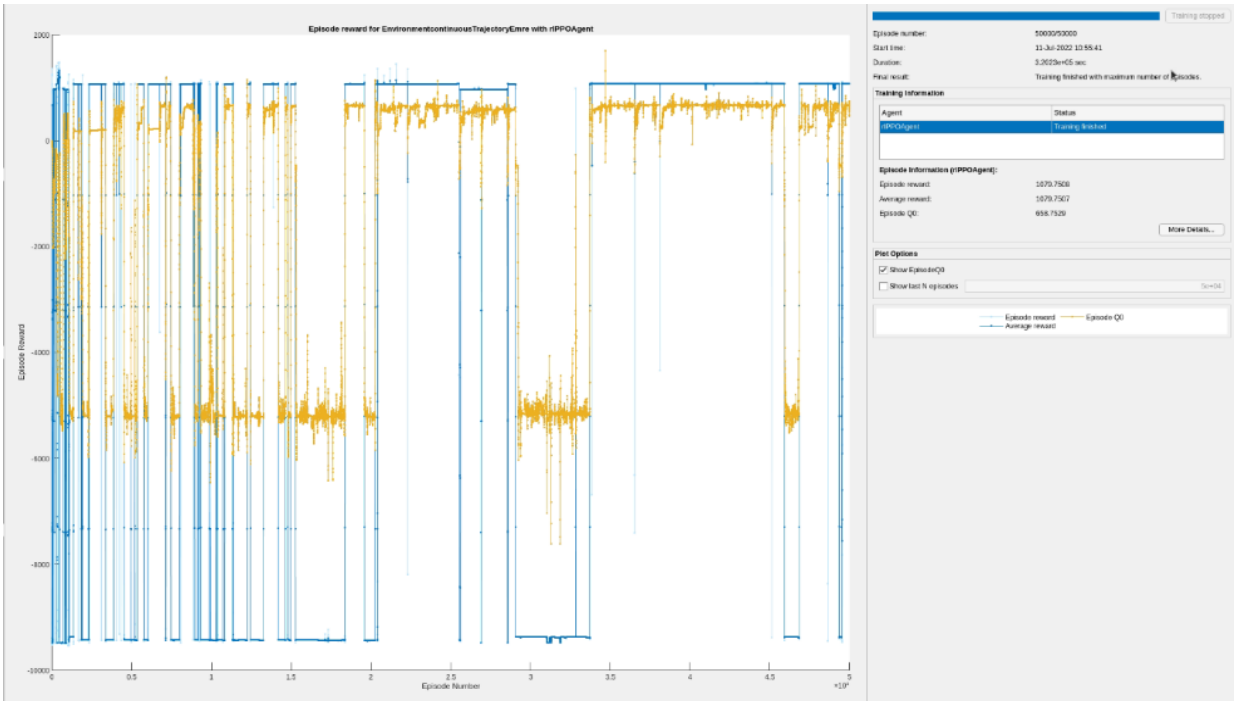

Figure 4.12: Train Statistics for PPO Agent.

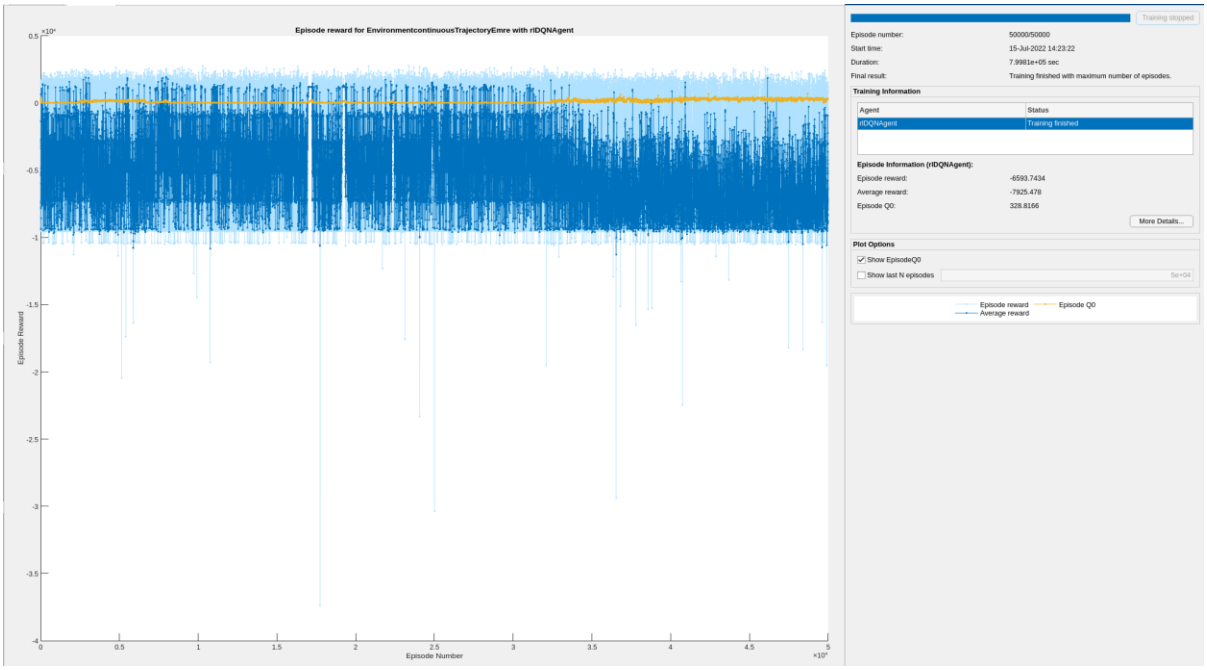

Figure 4.13: Train Statistics for DQN Agent.

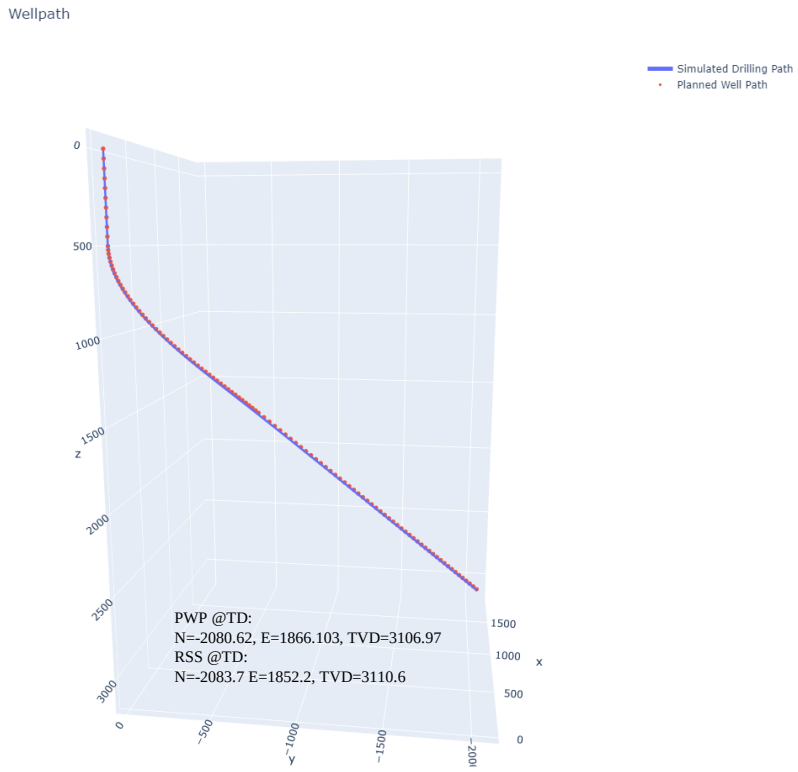

Figure 4.14: 3D view of Planned Well Path vs Path by RSS Simulator for PPO Agent with J Type Well.

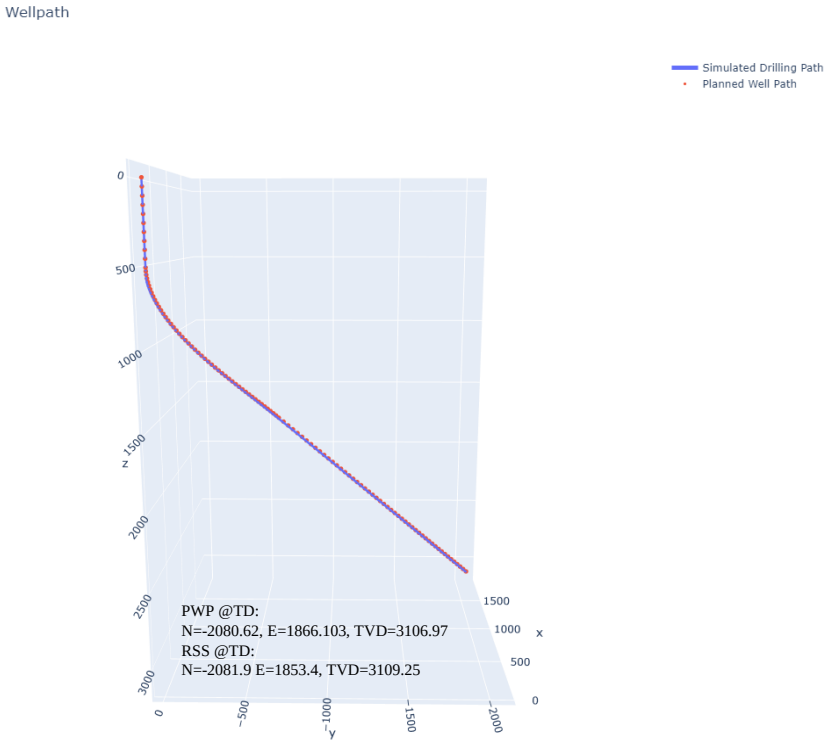

Figure 4.15: 3D view of Planned Well Path vs Path by RSS Simulator for DQN Agent with J Type Well.

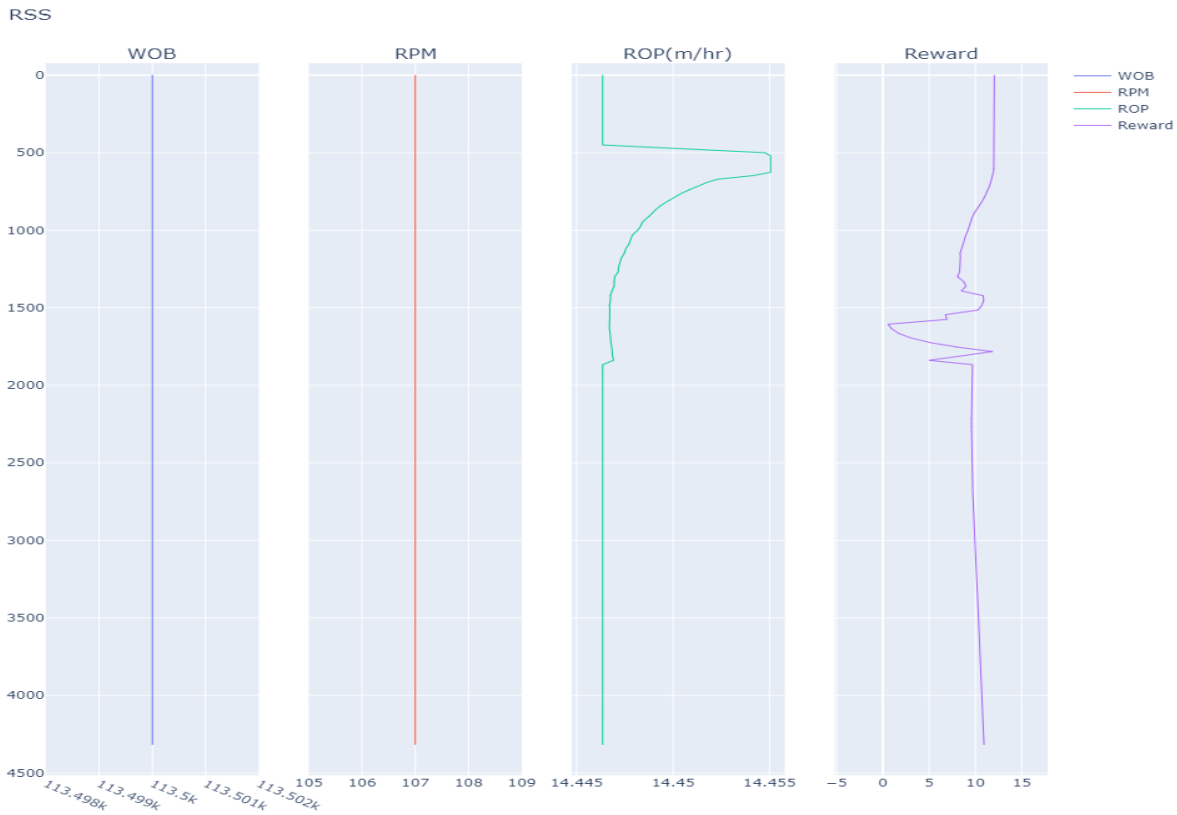

Figure 4.16: PPO agent observation and outputs with respect to depth.

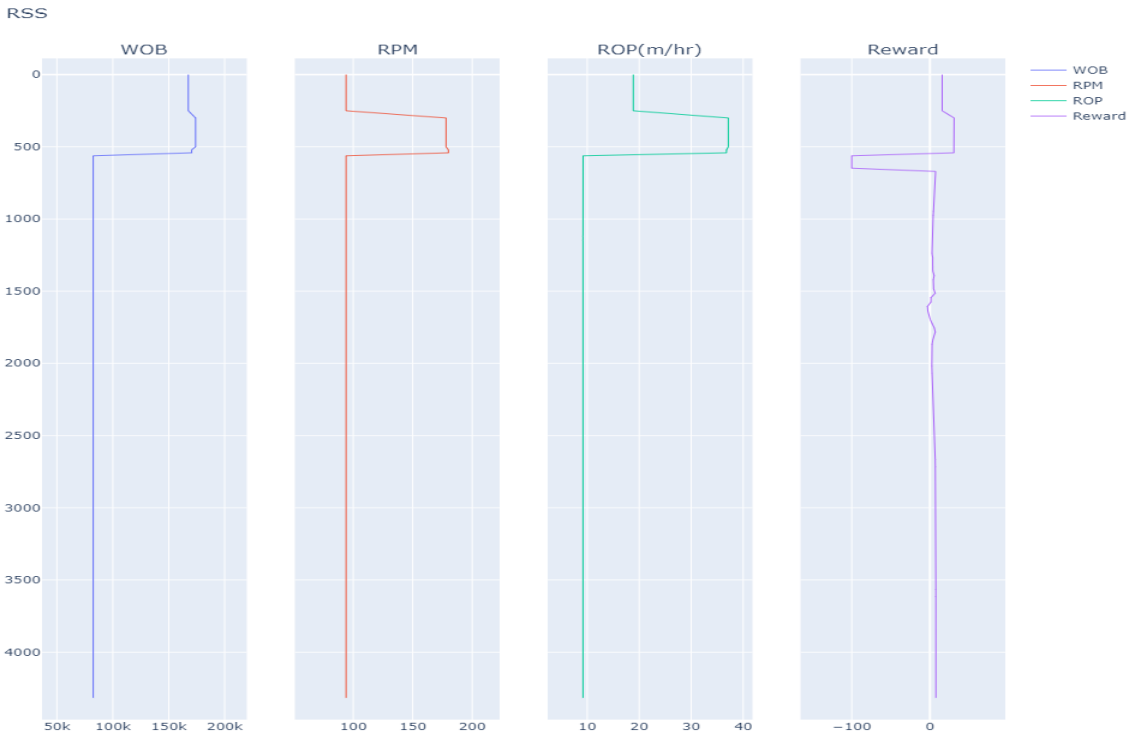

Figure 4.17: DQN agent observation and outputs with respect to depth.

4.2.2. “S” Shape Well with both PPO and DQN Agent

For this case there was no training established before simulation. The trained agent from J shape well used to simulate this type of well. To simulate this well, environment inside Reinforcement Learning Toolbox changed from J shape to S shape.

The PPO agent simulations show a good performance to match with planned path. However, after kick off point RSS simulator could not follow ellipse guidance till drop section. Even with this result, PPO agent performance is much better than DQN agent in terms of path mapping (Figure 4.18 & 4.19).

Interestingly, even without good match, DQN agent showed much better performance for ROP of RSS simulator. On the contrary, PPO agent simulation has consistent and low ROP during the simulation (Figure 4.20 & 4.21).

The result table of Figure 4.20 & 4.21 detailly given in appendix D.

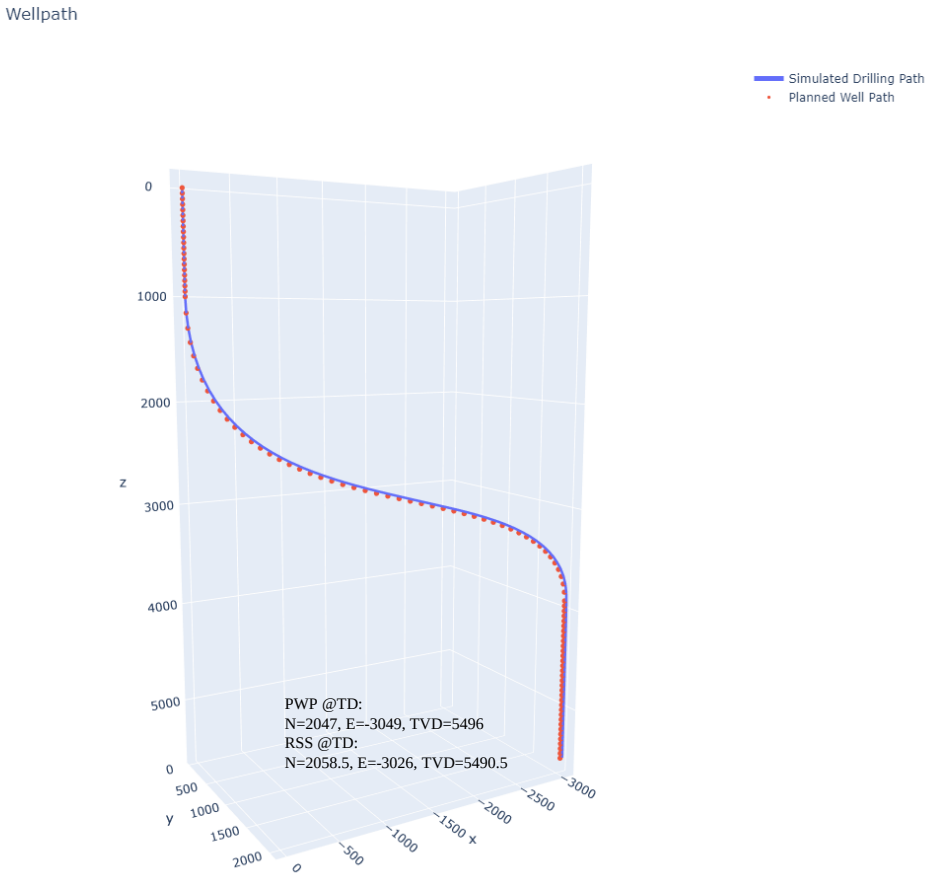

Figure 4.18: 3D view of Planned Well Path vs Path by RSS Simulator for PPO Agent with S Type Well.

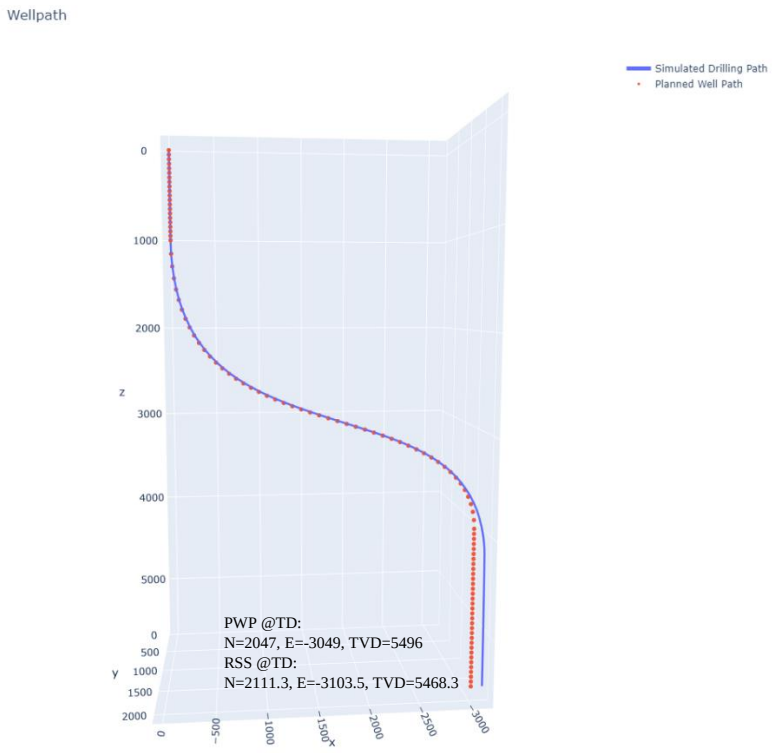

Figure 4.19: 3D view of Planned Well Path vs Path by RSS Simulator for DQN Agent with S Type Well.

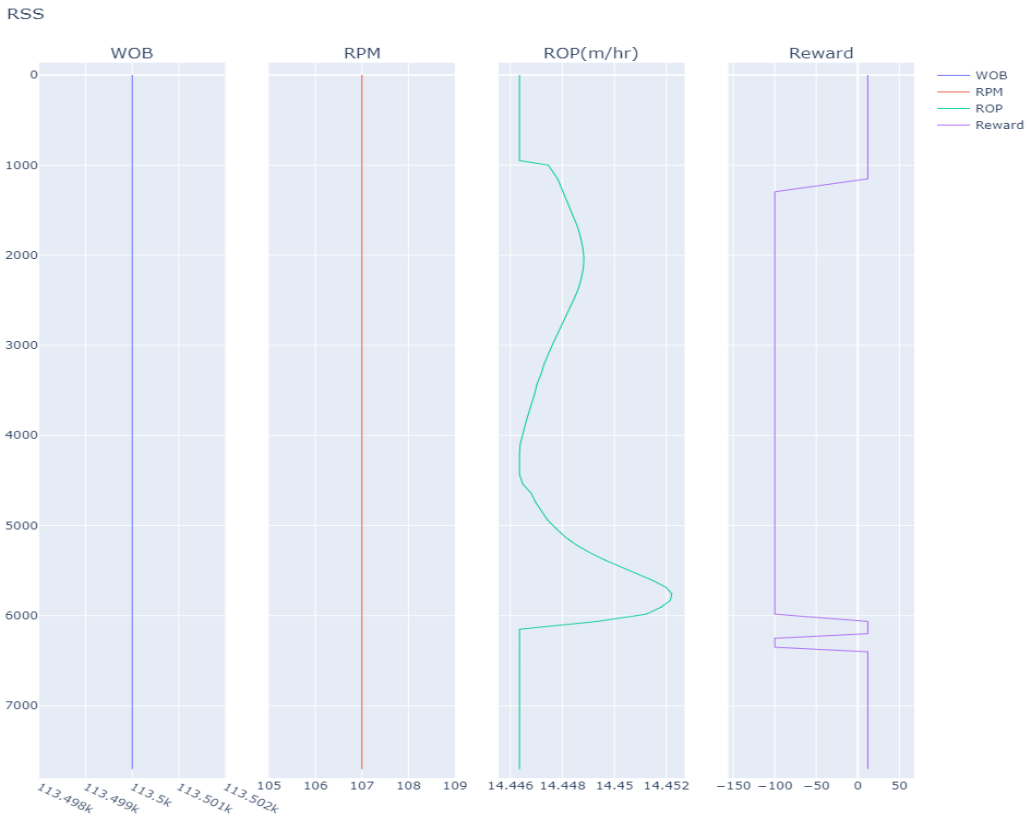

Figure 4.20: PPO agent observation and outputs with respect to depth.

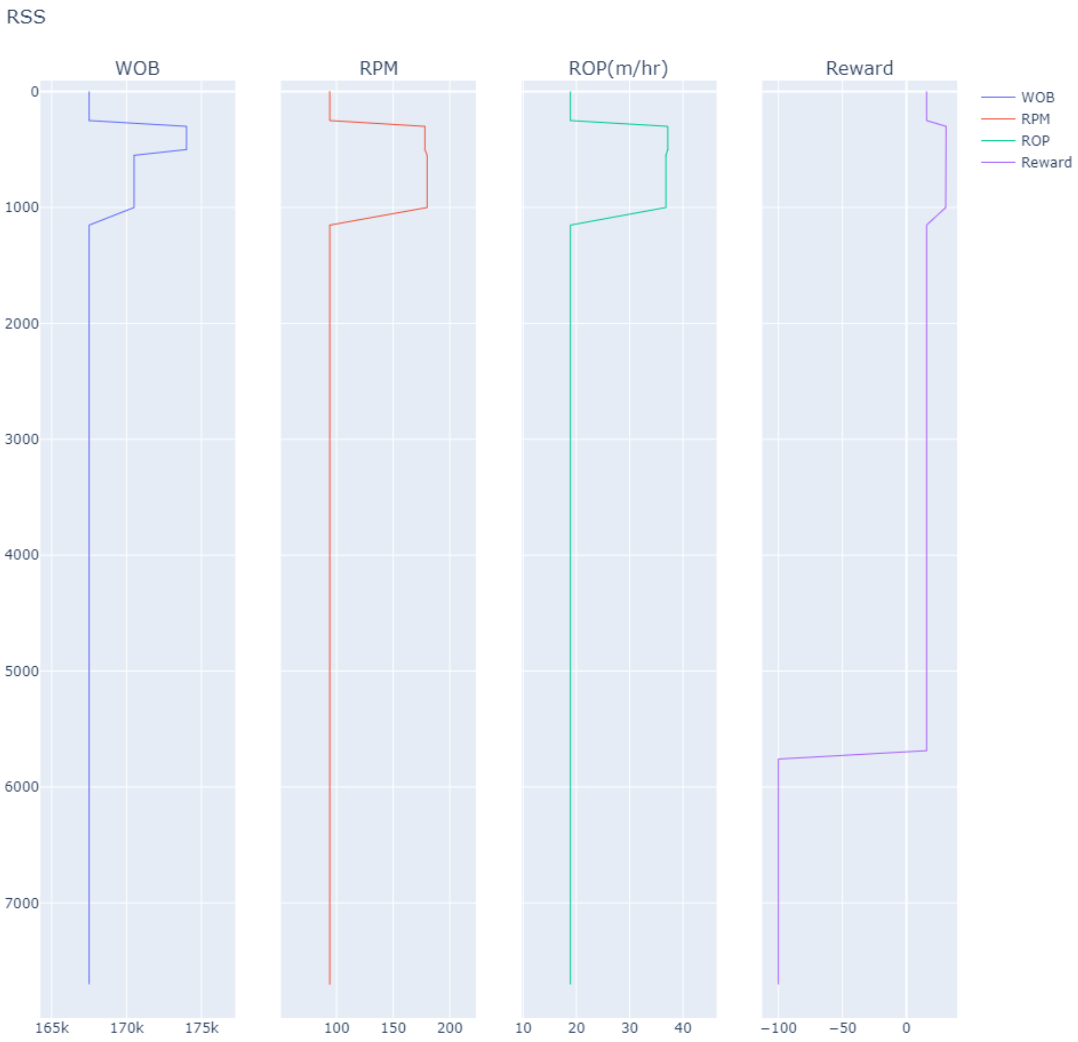

Figure 4.21: DQN agent observation and outputs with respect to depth.

4.2.3. Complex Shape Well with both PPO and DQN Agent

For this case there was no training established before simulation. The trained agent from J shape well used to simulate this type of well. To simulate this well, environment inside Reinforcement Learning Toolbox changed from J shape to complex shape.

The PPO agent simulations shows weak performance to match with planned path. However, after kick off point RSS simulator could not follow ellipse guidance till target. Even with this result, PPO agent performance is much better than DQN agent in terms of path mapping (Figure 4.22 & 4.23).

Interestingly, even without good match, DQN agent showed much better performance for ROP of RSS simulator. On the contrary, PPO agent simulation has consistent and low ROP during the simulation (Figure 4.24 & 4.25). The result table of Figure 4.24 & 4.25 detailly given in appendix D.

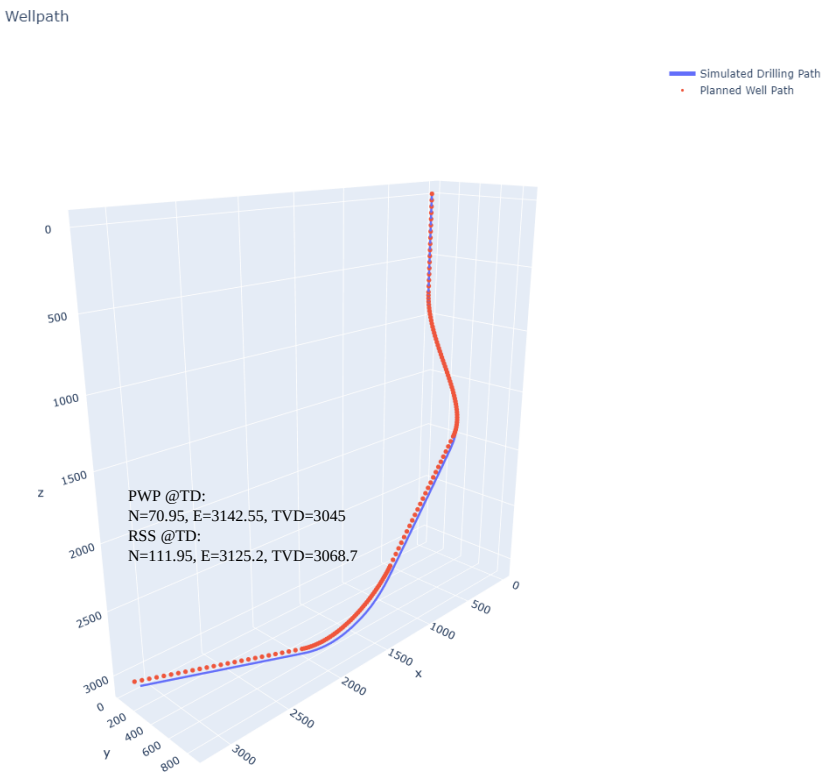

Figure 4.22: 3D view of Planned Well Path vs Path by RSS Simulator for PPO Agent with Complex Shape Well.

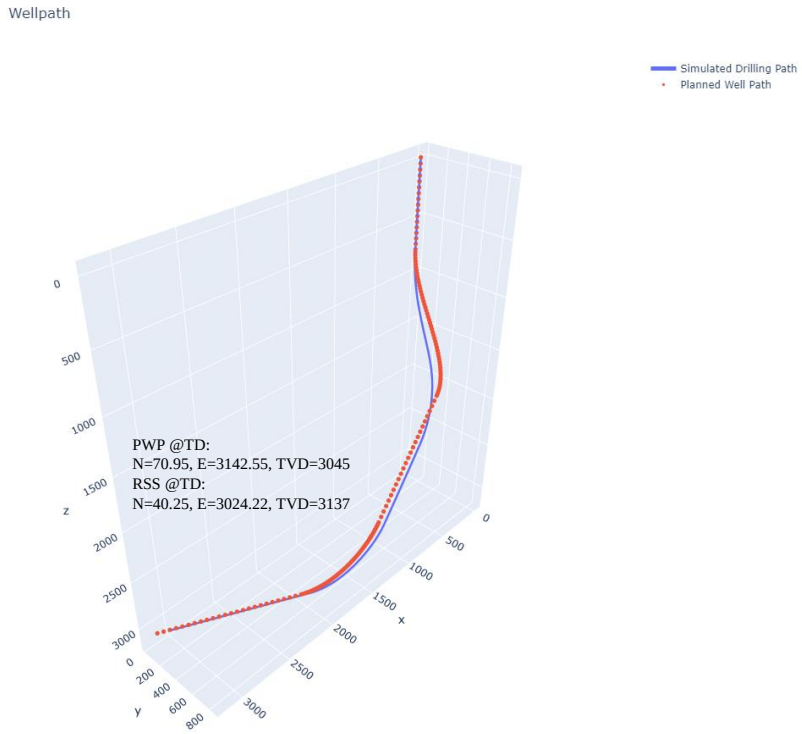

Figure 4.23: 3D view of Planned Well Path vs Path by RSS Simulator for DQN Agent with Complex Shape Well.

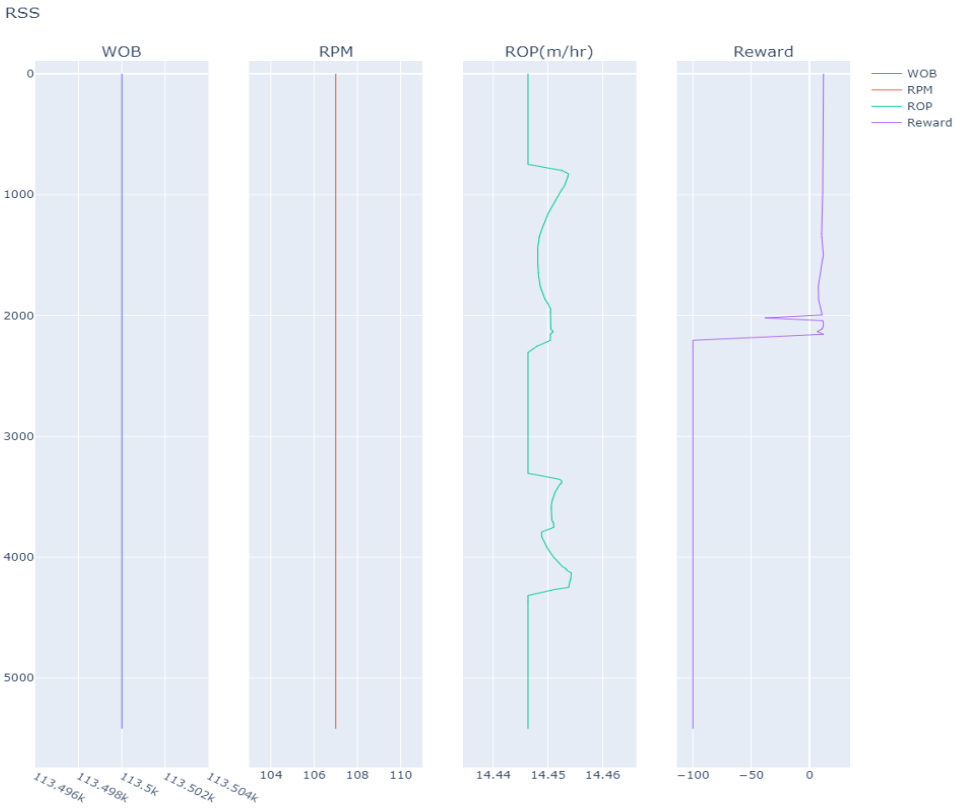

Figure 4.24: PPO agent observation and outputs with respect to depth.

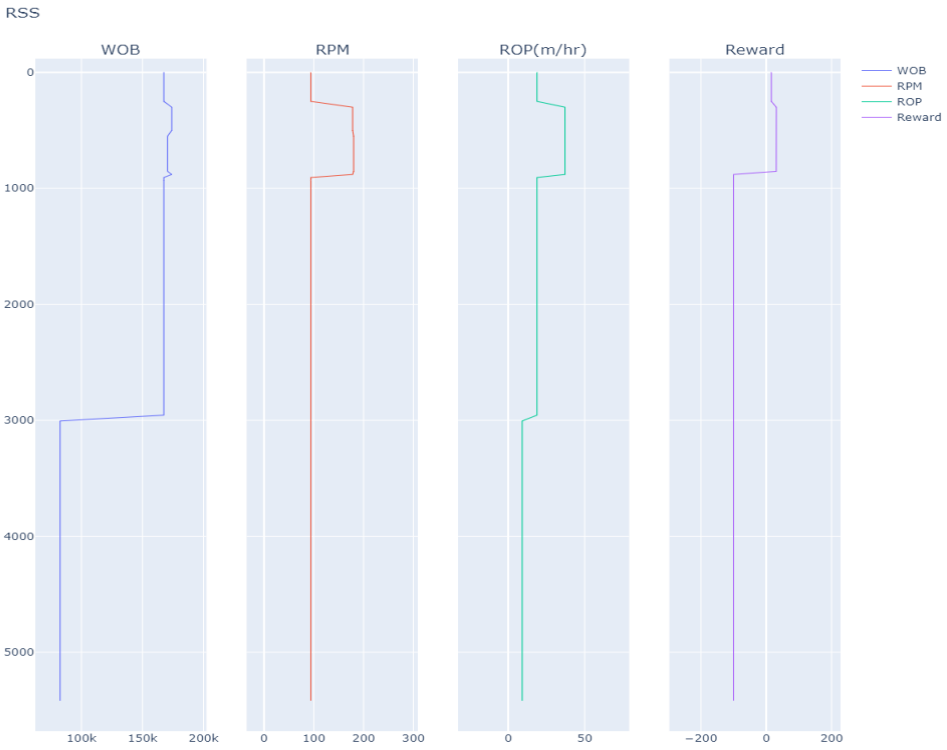

Figure 4.25: DQN agent observation and outputs with respect to depth.

4.3. Discussion

After countless tries and more than 50 days of work on Reinforcement Learning Toolbox of MATLAB, there is significant results obtained. However, the perfect results haven't achieved yet because of many reasons explained detailly below.

- RSS simulator is very complex and prone to errors or faulty results. This causes challenges in learning for agents.
- Ellipses matrix selection is not stable because there is no physical experience or source for selection.
- Structure and behavior of agents is almost mystery, it is hard to optimize their learning and behavior according to each case. Because they are not always giving correlated outcomes.
- Reward function is not mature enough to push agents to learn with optimum possibilities and for every condition. Have not had chance to try, but higher episode numbers give a good result with current reward function. Most importantly, the weight of each element in reward function should be arranged precisely and should be well tested.
- To increase the episode number could boost the performance of trainings. However, it is necessary to develop computationally cheap algorithms for RSS simulator.

Also, as mentioned in section 4.1.2 tool face angle and DLS values are excluded from observation space. Because these parameters are causing problem to learn of agents. They cannot figure out the logic behind of this parameter.

5. Conclusion and Future Work

The synthesis of RSS model with Reinforcement Learning environment did not give perfect results. However, the results of analysis are very promising to make RSS simulator enhanced with optimized parameters.

One of the core objectives of this work, following planned path and reach target point with minimum deviation with parameter optimization during RSS simulation is running. To optimize WOB and RPM reinforcement learning is the sole responsible algorithm inside the structure. Also, improvement in these two parameters not only helps trajectory control also increase the performance of drilling operation as simulated by RSS model.

However, the base of this structure starts with establishing smoothest and shortest path designed by PWP function by using the given survey points. This unique function developed by Jerez in 2021, make the base of structure available.

On the top of the base, in other words the PWP, RSS model and RL environment works with an incredible harmony. This harmony constructs unique environment for this study with promising results and milestone for future research in this area.

Besides, this structure gives some important information and results for the base cases. Training of J shape well and simulation of this well gave important results in terms of well path control and ROP performance. However, testing these trained agents on other well shapes do not show the same performance especially, path control side. There are multiple reasons behind of it, but algorithms should be tuned for more sensitive trainings.

Most important challenge of simulations in Reinforcement Learning module is time demand. This problem prevents both deterministic results and further improvements in this study. However, with the improvement in computational cost of RSS simulator and RL environment increase performance tremendously.

5.1. Future Work

The RSS module developed at University of Stavanger in 2021 is open to further enhancement and open to cooperate with other type of environments like Reinforcement Learning.

In this work, synthesis of RL and RSS model opened multiple doors for new research. The RL environment developed in this study put RSS simulator in a good shape to ease for future works. Some of the topics can be constructed over this work as named:

- Increasing time efficiency of RSS module to be able to make quick training for RL agents.
- Convert action space to continuous action space with finding a way to limit the intervals.
- Training for different shapes and comparing results of simulations with each other.
- Manipulating more parameters as action from RL environment.
- Adding control knowledge to this work, could make available to manipulate/control RSS tool actuators via RL agent.
- Making performance analysis for ROP and preventing possible incidents like preventing high DLS and tool face angle changes.

6. References

Adams, N., and T. Charrier, 1985, Drilling Engineering: A Complete Well Planning Approach: Tulsa, Okla, PennWell Pub. Co, 960 p.

Bourgoyne, A. T. (ed.), 1986, Applied Drilling Engineering: Richardson, TX, Society of Petroleum Engineers, SPE textbook series vol. 2, 502 p.

Esmaeili, A., B. Elahifar, R. K. Fruhwirth, and G. Thonhauser, 2012, ROP Modeling Using Neural Network and Drill String Vibration Data, *in* All Days, SPE Kuwait International Petroleum Conference and Exhibition, Kuwait City, Kuwait: SPE, p. SPE-163330-MS, doi:10.2118/163330-MS.

Farah, F. O., n.d., Directional Well Design, Trajectory and Survey Calculations, With A Case Study in Fiale, Asal Rift, Djibouti: p. 34.

Hegde, C., C. Soares, and K. E. Gray, 2018, Rate of Penetration (ROP) Modelling Using Hybrid Models: Deterministic and Machine Learning, *in* Proceedings of the 6th Unconventional Resources Technology Conference, Unconventional Resources Technology Conference, Houston, Texas, USA: American Association of Petroleum Geologists, doi:10.15530/urtec-2018-2896522.

Jerez, L. A. S., 2021, Trajectory Control Optimization Using the RSS Model, Master's: University of Stavanger, Stavanger, Norway, 138 p.

Joshi, D. R., and R. Samuel, 2017a, Automated Geometric Path Correction in Directional Drilling, *in* Day 2 Tue, October 10, 2017, SPE Annual Technical Conference and Exhibition, San Antonio, Texas, USA: SPE, p. D021S024R003, doi:10.2118/187209-MS.

Joshi, D. R., and R. Samuel, 2017b, Automated Geometric Path Correction in Directional Drilling, *in* Day 2 Tue, October 10, 2017, SPE Annual Technical Conference and Exhibition, San Antonio, Texas, USA: SPE, p. D021S024R003, doi:10.2118/187209-MS.

Kuznetcov, A., 2016, ROP Optimization and Modelling in Directional Drilling Process, Master's: University of Stavanger, Stavanger, Norway, 105 p.

Li, F., X. Ma, and Y. Tan, 2020, Review of the Development of Rotary Steerable Systems: Journal of Physics: Conference Series, v. 1617, no. 1, p. 012085, doi:10.1088/1742-6596/1617/1/012085.

Liu, Z., and R. Samuel, 2016, Wellbore-Trajectory Control by Use of Minimum Well-Profile-Energy Criterion for Drilling Automation: SPE Journal, v. 21, no. 02, p. 449–458, doi:10.2118/170861-PA.

Create MATLAB Reinforcement Learning Environments, 2022: MATLAB Reinforcement Learning Toolbox. https://se.mathworks.com/help/reinforcement-learning/ug/create-matlab-environments-for-reinforcement-learning.html.

Mitchell, R. F., S. Miska, B. S. Aadnøy, and Society of Petroleum Engineers (U.S.) (eds.), 2011, Fundamentals of Drilling Engineering: Richardson, TX, Society of Petroleum Engineers, SPE textbook series v. 12, 696 p.

Mittal, M., and R. Samuel, 2016, 3D Downhole Drilling Automation Based on Minimum Well Profile Energy, *in* Day 3 Wed, September 28, 2016, SPE Annual Technical Conference and Exhibition, Dubai, UAE: SPE, p. D031S041R001, doi:10.2118/181381-MS.

Nabors Industrıes Ltd., 2021, OrientXpress® Rotary Steering System: Nabor.com https://www.nabors.com/drilling-solutions/directional-automation/automated-wellbore-placement/orientxpress-rotary-steering.

Nkengele, J., 2019, Determination of Dogleg Severity and Side Force for Stuck Pipe Prevention, Master's.

Reinforcement Learning with MATLAB, 2022: The MathWorks Inc.

Ruszka, J., 2003, Rotary Steerable Drilling Technology Matures: Drilling Contractor, v. 59(4), p. 44–45.

Sampaio, J. H. B., 2017, Designing Three-Dimensional Directional Well Trajectories Using Bézier Curves: Journal of Energy Resources Technology, v. 139, no. 3, p. 032901, doi:10.1115/1.4034810.

Saramago, C. P., 2020, Rotary Steerable System Modelling and Simulator, Master's: University of Stavanger, Stavanger, Norway, 111 p.

Sutton, R. S., and A. G. Barto, 2018, Reinforcement Learning: An Introduction, Second edition ed. (revised): Cambridge, Massachusetts, The MIT Press, Adaptive computation and machine learning series, 526 p.

Teale, R., 1965, The Concept of Specific Energy in Rock Drilling: International Journal of Rock Mechanics and Mining Sciences & Geomechanics Abstracts, v. 2, no. 1, p. 57–73, doi:10.1016/0148-9062(65)90022-7.

Wang, H., Z.-C. Guan, Y.-C. Shi, and D.-Y. Liang, n.d., Study on Build-up Rate of Push-the-bit Rotary Steerable Bottom Hole Assembly: p. 8.

Wiktorski, E., A. Kuznetcov, and D. Sui, 2017, ROP Optimization and Modeling in Directional Drilling Process, *in* Day 1 Wed, April 05, 2017, SPE Bergen One Day Seminar, Bergen, Norway: SPE, p. D011S003R002, doi:10.2118/185909-MS.

Willerth, M., 2016, How Much Ellipse Do You Need? p. 11.

Yu, Y., W. Chen, Q. Liu, M. Chau, V. Vesselinov, and R. Meehan, 2021, Training an Automated Directional Drilling Agent with Deep Reinforcement Learning in a Simulated Environment, *in* Day 4 Thu, March 11, 2021, SPE/IADC International Drilling Conference and Exhibition, Virtual: SPE, p. D041S013R002, doi:10.2118/204105-MS.

Appendix A

Data Inputs and Outputs

Simulators usually manage many parameters simultaneously; for that reason, it is helpful to organize the different variables that are going to be asked to the user, obtained from the survey stations file, or transferred from other models. As a result, the most relevant inputs and outputs will be shown in a collection of different tables in this section.

Inputs

Table A 1: Relevant Inputs Used in the PWP Module

Planned Well Path (PWP)		
Parameter	**Symbol**	**Unit**
Tolerance for consider 2 different segments	$Tolerance$	°
Survey points for the hold section	Sur_{pts}	m
Step for "u" in the Beziér curve calculation	$Step_u$	-
Range tolerance for searching for the best D_S and D_E value	Ran_{Tol}	m
Maximum DLS for the PWP	Max_{DLS}	°/30m

Table A 2: Inputs Used in the RSS Module

RSS Model		
Parameter	**Symbol**	**Unit**
Time step for the Simulation (Resolution)	Δt	s
OD of the RSS tool	OD	m
ID of the RSS tool	ID	m
Distance actuator - bit	a	m
Distance actuator - stabilizer	b	m
Borehole diameter	Db	m
Delta between simulated survey points	$Delta_{Sur}$	m

Error Noise that will be added to the other modules data	$Error_{input}$	-
Maximum opening offset of the tool (0% to 100%)	$maxoff$	-
Elasticity modulus	E	Pa
Maximum physical opening of the offset	$Offset_L$	m
Maximum degree of tolerance for the activation of offset	Max_{deg}	°

Table A 3: Inputs Coming from External Modules

Variables Given by Other Modules (Models)		
Parameter	**Symbol**	**Unit**
Sliding factor coefficient	μ	-
RPM	N	rpm
Weight On Bit (WOB)	WOB	N
Specific energy of the rock	Es	Pa
Steerability of the bit	$alpha$	-

Table A 4: Inputs Imported from the Survey Data Points

Survey Data Points (Excel)		
Parameter	**Symbol**	**Unit**
Vertical coordinate	V	m
North coordinate	N	m
East coordinate	E	M

Outputs

Table 2.5: Outputs from the PWP module

Planned Well Path (PWP)		
Parameter	**Symbol**	**Unit**
Vertical coordinate	V	m
North coordinate	N	m
East coordinate	E	m
Measured depth	MD	m
Inclination	Inc	°
Azimuth	Azi	°
Dogleg Severity	DLS	°/30m

Table 2.6: Outputs from the RSS Module

Simulation Results		
Parameter	**Symbol**	**Unit**
Measure depth	MD	m
Time	t	min
Inclination	Inc	°
Azimuth	Azi	°
Horizontal Displacement	HD	m
True Vertical Depth	TVD	m
East coordinate	E	m
North coordinate	N	m
Offset applied (percentage of opening of the actuator)	$Offset$	-
Dog Leg Severity	DLS	°/30m

Total force on the bit for the inclination	$Tot\ F_{Inc}$	N
Total force on the bit for the azimuth	$Tot\ F_{Azi}$	N
ROP axial	ROP_{Axial}	m/hr
ROP inclination	ROP_{Inc}	m/hr
ROP azimuth	ROP_{Azi}	m/hr

Appendix B

Assumption and constraints

According to the Jerez work some assumptions and constraints established by him and indicated below:

The assumptions in the RSS Simulator are the following modified from Jerez (2021):

- The maximum length of the opening of the actuator or offset of the OrientXpress® RSS BHA tool is 6 mm.
- The u value used in the Bezier function is 0.05 when the optimizer is called.
- The maximum DLS of the BHA tool is 15 °/30m.
- The BHA tool is located just after the bit, so there is no necessity of bit projection prediction.
- The simulation follows a planned trajectory because it is assumed that the trajectory is given after some geological considerations have been discussed before initiating the drilling operations.
- The study cases use some constant external parameters (2.3) since at the moment of the creation of the thesis, the rest of the models of the Real-Time Drilling Simulator are not finished yet.

The limitations or constraints of the RSS Simulator are the following modified from Jerez (2021):

- The survey points input should be arranged in the next order: Vertical, North, and East.
- There must be at least 3 points indicating a holding section in the survey points given and at least 2 points in for indicating a curvature section.
- The gravity and reactive torque have not been taken into count in the forces affecting the bit direction.
- The first and last section of the well should be a hold section.
- The planned trajectory cannot be updated or changed after the simulation has started.
- The formation information was not considered in the simulation, which should be improved in future work with the simulator.
- The simulator did not use a BHA model that might be a good added feature in the future development.

Appendix C

Table for planned well path and radius of ellipses used in training and simulation sessions for agents given below:

PWP and Ellipse Data for J Shape Well

Index	V[m]	N[m]	E[m]	MD[m]	Inc [°]		DLS	r_N[m]	r_E[m]	r_V[m]
1	0.00	0.00	0.00	0.00	0.00	0.00	0.00	1.00	1.00	1.00
2	50.00	0.00	0.00	50.00	0.00	0.00	0.00	1.20	1.20	1.20
3	100.00	0.00	0.00	100.00	0.00	0.00	0.00	1.40	1.40	1.40
4	150.00	0.00	0.00	150.00	0.00	0.00	0.00	1.60	1.60	1.60
5	200.00	0.00	0.00	200.00	0.00	0.00	0.00	1.80	1.80	1.80
6	250.00	0.00	0.00	250.00	0.00	0.00	0.00	2.00	2.00	2.00
7	300.00	0.00	0.00	300.00	0.00	0.00	0.00	2.20	2.20	2.20
8	350.00	0.00	0.00	350.00	0.00	0.00	0.00	2.40	2.40	2.40
9	400.00	0.00	0.00	400.00	0.00	0.00	0.00	2.60	2.60	2.60
10	450.00	0.00	0.00	450.00	0.00	0.00	0.00	2.80	2.80	2.80
11	500.00	0.00	0.00	500.00	0.00	0.00	5.27	3.00	3.00	3.00
12	520.45	-0.50	0.38	520.46	3.52	142.80	5.05	3.20	3.20	3.20
13	540.95	-2.00	1.52	541.05	6.91	142.76	4.80	3.40	3.40	3.40
14	561.51	-4.45	3.39	561.84	10.13	142.72	4.51	3.60	3.60	3.60
15	582.12	-7.84	5.97	582.88	13.19	142.68	4.21	3.80	3.80	3.80
16	602.77	-12.14	9.24	604.23	16.08	142.64	3.91	4.00	4.00	4.00
17	623.46	-17.31	13.19	625.91	18.79	142.59	3.60	4.20	4.20	4.20
18	644.18	-23.32	17.80	647.98	21.34	142.55	3.31	4.40	4.40	4.40
19	664.93	-30.16	23.04	670.45	23.71	142.50	3.03	4.60	4.60	4.60
20	685.71	-37.78	28.89	693.34	25.93	142.45	2.77	4.80	4.80	4.80
21	706.51	-46.17	35.35	716.68	27.99	142.40	2.53	5.00	5.00	5.00
22	727.32	-55.29	42.38	740.46	29.91	142.35	2.31	5.20	5.20	5.20
23	748.14	-65.12	49.97	764.71	31.69	142.30	2.10	5.40	5.40	5.40
24	768.97	-75.63	58.10	789.41	33.34	142.24	1.92	5.60	5.60	5.60
25	789.80	-86.78	66.75	814.57	34.88	142.18	1.75	5.80	5.80	5.80
26	810.62	-98.55	75.89	840.18	36.30	142.12	1.59	6.00	6.00	6.00
27	831.44	-110.92	85.52	866.23	37.63	142.06	1.46	6.20	6.20	6.20
28	852.24	-123.84	95.61	892.72	38.85	142.00	1.33	6.40	6.40	6.40
29	873.02	-137.30	106.14	919.63	39.99	141.93	1.22	6.60	6.60	6.60
30	893.78	-151.27	117.09	946.94	41.05	141.87	1.11	6.80	6.80	6.80
31	914.51	-165.72	128.45	974.64	42.03	141.79	1.02	7.00	7.00	7.00
32	935.21	-180.61	140.19	1002.72	42.94	141.72	0.93	7.20	7.20	7.20
33	955.88	-195.93	152.29	1031.14	43.79	141.65	0.85	7.40	7.40	7.40
34	976.50	-211.63	164.73	1059.90	44.57	141.57	0.78	7.60	7.60	7.60
35	997.07	-227.70	177.51	1088.96	45.29	141.49	0.72	7.80	7.80	7.80

36	1017.59	-244.11	190.58	1118.31	45.96	141.40	0.66	8.00	8.00	8.00
37	1038.06	-260.82	203.95	1147.92	46.58	141.31	0.60	8.20	8.20	8.20
38	1058.46	-277.82	217.58	1177.77	47.15	141.22	0.55	8.40	8.40	8.40
39	1078.80	-295.06	231.45	1207.82	47.68	141.12	0.51	8.60	8.60	8.60
40	1099.07	-312.52	245.56	1238.07	48.16	141.02	0.46	8.80	8.80	8.80
41	1119.27	-330.18	259.87	1268.47	48.60	140.92	0.42	9.00	9.00	9.00
42	1139.38	-348.00	274.37	1299.01	49.00	140.81	0.38	9.20	9.20	9.20
43	1159.41	-365.95	289.05	1329.65	49.36	140.69	0.35	9.40	9.40	9.40
44	1179.35	-384.02	303.87	1360.37	49.69	140.57	0.31	9.60	9.60	9.60
45	1199.19	-402.16	318.82	1391.13	49.98	140.44	0.28	9.80	9.80	9.80
46	1218.94	-420.35	333.88	1421.92	50.23	140.31	0.25	10.00	10.00	10.00
47	1238.58	-438.57	349.04	1452.70	50.45	140.17	0.23	10.20	10.20	10.20
48	1258.11	-456.78	364.27	1483.44	50.64	140.02	0.20	10.40	10.40	10.40
49	1277.53	-474.96	379.55	1514.12	50.80	139.86	0.18	10.60	10.60	10.60
50	1296.83	-493.07	394.87	1544.70	50.92	139.70	0.17	10.80	10.80	10.80
51	1316.01	-511.09	410.20	1575.15	51.01	139.53	0.16	11.00	11.00	11.00
52	1335.06	-528.99	425.52	1605.46	51.07	139.34	0.15	11.20	11.20	11.20
53	1353.98	-546.74	440.82	1635.57	51.10	139.14	0.16	11.40	11.40	11.40
54	1372.76	-564.32	456.08	1665.48	51.09	138.94	0.17	11.60	11.60	11.60
55	1391.40	-581.69	471.27	1695.15	51.05	138.71	0.19	11.80	11.80	11.80
56	1409.90	-598.82	486.38	1724.54	50.97	138.48	0.22	12.00	12.00	12.00
57	1428.24	-615.70	501.38	1753.63	50.85	138.22	0.25	12.20	12.20	12.20
58	1446.43	-632.28	516.27	1782.39	50.70	137.95	0.29	12.40	12.40	12.40
59	1464.45	-648.54	531.01	1810.80	50.51	137.66	0.34	12.60	12.60	12.60
60	1482.31	-664.46	545.60	1838.81	50.28	137.34	0.39	12.80	12.80	12.80
61	1500.00	-680.00	560.00	1866.42	50.00	137.00	0.00	13.00	13.00	13.00
62	1532.14	-708.01	586.12	1916.42	50.00	137.00	0.00	13.20	13.20	13.20
63	1564.28	-736.03	612.24	1966.42	50.00	137.00	0.00	13.40	13.40	13.40
64	1596.42	-764.04	638.37	2016.42	50.00	137.00	0.00	13.60	13.60	13.60
65	1628.56	-792.06	664.49	2066.42	50.00	137.00	0.00	13.80	13.80	13.80
66	1660.70	-820.07	690.61	2116.42	50.00	137.00	0.00	14.00	14.00	14.00
67	1692.84	-848.09	716.73	2166.42	50.00	137.00	0.00	14.20	14.20	14.20
68	1724.98	-876.10	742.85	2216.42	50.00	137.00	0.00	14.40	14.40	14.40
69	1757.12	-904.11	768.98	2266.42	50.00	137.00	0.00	14.60	14.60	14.60
70	1789.25	-932.13	795.10	2316.42	50.00	137.00	0.00	14.80	14.80	14.80
71	1821.39	-960.14	821.22	2366.42	50.00	137.00	0.00	15.00	15.00	15.00
72	1853.53	-988.16	847.34	2416.42	50.00	137.00	0.00	15.20	15.20	15.20
73	1885.67	-1016.17	873.46	2466.42	50.00	137.00	0.00	15.40	15.40	15.40
74	1917.81	-1044.19	899.59	2516.42	50.00	137.00	0.00	15.60	15.60	15.60
75	1949.95	-1072.20	925.71	2566.42	50.00	137.00	0.00	15.80	15.80	15.80
76	1982.09	-1100.21	951.83	2616.42	50.00	137.00	0.00	16.00	16.00	16.00
77	2014.23	-1128.23	977.95	2666.42	50.00	137.00	0.00	16.20	16.20	16.20
78	2046.37	-1156.24	1004.07	2716.42	50.00	137.00	0.00	16.40	16.40	16.40

79	2078.51	-1184.26	1030.20	2766.42	50.00	137.00	0.00	16.60	16.60	16.60
80	2110.65	-1212.27	1056.32	2816.42	50.00	137.00	0.00	16.80	16.80	16.80
81	2142.79	-1240.28	1082.44	2866.42	50.00	137.00	0.00	17.00	17.00	17.00
82	2174.93	-1268.30	1108.56	2916.42	50.00	137.00	0.00	17.20	17.20	17.20
83	2207.07	-1296.31	1134.69	2966.42	50.00	137.00	0.00	17.40	17.40	17.40
84	2239.21	-1324.33	1160.81	3016.42	50.00	137.00	0.00	17.60	17.60	17.60
85	2271.35	-1352.34	1186.93	3066.42	50.00	137.00	0.00	17.80	17.80	17.80
86	2303.48	-1380.36	1213.05	3116.42	50.00	137.00	0.00	18.00	18.00	18.00
87	2335.62	-1408.37	1239.17	3166.42	50.00	137.00	0.00	18.20	18.20	18.20
88	2367.76	-1436.38	1265.30	3216.42	50.00	137.00	0.00	18.40	18.40	18.40
89	2399.90	-1464.40	1291.42	3266.42	50.00	137.00	0.00	18.60	18.60	18.60
90	2432.04	-1492.41	1317.54	3316.42	50.00	137.00	0.00	18.80	18.80	18.80
91	2464.18	-1520.43	1343.66	3366.42	50.00	137.00	0.00	19.00	19.00	19.00
92	2496.32	-1548.44	1369.78	3416.42	50.00	137.00	0.00	19.20	19.20	19.20
93	2528.46	-1576.46	1395.91	3466.42	50.00	137.00	0.00	19.40	19.40	19.40
94	2560.60	-1604.47	1422.03	3516.42	50.00	137.00	0.00	19.60	19.60	19.60
95	2592.74	-1632.48	1448.15	3566.42	50.00	137.00	0.00	19.80	19.80	19.80
96	2624.88	-1660.50	1474.27	3616.42	50.00	137.00	0.00	20.00	20.00	20.00
97	2657.02	-1688.51	1500.39	3666.42	50.00	137.00	0.00	20.20	20.20	20.20
98	2689.16	-1716.53	1526.52	3716.42	50.00	137.00	0.00	20.40	20.40	20.40
99	2721.30	-1744.54	1552.64	3766.42	50.00	137.00	0.00	20.60	20.60	20.60
100	2753.44	-1772.56	1578.76	3816.42	50.00	137.00	0.00	20.80	20.80	20.80
101	2785.58	-1800.57	1604.88	3866.42	50.00	137.00	0.00	21.00	21.00	21.00
102	2817.71	-1828.58	1631.00	3916.42	50.00	137.00	0.00	21.20	21.20	21.20
103	2849.85	-1856.60	1657.13	3966.42	50.00	137.00	0.00	21.40	21.40	21.40
104	2881.99	-1884.61	1683.25	4016.42	50.00	137.00	0.00	21.60	21.60	21.60
105	2914.13	-1912.63	1709.37	4066.42	50.00	137.00	0.00	21.80	21.80	21.80
106	2946.27	-1940.64	1735.49	4116.42	50.00	137.00	0.00	22.00	22.00	22.00
107	2978.41	-1968.66	1761.61	4166.42	50.00	137.00	0.00	22.20	22.20	22.20
108	3010.55	-1996.67	1787.74	4216.42	50.00	137.00	0.00	22.40	22.40	22.40
109	3042.69	-2024.68	1813.86	4266.42	50.00	137.00	0.00	22.60	22.60	22.60
110	3074.83	-2052.70	1839.98	4316.42	50.00	137.00	0.00	22.80	22.80	22.80
111	3106.97	-2080.62	1866.10	4366.37	50.00	137.00	0.00	23.00	23.00	23.00

PWP and Ellipse Data for S Shape Well

Index	V[m]	N[m]	E[m]	MD[m]	Inc [°]	Azi [°]	DLS	r_N[m]	r_E[m]	r_V[m]
1	0.00	0.00	0.00	0.00	0.00	0.00	0.00	1.00	1.00	1.00
2	50.00	0.00	0.00	50.00	0.00	0.00	0.00	1.20	1.20	1.20
3	100.00	0.00	0.00	100.00	0.00	0.00	0.00	1.40	1.40	1.40
4	150.00	0.00	0.00	150.00	0.00	0.00	0.00	1.60	1.60	1.60
5	200.00	0.00	0.00	200.00	0.00	0.00	0.00	1.80	1.80	1.80
6	250.00	0.00	0.00	250.00	0.00	0.00	0.00	2.00	2.00	2.00

7	300.00	0.00	0.00	300.00	0.00	0.00	0.00	2.20	2.20	2.20
8	350.00	0.00	0.00	350.00	0.00	0.00	0.00	2.40	2.40	2.40
9	400.00	0.00	0.00	400.00	0.00	0.00	0.00	2.60	2.60	2.60
10	450.00	0.00	0.00	450.00	0.00	0.00	0.00	2.80	2.80	2.80
11	500.00	0.00	0.00	500.00	0.00	0.00	0.00	3.00	3.00	3.00
12	550.00	0.00	0.00	550.00	0.00	0.00	0.00	3.20	3.20	3.20
13	600.00	0.00	0.00	600.00	0.00	0.00	0.00	3.40	3.40	3.40
14	650.00	0.00	0.00	650.00	0.00	0.00	0.00	3.60	3.60	3.60
15	700.00	0.00	0.00	700.00	0.00	0.00	0.00	3.80	3.80	3.80
16	750.00	0.00	0.00	750.00	0.00	0.00	0.00	4.00	4.00	4.00
17	800.00	0.00	0.00	800.00	0.00	0.00	0.00	4.20	4.20	4.20
18	850.00	0.00	0.00	850.00	0.00	0.00	0.00	4.40	4.40	4.40
19	900.00	0.00	0.00	900.00	0.00	0.00	0.00	4.60	4.60	4.60
20	950.00	0.00	0.00	950.00	0.00	0.00	0.00	4.80	4.80	4.80
21	1000.00	0.00	0.00	1000.00	0.00	0.00	0.61	5.00	5.00	5.00
22	1152.17	2.42	-3.56	1152.23	3.32	304.23	0.70	5.20	5.20	5.20
23	1295.49	9.56	-14.06	1296.11	6.88	304.23	0.79	5.40	5.40	5.40
24	1430.26	21.22	-31.20	1432.47	10.68	304.23	0.88	5.60	5.60	5.60
25	1556.80	37.21	-54.69	1562.16	14.70	304.23	0.98	5.80	5.80	5.80
26	1675.43	57.32	-84.25	1686.06	18.90	304.23	1.06	6.00	6.00	6.00
27	1786.46	81.36	-119.59	1805.03	23.25	304.23	1.13	6.20	6.20	6.20
28	1890.19	109.13	-160.42	1919.91	27.69	304.23	1.18	6.40	6.40	6.40
29	1986.94	140.44	-206.44	2031.54	32.15	304.23	1.21	6.60	6.60	6.60
30	2077.04	175.09	-257.38	2140.68	36.58	304.23	1.22	6.80	6.80	6.80
31	2160.78	212.89	-312.94	2248.05	40.90	304.23	1.19	7.00	7.00	7.00
32	2238.48	253.63	-372.83	2354.27	45.06	304.23	1.15	7.20	7.20	7.20
33	2310.45	297.13	-436.76	2459.92	49.01	304.23	1.09	7.40	7.40	7.40
34	2377.02	343.18	-504.45	2565.43	52.72	304.23	1.02	7.60	7.60	7.60
35	2438.48	391.58	-575.61	2671.19	56.16	304.23	0.94	7.80	7.80	7.80
36	2495.16	442.15	-649.94	2777.47	59.33	304.23	0.85	8.00	8.00	8.00
37	2547.37	494.69	-727.17	2884.47	62.21	304.23	0.77	8.20	8.20	8.20
38	2595.41	548.99	-806.99	2992.30	64.82	304.23	0.68	8.40	8.40	8.40
39	2639.61	604.86	-889.12	3101.03	67.16	304.23	0.61	8.60	8.60	8.60
40	2680.28	662.11	-973.28	3210.64	69.24	304.23	0.53	8.80	8.80	8.80
41	2717.72	720.54	-1059.17	3321.06	71.07	304.23	0.46	9.00	9.00	9.00
42	2752.26	779.96	-1146.50	3432.19	72.67	304.23	0.40	9.20	9.20	9.20
43	2784.20	840.15	-1234.99	3543.87	74.05	304.23	0.34	9.40	9.40	9.40
44	2813.86	900.94	-1324.35	3655.94	75.22	304.23	0.28	9.60	9.60	9.60
45	2841.55	962.12	-1414.28	3768.18	76.18	304.23	0.23	9.80	9.80	9.80
46	2867.58	1023.50	-1504.50	3880.36	76.95	304.23	0.18	10.00	10.00	10.00
47	2892.28	1084.88	-1594.72	3992.24	77.52	304.23	0.13	10.20	10.20	10.20
48	2915.94	1146.06	-1684.65	4103.56	77.90	304.23	0.08	10.40	10.40	10.40
49	2938.88	1206.85	-1774.01	4214.04	78.09	304.23	0.03	10.60	10.60	10.60

50	2961.43	1267.04	-1862.50	4323.41	78.09	304.23	0.03	10.80	10.80	10.80
51	2983.88	1326.46	-1949.83	4431.40	77.88	304.23	0.09	11.00	11.00	11.00
52	3006.55	1384.89	-2035.72	4537.72	77.46	304.23	0.15	11.20	11.20	11.20
53	3029.76	1442.14	-2119.88	4642.12	76.81	304.23	0.22	11.40	11.40	11.40
54	3053.82	1498.01	-2202.01	4744.33	75.92	304.23	0.30	11.60	11.60	11.60
55	3079.04	1552.31	-2281.83	4844.11	74.75	304.23	0.40	11.80	11.80	11.80
56	3105.74	1604.85	-2359.06	4941.25	73.29	304.23	0.51	12.00	12.00	12.00
57	3134.22	1655.42	-2433.39	5035.56	71.49	304.23	0.64	12.20	12.20	12.20
58	3164.81	1703.82	-2504.55	5126.89	69.31	304.23	0.80	12.40	12.40	12.40
59	3197.80	1749.87	-2572.24	5215.16	66.70	304.23	0.98	12.60	12.60	12.60
60	3233.53	1793.37	-2636.17	5300.34	63.61	304.23	1.20	12.80	12.80	12.80
61	3272.29	1834.11	-2696.06	5382.50	59.97	304.23	1.46	13.00	13.00	13.00
62	3314.41	1871.91	-2751.62	5461.80	55.74	304.23	1.75	13.20	13.20	13.20
63	3360.19	1906.56	-2802.56	5538.56	50.89	304.23	2.05	13.40	13.40	13.40
64	3409.95	1937.87	-2848.58	5613.22	45.40	304.23	2.35	13.60	13.60	13.60
65	3464.01	1965.64	-2889.41	5686.43	39.32	304.23	2.61	13.80	13.80	13.80
66	3522.67	1989.68	-2924.75	5759.01	32.77	304.23	2.78	14.00	14.00	14.00
67	3586.25	2009.79	-2954.31	5831.95	25.92	304.23	2.82	14.20	14.20	14.20
68	3655.06	2025.78	-2977.80	5906.40	19.00	304.23	2.72	14.40	14.40	14.40
69	3729.41	2037.44	-2994.94	5983.59	12.25	304.23	2.50	14.60	14.60	14.60
70	3809.62	2044.58	-3005.44	6064.80	5.87	304.23	2.20	14.80	14.80	14.80
71	3896.00	2047.00	-3009.00	6151.28	0.00	0.00	0.00	15.00	15.00	15.00
72	3946.00	2047.00	-3009.00	6201.28	0.00	0.00	0.00	15.20	15.20	15.20
73	3996.00	2047.00	-3009.00	6251.28	0.00	0.00	0.00	15.40	15.40	15.40
74	4046.00	2047.00	-3009.00	6301.28	0.00	0.00	0.00	15.60	15.60	15.60
75	4096.00	2047.00	-3009.00	6351.28	0.00	0.00	0.00	15.80	15.80	15.80
76	4146.00	2047.00	-3009.00	6401.28	0.00	0.00	0.00	16.00	16.00	16.00
77	4196.00	2047.00	-3009.00	6451.28	0.00	0.00	0.00	16.20	16.20	16.20
78	4246.00	2047.00	-3009.00	6501.28	0.00	0.00	0.00	16.40	16.40	16.40
79	4296.00	2047.00	-3009.00	6551.28	0.00	0.00	0.00	16.60	16.60	16.60
80	4346.00	2047.00	-3009.00	6601.28	0.00	0.00	0.00	16.80	16.80	16.80
81	4396.00	2047.00	-3009.00	6651.28	0.00	0.00	0.00	17.00	17.00	17.00
82	4446.00	2047.00	-3009.00	6701.28	0.00	0.00	0.00	17.20	17.20	17.20
83	4496.00	2047.00	-3009.00	6751.28	0.00	0.00	0.00	17.40	17.40	17.40
84	4546.00	2047.00	-3009.00	6801.28	0.00	0.00	0.00	17.60	17.60	17.60
85	4596.00	2047.00	-3009.00	6851.28	0.00	0.00	0.00	17.80	17.80	17.80
86	4646.00	2047.00	-3009.00	6901.28	0.00	0.00	0.00	18.00	18.00	18.00
87	4696.00	2047.00	-3009.00	6951.28	0.00	0.00	0.00	18.20	18.20	18.20
88	4746.00	2047.00	-3009.00	7001.28	0.00	0.00	0.00	18.40	18.40	18.40
89	4796.00	2047.00	-3009.00	7051.28	0.00	0.00	0.00	18.60	18.60	18.60
90	4846.00	2047.00	-3009.00	7101.28	0.00	0.00	0.00	18.80	18.80	18.80
91	4896.00	2047.00	-3009.00	7151.28	0.00	0.00	0.00	19.00	19.00	19.00
92	4946.00	2047.00	-3009.00	7201.28	0.00	0.00	0.00	19.20	19.20	19.20

93	4996.00	2047.00	-3009.00	7251.28	0.00	0.00	0.00	19.40	19.40	19.40
94	5046.00	2047.00	-3009.00	7301.28	0.00	0.00	0.00	19.60	19.60	19.60
95	5096.00	2047.00	-3009.00	7351.28	0.00	0.00	0.00	19.80	19.80	19.80
96	5146.00	2047.00	-3009.00	7401.28	0.00	0.00	0.00	20.00	20.00	20.00
97	5196.00	2047.00	-3009.00	7451.28	0.00	0.00	0.00	20.20	20.20	20.20
98	5246.00	2047.00	-3009.00	7501.28	0.00	0.00	0.00	20.40	20.40	20.40
99	5296.00	2047.00	-3009.00	7551.28	0.00	0.00	0.00	20.60	20.60	20.60
100	5346.00	2047.00	-3009.00	7601.28	0.00	0.00	0.00	20.80	20.80	20.80
101	5396.00	2047.00	-3009.00	7651.28	0.00	0.00	0.00	21.00	21.00	21.00
102	5446.00	2047.00	-3009.00	7701.28	0.00	0.00	0.00	21.20	21.20	21.20
103	5496.00	2047.00	-3009.00	7751.28	0.00	0.00	0.00	21.40	21.40	21.40

PWP and Ellipse Data for Complex Shape Well

Index	V[m]	N[m]	E[m]	MD[m]	Inc [°]	Azi [°]	DLS	r_N[m]	r_E[m]	r_V[m]
1	0.00	0.00	0.00	0.00	0.00	0.00	0.00	1.00	1.00	1.00
2	50.00	0.00	0.00	50.00	0.00	0.00	0.00	1.20	1.20	1.20
3	100.00	0.00	0.00	100.00	0.00	0.00	0.00	1.40	1.40	1.40
4	150.00	0.00	0.00	150.00	0.00	0.00	0.00	1.60	1.60	1.60
5	200.00	0.00	0.00	200.00	0.00	0.00	0.00	1.80	1.80	1.80
6	250.00	0.00	0.00	250.00	0.00	0.00	0.00	2.00	2.00	2.00
7	300.00	0.00	0.00	300.00	0.00	0.00	0.00	2.20	2.20	2.20
8	350.00	0.00	0.00	350.00	0.00	0.00	0.00	2.40	2.40	2.40
9	400.00	0.00	0.00	400.00	0.00	0.00	0.00	2.60	2.60	2.60
10	450.00	0.00	0.00	450.00	0.00	0.00	0.00	2.80	2.80	2.80
11	500.00	0.00	0.00	500.00	0.00	0.00	0.00	3.00	3.00	3.00
12	550.00	0.00	0.00	550.00	0.00	0.00	0.00	3.20	3.20	3.20
13	600.00	0.00	0.00	600.00	0.00	0.00	0.00	3.40	3.40	3.40
14	650.00	0.00	0.00	650.00	0.00	0.00	0.00	3.60	3.60	3.60
15	700.00	0.00	0.00	700.00	0.00	0.00	0.00	3.80	3.80	3.80
16	750.00	0.00	0.00	750.00	0.00	0.00	0.00	4.00	4.00	4.00
17	800.00	0.00	0.00	800.00	0.00	0.00	3.68	4.20	4.20	4.20
18	826.88	0.74	0.23	826.89	3.28	17.06	3.64	4.40	4.40	4.40
19	853.47	2.91	0.90	853.57	6.50	17.30	3.58	4.60	4.60	4.60
20	879.76	6.47	2.01	880.13	9.62	17.54	3.48	4.80	4.80	4.80
21	905.76	11.35	3.57	906.63	12.64	17.80	3.35	5.00	5.00	5.00
22	931.47	17.50	5.56	933.14	15.54	18.06	3.21	5.20	5.20	5.20
23	956.89	24.85	7.98	959.71	18.32	18.34	3.05	5.40	5.40	5.40
24	982.01	33.36	10.82	986.39	20.95	18.63	2.88	5.60	5.60	5.60
25	1006.85	42.96	14.09	1013.22	23.45	18.93	2.71	5.80	5.80	5.80
26	1031.40	53.60	17.77	1040.22	25.80	19.24	2.53	6.00	6.00	6.00
27	1055.66	65.22	21.86	1067.43	28.02	19.57	2.37	6.20	6.20	6.20
28	1079.63	77.76	26.36	1094.86	30.10	19.91	2.20	6.40	6.40	6.40

29	1103.31	91.17	31.27	1122.51	32.05	20.26	2.04	6.60	6.60	6.60
30	1126.71	105.39	36.57	1150.40	33.87	20.64	1.90	6.80	6.80	6.80
31	1149.81	120.36	42.27	1178.52	35.57	21.03	1.76	7.00	7.00	7.00
32	1172.64	136.03	48.35	1206.86	37.15	21.43	1.63	7.20	7.20	7.20
33	1195.18	152.33	54.82	1235.42	38.62	21.86	1.51	7.40	7.40	7.40
34	1217.43	169.22	61.67	1264.18	39.98	22.31	1.40	7.60	7.60	7.60
35	1239.40	186.62	68.90	1293.13	41.25	22.79	1.30	7.80	7.80	7.80
36	1261.08	204.50	76.50	1322.24	42.43	23.28	1.21	8.00	8.00	8.00
37	1282.49	222.78	84.47	1351.49	43.51	23.81	1.13	8.20	8.20	8.20
38	1303.61	241.41	92.80	1380.86	44.52	24.36	1.06	8.40	8.40	8.40
39	1324.45	260.34	101.48	1410.33	45.44	24.95	1.00	8.60	8.60	8.60
40	1345.00	279.51	110.53	1439.85	46.29	25.56	0.95	8.80	8.80	8.80
41	1365.28	298.86	119.92	1469.41	47.07	26.22	0.91	9.00	9.00	9.00
42	1385.28	318.33	129.65	1498.97	47.78	26.92	0.87	9.20	9.20	9.20
43	1405.00	337.86	139.73	1528.50	48.43	27.65	0.85	9.40	9.40	9.40
44	1424.44	357.41	150.14	1557.97	49.01	28.44	0.84	9.60	9.60	9.60
45	1443.60	376.91	160.88	1587.34	49.54	29.28	0.85	9.80	9.80	9.80
46	1462.48	396.30	171.95	1616.58	50.01	30.17	0.86	10.00	10.00	10.00
47	1481.09	415.53	183.34	1645.66	50.43	31.13	0.89	10.20	10.20	10.20
48	1499.42	434.54	195.05	1674.55	50.79	32.15	0.93	10.40	10.40	10.40
49	1517.47	453.27	207.07	1703.21	51.11	33.25	0.98	10.60	10.60	10.60
50	1535.25	471.67	219.41	1731.62	51.38	34.43	1.05	10.80	10.80	10.80
51	1552.76	489.68	232.04	1759.73	51.60	35.70	1.13	11.00	11.00	11.00
52	1569.99	507.24	244.98	1787.53	51.78	37.08	1.23	11.20	11.20	11.20
53	1586.95	524.30	258.21	1814.98	51.91	38.56	1.34	11.40	11.40	11.40
54	1603.63	540.79	271.74	1842.06	52.01	40.17	1.47	11.60	11.60	11.60
55	1620.05	556.66	285.55	1868.74	52.07	41.91	1.62	11.80	11.80	11.80
56	1636.19	571.86	299.64	1895.01	52.10	43.80	1.79	12.00	12.00	12.00
57	1652.06	586.32	314.01	1920.85	52.10	45.86	1.99	12.20	12.20	12.20
58	1667.66	599.99	328.65	1946.24	52.08	48.11	2.20	12.40	12.40	12.40
59	1682.99	612.81	343.57	1971.18	52.05	50.55	2.44	12.60	12.60	12.60
60	1698.05	624.73	358.74	1995.65	52.01	53.21	2.71	12.80	12.80	12.80
61	1712.85	635.69	374.18	2019.68	51.98	56.11	3.00	13.00	13.00	13.00
62	1727.37	645.62	389.87	2043.26	51.97	59.26	3.32	13.20	13.20	13.20
63	1741.63	654.48	405.81	2066.41	52.01	62.68	3.66	13.40	13.40	13.40
64	1755.62	662.20	422.00	2089.15	52.10	66.36	4.02	13.60	13.60	13.60
65	1769.35	668.74	438.43	2111.54	52.28	70.32	4.38	13.80	13.80	13.80
66	1782.81	674.02	455.10	2133.60	52.57	74.54	4.74	14.00	14.00	14.00
67	1796.00	678.00	472.00	2155.41	53.17	78.94	0.00	14.20	14.20	14.20
68	1825.97	685.68	511.28	2205.41	53.17	78.94	0.00	14.40	14.40	14.40
69	1855.94	693.36	550.56	2255.41	53.17	78.94	0.00	14.60	14.60	14.60
70	1885.91	701.04	589.84	2305.41	53.17	78.94	0.00	14.80	14.80	14.80
71	1915.88	708.72	629.12	2355.41	53.17	78.94	0.00	15.00	15.00	15.00

72	1945.85	716.40	668.39	2405.41	53.17	78.94	0.00	15.20	15.20	15.20
73	1975.82	724.08	707.67	2455.41	53.17	78.94	0.00	15.40	15.40	15.40
74	2005.79	731.76	746.95	2505.41	53.17	78.94	0.00	15.60	15.60	15.60
75	2035.76	739.44	786.23	2555.41	53.17	78.94	0.00	15.80	15.80	15.80
76	2065.73	747.12	825.51	2605.41	53.17	78.94	0.00	16.00	16.00	16.00
77	2095.70	754.80	864.79	2655.41	53.17	78.94	0.00	16.20	16.20	16.20
78	2125.67	762.48	904.07	2705.41	53.17	78.94	0.00	16.40	16.40	16.40
79	2155.64	770.16	943.35	2755.41	53.17	78.94	0.00	16.60	16.60	16.60
80	2185.61	777.84	982.63	2805.41	53.17	78.94	0.00	16.80	16.80	16.80
81	2215.58	785.52	1021.91	2855.41	53.17	78.94	0.00	17.00	17.00	17.00
82	2245.55	793.20	1061.18	2905.41	53.17	78.94	0.00	17.20	17.20	17.20
83	2275.52	800.89	1100.46	2955.41	53.17	78.94	0.00	17.40	17.40	17.40
84	2305.49	808.57	1139.74	3005.41	53.17	78.94	0.00	17.60	17.60	17.60
85	2335.46	816.25	1179.02	3055.41	53.17	78.94	0.00	17.80	17.80	17.80
86	2365.43	823.93	1218.30	3105.41	53.17	78.94	0.00	18.00	18.00	18.00
87	2395.40	831.61	1257.58	3155.41	53.17	78.94	0.00	18.20	18.20	18.20
88	2425.37	839.29	1296.86	3205.41	53.17	78.94	0.00	18.40	18.40	18.40
89	2455.34	846.97	1336.14	3255.41	53.17	78.94	0.00	18.60	18.60	18.60
90	2485.31	854.65	1375.42	3305.41	53.17	78.94	0.00	18.80	18.80	18.80
91	2518.00	861.00	1413.00	3355.63	53.00	79.00	4.86	19.00	19.00	19.00
92	2527.75	863.15	1425.35	3371.50	51.30	81.29	4.51	19.20	19.20	19.20
93	2537.97	864.78	1437.65	3387.58	49.78	83.56	4.17	19.40	19.40	19.40
94	2548.64	865.92	1449.92	3403.88	48.43	85.82	3.84	19.60	19.60	19.60
95	2559.74	866.58	1462.14	3420.40	47.25	88.04	3.53	19.80	19.80	19.80
96	2571.22	866.76	1474.34	3437.16	46.22	90.22	3.25	20.00	20.00	20.00
97	2583.08	866.49	1486.51	3454.15	45.33	92.35	2.98	20.20	20.20	20.20
98	2595.27	865.77	1498.65	3471.38	44.58	94.41	2.74	20.40	20.40	20.40
99	2607.77	864.62	1510.78	3488.83	43.96	96.41	2.52	20.60	20.60	20.60
100	2620.56	863.05	1522.90	3506.52	43.46	98.34	2.32	20.80	20.80	20.80
101	2633.60	861.07	1535.00	3524.42	43.06	100.19	2.13	21.00	21.00	21.00
102	2646.86	858.70	1547.11	3542.53	42.77	101.95	1.97	21.20	21.20	21.20
103	2660.33	855.95	1559.21	3560.84	42.58	103.64	1.82	21.40	21.40	21.40
104	2673.97	852.84	1571.32	3579.34	42.47	105.23	1.69	21.60	21.60	21.60
105	2687.75	849.36	1583.43	3598.02	42.44	106.74	1.58	21.80	21.80	21.80
106	2701.64	845.55	1595.56	3616.86	42.49	108.16	1.48	22.00	22.00	22.00
107	2715.63	841.40	1607.71	3635.84	42.62	109.49	1.40	22.20	22.20	22.20
108	2729.67	836.95	1619.88	3654.95	42.81	110.74	1.33	22.40	22.40	22.40
109	2743.75	832.18	1632.08	3674.18	43.07	111.90	1.27	22.60	22.60	22.60
110	2757.83	827.13	1644.31	3693.50	43.39	112.98	1.23	22.80	22.80	22.80
111	2771.89	821.80	1656.58	3712.91	43.77	113.98	1.20	23.00	23.00	23.00
112	2785.90	816.21	1668.89	3732.37	44.21	114.90	1.19	23.20	23.20	23.20
113	2799.83	810.36	1681.24	3751.89	44.71	115.74	1.19	23.40	23.40	23.40
114	2813.65	804.28	1693.65	3771.43	45.27	116.51	1.20	23.60	23.60	23.60

115	2827.34	797.97	1706.10	3790.99	45.89	117.20	1.23	23.80	23.80	23.80
116	2840.86	791.44	1718.62	3810.54	46.56	117.83	1.27	24.00	24.00	24.00
117	2854.20	784.72	1731.20	3830.06	47.30	118.39	1.32	24.20	24.20	24.20
118	2867.32	777.81	1743.85	3849.55	48.10	118.89	1.38	24.40	24.40	24.40
119	2880.19	770.73	1756.57	3868.99	48.96	119.32	1.46	24.60	24.60	24.60
120	2892.79	763.48	1769.37	3888.35	49.88	119.69	1.54	24.80	24.80	24.80
121	2905.09	756.09	1782.25	3907.64	50.88	120.00	1.64	25.00	25.00	25.00
122	2917.06	748.56	1795.22	3926.82	51.94	120.26	1.75	25.20	25.20	25.20
123	2928.67	740.91	1808.28	3945.90	53.08	120.46	1.87	25.40	25.40	25.40
124	2939.90	733.15	1821.43	3964.85	54.29	120.61	2.00	25.60	25.60	25.60
125	2950.71	725.30	1834.68	3983.68	55.59	120.70	2.14	25.80	25.80	25.80
126	2961.09	717.36	1848.04	4002.36	56.97	120.75	2.30	26.00	26.00	26.00
127	2970.99	709.35	1861.51	4020.90	58.44	120.74	2.47	26.20	26.20	26.20
128	2980.41	701.28	1875.09	4039.29	60.00	120.69	2.65	26.40	26.40	26.40
129	2989.29	693.16	1888.78	4057.52	61.67	120.58	2.84	26.60	26.60	26.60
130	2997.63	685.02	1902.60	4075.60	63.43	120.44	3.04	26.80	26.80	26.80
131	3005.39	676.85	1916.55	4093.52	65.30	120.24	3.25	27.00	27.00	27.00
132	3012.54	668.68	1930.63	4111.30	67.29	120.01	3.47	27.20	27.20	27.20
133	3019.06	660.52	1944.84	4128.94	69.38	119.73	3.70	27.40	27.40	27.40
134	3024.91	652.37	1959.20	4146.45	71.59	119.40	3.93	27.60	27.60	27.60
135	3030.07	644.26	1973.70	4163.85	73.91	119.04	4.16	27.80	27.80	27.80
136	3034.52	636.20	1988.35	4181.16	76.34	118.63	4.39	28.00	28.00	28.00
137	3038.22	628.19	2003.15	4198.39	78.88	118.18	4.60	28.20	28.20	28.20
138	3041.14	620.25	2018.12	4215.58	81.53	117.70	4.79	28.40	28.40	28.40
139	3043.27	612.40	2033.24	4232.75	84.27	117.17	4.96	28.60	28.60	28.60
140	3044.56	604.65	2048.53	4249.95	87.10	116.60	5.09	28.80	28.80	28.80
141	3045.00	597.00	2064.00	4267.21	90.00	116.00	0.00	29.00	29.00	29.00
142	3045.00	575.08	2108.94	4317.21	90.00	116.00	0.00	29.20	29.20	29.20
143	3045.00	553.16	2153.88	4367.21	90.00	116.00	0.00	29.40	29.40	29.40
144	3045.00	531.24	2198.82	4417.21	90.00	116.00	0.00	29.60	29.60	29.60
145	3045.00	509.32	2243.76	4467.21	90.00	116.00	0.00	29.80	29.80	29.80
146	3045.00	487.40	2288.70	4517.21	90.00	116.00	0.00	30.00	30.00	30.00
147	3045.00	465.48	2333.64	4567.21	90.00	116.00	0.00	30.20	30.20	30.20
148	3045.00	443.56	2378.58	4617.21	90.00	116.00	0.00	30.40	30.40	30.40
149	3045.00	421.64	2423.52	4667.21	90.00	116.00	0.00	30.60	30.60	30.60
150	3045.00	399.72	2468.46	4717.21	90.00	116.00	0.00	30.80	30.80	30.80
151	3045.00	377.80	2513.40	4767.21	90.00	116.00	0.00	31.00	31.00	31.00
152	3045.00	355.88	2558.34	4817.21	90.00	116.00	0.00	31.20	31.20	31.20
153	3045.00	333.96	2603.28	4867.21	90.00	116.00	0.00	31.40	31.40	31.40
154	3045.00	312.04	2648.22	4917.21	90.00	116.00	0.00	31.60	31.60	31.60
155	3045.00	290.12	2693.16	4967.21	90.00	116.00	0.00	31.80	31.80	31.80
156	3045.00	268.20	2738.10	5017.21	90.00	116.00	0.00	32.00	32.00	32.00
157	3045.00	246.28	2783.04	5067.21	90.00	116.00	0.00	32.20	32.20	32.20

158	3045.00	224.36	2827.97	5117.21	90.00	116.00	0.00	32.40	32.40	32.40
159	3045.00	202.44	2872.91	5167.21	90.00	116.00	0.00	32.60	32.60	32.60
160	3045.00	180.52	2917.85	5217.21	90.00	116.00	0.00	32.80	32.80	32.80
161	3045.00	158.60	2962.79	5267.21	90.00	116.00	0.00	33.00	33.00	33.00
162	3045.00	136.68	3007.73	5317.21	90.00	116.00	0.00	33.20	33.20	33.20
163	3045.00	114.76	3052.67	5367.21	90.00	116.00	0.00	33.40	33.40	33.40
164	3045.00	92.84	3097.61	5417.21	90.00	116.00	0.00	33.60	33.60	33.60
165	3045.00	70.95	3142.55	5467.19	90.00	116.00	0.00	33.80	33.80	33.80

Appendix D

Output results of section 4.2 given in tables below:

Simulation Results of J Shape Well with Trained PPO Agent

Index	N[m]	E[m]	V[m]	MD[m]	T[min]	WOB[N]	RPM	Reward	ROP[m/hr]
0	0.00	0.00	0.00	0.00	0.00	113500.00	107.00	12.04	14.45
1	0.00	0.00	50.08	50.08	208.00	113500.00	107.00	12.04	14.45
2	0.00	0.00	100.16	100.16	416.00	113500.00	107.00	12.04	14.45
3	0.00	0.00	150.00	150.00	623.00	113500.00	107.00	12.04	14.45
4	0.00	0.00	200.08	200.08	831.00	113500.00	107.00	12.04	14.45
5	0.00	0.00	250.16	250.16	1039.00	113500.00	107.00	12.04	14.45
6	0.00	0.00	300.00	300.00	1246.00	113500.00	107.00	12.04	14.45
7	0.00	0.00	350.08	350.08	1454.00	113500.00	107.00	12.04	14.45
8	0.00	0.00	400.16	400.16	1662.00	113500.00	107.00	12.04	14.45
9	0.00	0.00	450.00	450.00	1869.00	113500.00	107.00	12.04	14.45
10	0.00	0.00	500.08	500.08	2077.00	113500.00	107.00	12.05	14.45
11	-0.39	0.30	520.55	520.56	2162.00	113500.00	107.00	12.04	14.46
12	-1.60	1.22	541.22	541.28	2248.00	113500.00	107.00	12.03	14.46
13	-3.63	2.76	561.77	562.00	2334.00	113500.00	107.00	12.02	14.46
14	-6.51	4.94	582.42	582.96	2421.00	113500.00	107.00	12.00	14.46
15	-10.30	7.82	603.32	604.40	2510.00	113500.00	107.00	11.98	14.46
16	-15.01	11.40	624.18	626.08	2600.00	113500.00	107.00	11.93	14.46
17	-20.63	15.67	644.93	648.01	2691.00	113500.00	107.00	11.86	14.45
18	-27.35	20.78	665.95	670.65	2785.00	113500.00	107.00	11.74	14.45
19	-34.91	26.53	686.76	693.54	2880.00	113500.00	107.00	11.63	14.45
20	-43.27	32.90	707.62	716.90	2977.00	113500.00	107.00	11.50	14.45
21	-52.30	39.77	728.32	740.50	3075.00	113500.00	107.00	11.36	14.45
22	-62.15	47.28	749.25	764.83	3176.00	113500.00	107.00	11.17	14.45
23	-72.71	55.33	770.21	789.63	3279.00	113500.00	107.00	10.95	14.45
24	-83.82	63.81	790.99	814.68	3383.00	113500.00	107.00	10.70	14.45
25	-95.58	72.78	811.79	840.21	3489.00	113500.00	107.00	10.41	14.45
26	-108.07	82.32	832.82	866.46	3598.00	113500.00	107.00	10.07	14.45
27	-121.05	92.23	853.68	892.95	3708.00	113500.00	107.00	9.83	14.45
28	-134.47	102.51	874.38	919.68	3819.00	113500.00	107.00	9.64	14.45
29	-148.56	113.32	895.32	947.13	3933.00	113500.00	107.00	9.50	14.45
30	-163.04	124.46	916.13	974.82	4048.00	113500.00	107.00	9.38	14.45
31	-177.91	135.92	936.81	1002.76	4164.00	113500.00	107.00	9.18	14.45
32	-193.26	147.80	957.56	1031.17	4282.00	113500.00	107.00	8.97	14.45
33	-209.09	160.08	978.38	1060.07	4402.00	113500.00	107.00	8.80	14.45
34	-225.11	172.54	998.95	1088.96	4522.00	113500.00	107.00	8.71	14.45
35	-241.58	185.38	1019.61	1118.34	4644.00	113500.00	107.00	8.53	14.45

36	-258.33	198.50	1040.21	1147.96	4767.00	113500.00	107.00	8.35	14.45
37	-275.37	211.87	1060.76	1177.82	4891.00	113500.00	107.00	8.38	14.45
38	-292.67	225.51	1081.27	1207.92	5016.00	113500.00	107.00	8.35	14.45
39	-310.22	239.38	1101.76	1238.25	5142.00	113500.00	107.00	8.25	14.45
40	-327.87	253.39	1122.08	1268.59	5268.00	113500.00	107.00	8.29	14.45
41	-345.75	267.64	1142.39	1299.17	5395.00	113500.00	107.00	8.06	14.45
42	-363.70	282.00	1162.55	1329.75	5522.00	113500.00	107.00	8.72	14.45
43	-381.85	296.59	1182.75	1360.57	5650.00	113500.00	107.00	8.97	14.45
44	-399.90	311.17	1202.66	1391.15	5777.00	113500.00	107.00	8.48	14.45
45	-418.14	325.96	1222.63	1421.97	5905.00	113500.00	107.00	10.85	14.45
46	-436.39	340.84	1242.51	1452.79	6033.00	113500.00	107.00	10.89	14.45
47	-454.65	355.81	1262.31	1483.61	6161.00	113500.00	107.00	10.71	14.45
48	-472.77	370.75	1281.89	1514.19	6288.00	113500.00	107.00	10.27	14.45
49	-490.89	385.76	1301.43	1544.77	6415.00	113500.00	107.00	6.77	14.45
50	-508.97	400.85	1320.93	1575.35	6542.00	113500.00	107.00	6.92	14.45
51	-526.89	415.89	1340.24	1605.69	6668.00	113500.00	107.00	0.56	14.45
52	-544.61	430.88	1359.40	1635.78	6793.00	113500.00	107.00	0.96	14.45
53	-562.14	445.80	1378.41	1665.64	6917.00	113500.00	107.00	1.74	14.45
54	-579.47	460.68	1397.26	1695.26	7040.00	113500.00	107.00	3.07	14.45
55	-596.61	475.51	1415.95	1724.63	7162.00	113500.00	107.00	5.15	14.45
56	-613.54	490.29	1434.49	1753.77	7283.00	113500.00	107.00	8.03	14.45
57	-630.12	504.91	1452.72	1782.42	7402.00	113500.00	107.00	11.85	14.45
58	-646.49	519.50	1470.79	1810.83	7520.00	113500.00	107.00	8.22	14.45
59	-662.63	534.04	1488.71	1839.00	7637.00	113500.00	107.00	4.99	14.45
60	-678.28	548.31	1506.18	1866.45	7751.00	113500.00	107.00	9.68	14.45
61	-706.78	574.34	1538.09	1916.53	7959.00	113500.00	107.00	9.66	14.45
62	-735.23	600.38	1570.03	1966.61	8167.00	113500.00	107.00	9.63	14.45
63	-763.52	626.30	1601.85	2016.45	8374.00	113500.00	107.00	9.61	14.45
64	-791.90	652.35	1633.84	2066.53	8582.00	113500.00	107.00	9.60	14.45
65	-820.25	678.41	1665.86	2116.61	8790.00	113500.00	107.00	9.58	14.45
66	-848.44	704.35	1697.75	2166.45	8997.00	113500.00	107.00	9.58	14.45
67	-876.74	730.41	1729.80	2216.53	9205.00	113500.00	107.00	9.57	14.45
68	-905.02	756.49	1761.87	2266.61	9413.00	113500.00	107.00	9.57	14.45
69	-933.14	782.44	1793.81	2316.45	9620.00	113500.00	107.00	9.58	14.45
70	-961.38	808.52	1825.90	2366.54	9828.00	113500.00	107.00	9.59	14.45
71	-989.61	834.61	1858.01	2416.62	10036.00	113500.00	107.00	9.60	14.45
72	-1017.68	860.58	1889.98	2466.46	10243.00	113500.00	107.00	9.61	14.45
73	-1045.87	886.67	1922.10	2516.54	10451.00	113500.00	107.00	9.63	14.45
74	-1074.06	912.78	1954.24	2566.62	10659.00	113500.00	107.00	9.65	14.45
75	-1102.09	938.75	1986.22	2616.46	10866.00	113500.00	107.00	9.68	14.45
76	-1130.26	964.86	2018.37	2666.54	11074.00	113500.00	107.00	9.70	14.45
77	-1158.41	990.97	2050.52	2716.62	11282.00	113500.00	107.00	9.73	14.45
78	-1186.42	1016.96	2082.52	2766.46	11489.00	113500.00	107.00	9.76	14.45

79	-1214.56	1043.08	2114.68	2816.54	11697.00	113500.00	107.00	9.79	14.45
80	-1242.69	1069.20	2146.84	2866.62	11905.00	113500.00	107.00	9.83	14.45
81	-1270.68	1095.20	2178.85	2916.46	12112.00	113500.00	107.00	9.86	14.45
82	-1298.79	1121.33	2211.02	2966.54	12320.00	113500.00	107.00	9.90	14.45
83	-1326.91	1147.46	2243.19	3016.62	12528.00	113500.00	107.00	9.94	14.45
84	-1354.88	1173.46	2275.21	3066.46	12735.00	113500.00	107.00	9.98	14.45
85	-1382.99	1199.60	2307.38	3116.54	12943.00	113500.00	107.00	10.02	14.45
86	-1411.09	1225.73	2339.56	3166.62	13151.00	113500.00	107.00	10.06	14.45
87	-1439.05	1251.74	2371.58	3216.46	13358.00	113500.00	107.00	10.10	14.45
88	-1467.15	1277.88	2403.76	3266.54	13566.00	113500.00	107.00	10.14	14.45
89	-1495.24	1304.02	2435.94	3316.62	13774.00	113500.00	107.00	10.18	14.45
90	-1523.19	1330.04	2467.97	3366.46	13981.00	113500.00	107.00	10.22	14.45
91	-1551.28	1356.18	2500.15	3416.54	14189.00	113500.00	107.00	10.26	14.45
92	-1579.36	1382.33	2532.34	3466.62	14397.00	113500.00	107.00	10.30	14.45
93	-1607.31	1408.35	2564.37	3516.46	14604.00	113500.00	107.00	10.34	14.45
94	-1635.39	1434.49	2596.55	3566.55	14812.00	113500.00	107.00	10.38	14.45
95	-1663.47	1460.64	2628.74	3616.63	15020.00	113500.00	107.00	10.42	14.45
96	-1691.41	1486.67	2660.77	3666.47	15227.00	113500.00	107.00	10.46	14.45
97	-1719.49	1512.82	2692.95	3716.55	15435.00	113500.00	107.00	10.50	14.45
98	-1747.56	1538.97	2725.14	3766.63	15643.00	113500.00	107.00	10.54	14.45
99	-1775.50	1564.99	2757.17	3816.47	15850.00	113500.00	107.00	10.58	14.45
100	-1803.57	1591.15	2789.36	3866.55	16058.00	113500.00	107.00	10.62	14.45
101	-1831.64	1617.30	2821.55	3916.63	16266.00	113500.00	107.00	10.65	14.45
102	-1859.58	1643.33	2853.58	3966.47	16473.00	113500.00	107.00	10.69	14.45
103	-1887.65	1669.48	2885.77	4016.55	16681.00	113500.00	107.00	10.73	14.45
104	-1915.72	1695.64	2917.96	4066.63	16889.00	113500.00	107.00	10.76	14.45
105	-1943.65	1721.67	2950.00	4116.47	17096.00	113500.00	107.00	10.79	14.45
106	-1971.72	1747.83	2982.19	4166.55	17304.00	113500.00	107.00	10.83	14.45
107	-1999.78	1773.98	3014.38	4216.63	17512.00	113500.00	107.00	10.86	14.45
108	-2027.71	1800.01	3046.41	4266.47	17719.00	113500.00	107.00	10.89	14.45
109	-2055.78	1826.17	3078.60	4316.55	17927.00	113500.00	107.00	10.92	14.45
110	-2083.71	1852.20	3110.64	4366.39	18134.00				

Simulation Results of J Shape Well with Trained DQN Agent

Index	N[m]	E[m]	V[m]	MD[m]	T[min]	WOB[N]	RPM	Reward	ROP[m/hr]
0	0.00	0.00	0.00	0.00	0.00	167500.00	94.00	15.72	18.86
1	0.00	0.00	50.30	50.30	160.00	167500.00	94.00	15.72	18.86
2	0.00	0.00	100.29	100.29	319.00	167500.00	94.00	15.72	18.86
3	0.00	0.00	150.28	150.28	478.00	167500.00	94.00	15.72	18.86
4	0.00	0.00	200.27	200.27	637.00	167500.00	94.00	15.72	18.86
5	0.00	0.00	250.26	250.26	796.00	167500.00	94.00	15.72	18.86
6	0.00	0.00	300.25	300.25	955.00	174000.00	178.00	30.95	37.14

7	0.00	0.00	350.39	350.39	1036.00	174000.00	178.00	30.95	37.14
8	0.00	0.00	400.53	400.53	1117.00	174000.00	178.00	30.95	37.14
9	0.00	0.00	450.05	450.05	1197.00	174000.00	178.00	30.95	37.14
10	0.00	0.00	500.19	500.19	1278.00	174000.00	178.00	30.96	37.15
11	-0.09	0.07	520.62	520.62	1311.00	170500.00	180.00	30.66	36.79
12	-0.35	0.27	541.46	541.47	1345.00	170500.00	180.00	30.65	36.79
13	-0.80	0.61	562.30	562.32	1379.00	82500.00	94.00	-100.00	9.21
14	-2.50	1.90	582.89	583.03	1514.00	82500.00	94.00	-100.00	9.20
15	-6.64	5.04	603.55	604.34	1653.00	82500.00	94.00	-100.00	9.19
16	-11.97	9.09	624.08	625.95	1794.00	82500.00	94.00	-100.00	9.19
17	-18.16	13.80	644.73	648.00	1938.00	82500.00	94.00	-100.00	9.19
18	-25.20	19.15	665.44	670.52	2085.00	82500.00	94.00	7.28	9.19
19	-32.98	25.07	686.06	693.35	2234.00	82500.00	94.00	7.14	9.19
20	-41.58	31.61	706.85	716.78	2387.00	82500.00	94.00	6.99	9.19
21	-50.86	38.68	727.53	740.52	2542.00	82500.00	94.00	6.78	9.19
22	-60.84	46.28	748.22	764.72	2700.00	82500.00	94.00	6.55	9.19
23	-71.56	54.45	769.05	789.53	2862.00	82500.00	94.00	6.29	9.19
24	-82.85	63.06	789.77	814.65	3026.00	82500.00	94.00	6.01	9.19
25	-94.77	72.15	810.49	840.23	3193.00	82500.00	94.00	5.63	9.19
26	-107.29	81.71	831.22	866.26	3363.00	82500.00	94.00	5.26	9.19
27	-120.38	91.72	851.96	892.76	3536.00	82500.00	94.00	4.85	9.19
28	-134.03	102.17	872.73	919.71	3712.00	82500.00	94.00	4.66	9.19
29	-148.11	112.97	893.41	946.97	3890.00	82500.00	94.00	4.56	9.19
30	-162.70	124.20	914.13	974.68	4071.00	82500.00	94.00	4.18	9.19
31	-177.79	135.84	934.89	1002.86	4255.00	82500.00	94.00	4.04	9.19
32	-193.17	147.74	955.49	1031.19	4440.00	82500.00	94.00	3.90	9.19
33	-209.02	160.03	976.14	1059.98	4628.00	82500.00	94.00	3.56	9.19
34	-225.21	172.62	996.77	1089.07	4818.00	82500.00	94.00	3.58	9.19
35	-241.68	185.47	1017.25	1118.32	5009.00	82500.00	94.00	3.41	9.19
36	-258.54	198.67	1037.84	1148.03	5203.00	82500.00	94.00	3.14	9.19
37	-275.63	212.10	1058.31	1177.89	5398.00	82500.00	94.00	2.95	9.19
38	-292.93	225.73	1078.70	1207.90	5594.00	82500.00	94.00	3.22	9.19
39	-310.52	239.64	1099.10	1238.22	5792.00	82500.00	94.00	2.71	9.19
40	-328.20	253.68	1119.34	1268.54	5990.00	82500.00	94.00	3.58	9.19
41	-346.04	267.91	1139.53	1299.01	6189.00	82500.00	94.00	3.12	9.19
42	-364.14	282.40	1159.77	1329.79	6390.00	82500.00	94.00	3.60	9.19
43	-382.20	296.92	1179.80	1360.41	6590.00	82500.00	94.00	3.70	9.19
44	-400.39	311.62	1199.80	1391.19	6791.00	82500.00	94.00	5.44	9.19
45	-418.61	326.40	1219.72	1421.97	6992.00	82500.00	94.00	4.34	9.19
46	-436.85	341.28	1239.55	1452.75	7193.00	82500.00	94.00	5.01	9.19
47	-455.11	356.25	1259.29	1483.53	7394.00	82500.00	94.00	4.79	9.19
48	-473.27	371.22	1278.89	1514.15	7594.00	82500.00	94.00	6.71	9.19
49	-491.42	386.26	1298.43	1544.77	7794.00	82500.00	94.00	1.37	9.19

50	-509.45	401.30	1317.85	1575.25	7993.00	82500.00	94.00	1.32	9.19
51	-527.36	416.34	1337.15	1605.56	8191.00	82500.00	94.00	-3.10	9.19
52	-545.03	431.29	1356.25	1635.58	8387.00	82500.00	94.00	-2.72	9.19
53	-562.66	446.30	1375.35	1665.59	8583.00	82500.00	94.00	-1.60	9.19
54	-580.05	461.23	1394.24	1695.30	8777.00	82500.00	94.00	0.41	9.19
55	-597.11	476.01	1412.84	1724.54	8968.00	82500.00	94.00	2.85	9.19
56	-614.03	490.78	1431.33	1753.64	9158.00	82500.00	94.00	5.62	9.19
57	-630.70	505.50	1449.61	1782.42	9346.00	82500.00	94.00	6.85	9.19
58	-647.12	520.13	1467.70	1810.90	9532.00	82500.00	94.00	4.89	9.19
59	-663.19	534.62	1485.51	1838.93	9715.00	82500.00	94.00	3.63	9.19
60	-678.89	548.94	1503.06	1866.49	9895.00	82500.00	94.00	2.81	9.19
61	-707.33	574.96	1535.02	1916.56	10222.00	82500.00	94.00	2.46	9.19
62	-735.60	600.90	1566.95	1966.48	10548.00	82500.00	94.00	2.35	9.19
63	-763.90	626.93	1599.02	2016.55	10875.00	82500.00	94.00	2.46	9.19
64	-792.07	652.88	1631.03	2066.46	11201.00	82500.00	94.00	2.76	9.19
65	-820.29	678.93	1663.16	2116.53	11528.00	82500.00	94.00	3.17	9.19
66	-848.39	704.90	1695.21	2166.45	11854.00	82500.00	94.00	3.65	9.19
67	-876.56	730.97	1727.37	2216.52	12181.00	82500.00	94.00	4.13	9.19
68	-904.63	756.96	1759.44	2266.44	12507.00	82500.00	94.00	4.59	9.19
69	-932.77	783.04	1791.61	2316.51	12834.00	82500.00	94.00	5.01	9.19
70	-960.81	809.05	1823.68	2366.42	13160.00	82500.00	94.00	5.39	9.19
71	-988.93	835.15	1855.86	2416.49	13487.00	82500.00	94.00	5.72	9.19
72	-1017.04	861.26	1888.04	2466.57	13814.00	82500.00	94.00	6.00	9.19
73	-1045.05	887.29	1920.12	2516.48	14140.00	82500.00	94.00	6.25	9.19
74	-1073.15	913.40	1952.30	2566.55	14467.00	82500.00	94.00	6.46	9.19
75	-1101.15	939.44	1984.38	2616.47	14793.00	82500.00	94.00	6.64	9.19
76	-1129.24	965.57	2016.57	2666.54	15120.00	82500.00	94.00	6.79	9.19
77	-1157.23	991.62	2048.65	2716.46	15446.00	82500.00	94.00	6.92	9.19
78	-1185.31	1017.75	2080.83	2766.53	15773.00	82500.00	94.00	7.03	9.19
79	-1213.30	1043.80	2112.92	2816.44	16099.00	82500.00	94.00	7.13	9.19
80	-1241.37	1069.94	2145.10	2866.51	16426.00	82500.00	94.00	7.21	9.19
81	-1269.36	1096.00	2177.19	2916.43	16752.00	82500.00	94.00	7.27	9.19
82	-1297.43	1122.14	2209.37	2966.50	17079.00	82500.00	94.00	7.33	9.19
83	-1325.41	1148.20	2241.46	3016.42	17405.00	82500.00	94.00	7.38	9.19
84	-1353.47	1174.35	2273.64	3066.49	17732.00	82500.00	94.00	7.42	9.19
85	-1381.54	1200.50	2305.83	3116.56	18059.00	82500.00	94.00	7.46	9.19
86	-1409.51	1226.56	2337.91	3166.48	18385.00	82500.00	94.00	7.49	9.19
87	-1437.57	1252.71	2370.10	3216.55	18712.00	82500.00	94.00	7.51	9.19
88	-1465.55	1278.78	2402.18	3266.46	19038.00	82500.00	94.00	7.53	9.19
89	-1493.60	1304.94	2434.37	3316.53	19365.00	82500.00	94.00	7.55	9.19
90	-1521.58	1331.01	2466.45	3366.45	19691.00	82500.00	94.00	7.57	9.19
91	-1549.63	1357.16	2498.64	3416.52	20018.00	82500.00	94.00	7.58	9.19
92	-1577.61	1383.23	2530.72	3466.44	20344.00	82500.00	94.00	7.59	9.19

93	-1605.66	1409.39	2562.91	3516.51	20671.00	82500.00	94.00	7.60	9.19
94	-1633.63	1435.46	2595.00	3566.42	20997.00	82500.00	94.00	7.61	9.19
95	-1661.69	1461.62	2627.18	3616.49	21324.00	82500.00	94.00	7.62	9.19
96	-1689.74	1487.77	2659.36	3666.57	21651.00	82500.00	94.00	7.62	9.19
97	-1717.71	1513.85	2691.45	3716.48	21977.00	82500.00	94.00	7.63	9.19
98	-1745.76	1540.00	2723.63	3766.55	22304.00	82500.00	94.00	7.63	9.19
99	-1773.73	1566.08	2755.72	3816.47	22630.00	82500.00	94.00	7.64	9.19
100	-1801.79	1592.24	2787.91	3866.54	22957.00	82500.00	94.00	7.64	9.19
101	-1829.75	1618.31	2819.99	3916.46	23283.00	82500.00	94.00	7.64	9.19
102	-1857.81	1644.47	2852.18	3966.53	23610.00	82500.00	94.00	7.64	9.19
103	-1885.78	1670.55	2884.26	4016.44	23936.00	82500.00	94.00	7.65	9.19
104	-1913.83	1696.71	2916.45	4066.51	24263.00	82500.00	94.00	7.65	9.19
105	-1941.80	1722.78	2948.53	4116.43	24589.00	82500.00	94.00	7.65	9.19
106	-1969.85	1748.94	2980.72	4166.50	24916.00	82500.00	94.00	7.65	9.19
107	-1997.82	1775.02	3012.80	4216.42	25242.00	82500.00	94.00	7.65	9.19
108	-2025.87	1801.18	3044.99	4266.49	25569.00	82500.00	94.00	7.65	9.19
109	-2053.92	1827.33	3077.17	4316.56	25896.00	82500.00	94.00	7.65	9.19
110	-2081.89	1853.41	3109.26	4366.48	26222.00				

Simulation Results of S Shape Well with Trained PPO Agent

Index	N[m]	E[m]	V[m]	MD[m]	T[min]	WOB[N]	RPM	Reward	ROP[m/hr]
0	0.00	0.00	0.00	0.00	0.00	113500.00	107.00	12.04	14.45
1	0.00	0.00	50.08	50.08	208.00	113500.00	107.00	12.04	14.45
2	0.00	0.00	100.16	100.16	416.00	113500.00	107.00	12.04	14.45
3	0.00	0.00	150.00	150.00	623.00	113500.00	107.00	12.04	14.45
4	0.00	0.00	200.08	200.08	831.00	113500.00	107.00	12.04	14.45
5	0.00	0.00	250.16	250.16	1039.00	113500.00	107.00	12.04	14.45
6	0.00	0.00	300.00	300.00	1246.00	113500.00	107.00	12.04	14.45
7	0.00	0.00	350.08	350.08	1454.00	113500.00	107.00	12.04	14.45
8	0.00	0.00	400.16	400.16	1662.00	113500.00	107.00	12.04	14.45
9	0.00	0.00	450.00	450.00	1869.00	113500.00	107.00	12.04	14.45
10	0.00	0.00	500.08	500.08	2077.00	113500.00	107.00	12.04	14.45
11	0.00	0.00	550.17	550.17	2285.00	113500.00	107.00	12.04	14.45
12	0.00	0.00	600.01	600.01	2492.00	113500.00	107.00	12.04	14.45
13	0.00	0.00	650.09	650.09	2700.00	113500.00	107.00	12.04	14.45
14	0.00	0.00	700.17	700.17	2908.00	113500.00	107.00	12.04	14.45
15	0.00	0.00	750.01	750.01	3115.00	113500.00	107.00	12.04	14.45
16	0.00	0.00	800.09	800.09	3323.00	113500.00	107.00	12.04	14.45
17	0.00	0.00	850.17	850.17	3531.00	113500.00	107.00	12.04	14.45
18	0.00	0.00	900.01	900.01	3738.00	113500.00	107.00	12.04	14.45
19	0.00	0.00	950.09	950.09	3946.00	113500.00	107.00	12.04	14.45
20	0.00	0.00	1000.17	1000.17	4154.00	113500.00	107.00	12.04	14.45

21	3.90	-5.73	1152.18	1152.35	4786.00	113500.00	107.00	12.04	14.45
22	12.41	-18.24	1295.37	1296.35	5384.00	113500.00	107.00	-100.00	14.45
23	25.39	-37.32	1429.68	1432.64	5950.00	113500.00	107.00	-100.00	14.45
24	42.65	-62.69	1555.52	1562.19	6488.00	113500.00	107.00	-100.00	14.45
25	64.01	-94.09	1673.56	1686.21	7003.00	113500.00	107.00	-100.00	14.45
26	89.22	-131.16	1783.72	1805.17	7497.00	113500.00	107.00	-100.00	14.45
27	118.08	-173.57	1886.47	1920.03	7974.00	113500.00	107.00	-100.00	14.45
28	150.40	-221.08	1982.27	2031.77	8438.00	113500.00	107.00	-100.00	14.45
29	185.91	-273.28	2071.20	2140.86	8891.00	113500.00	107.00	-100.00	14.45
30	224.50	-330.01	2153.80	2248.26	9337.00	113500.00	107.00	-100.00	14.45
31	265.92	-390.89	2230.30	2354.46	9778.00	113500.00	107.00	-100.00	14.45
32	309.94	-455.60	2300.98	2459.94	10216.00	113500.00	107.00	-100.00	14.45
33	356.60	-524.19	2366.49	2565.65	10655.00	113500.00	107.00	-100.00	14.45
34	405.43	-595.96	2426.81	2671.36	11094.00	113500.00	107.00	-100.00	14.45
35	456.31	-670.76	2482.40	2777.56	11535.00	113500.00	107.00	-100.00	14.45
36	509.10	-748.36	2533.59	2884.47	11979.00	113500.00	107.00	-100.00	14.45
37	563.66	-828.56	2580.79	2992.35	12427.00	113500.00	107.00	-100.00	14.45
38	619.77	-911.04	2624.30	3101.19	12879.00	113500.00	107.00	-100.00	14.45
39	677.13	-995.35	2664.35	3210.75	13334.00	113500.00	107.00	-100.00	14.45
40	735.70	-1081.44	2701.40	3321.27	13793.00	113500.00	107.00	-100.00	14.45
41	795.10	-1168.76	2735.60	3432.27	14254.00	113500.00	107.00	-100.00	14.45
42	855.33	-1257.30	2767.44	3544.00	14718.00	113500.00	107.00	-100.00	14.45
43	916.06	-1346.57	2797.08	3655.96	15183.00	113500.00	107.00	-100.00	14.45
44	977.33	-1436.63	2824.99	3768.40	15650.00	113500.00	107.00	-100.00	14.45
45	1038.54	-1526.61	2851.32	3880.37	16115.00	113500.00	107.00	-100.00	14.45
46	1099.89	-1616.80	2876.55	3992.33	16580.00	113500.00	107.00	-100.00	14.45
47	1160.94	-1706.54	2900.91	4103.56	17042.00	113500.00	107.00	-100.00	14.45
48	1221.64	-1795.76	2924.77	4214.08	17501.00	113500.00	107.00	-100.00	14.45
49	1281.83	-1884.23	2948.24	4323.63	17956.00	113500.00	107.00	-100.00	14.45
50	1341.11	-1971.37	2971.23	4431.50	18404.00	113500.00	107.00	-100.00	14.45
51	1399.59	-2057.34	2993.92	4537.92	18846.00	113500.00	107.00	-100.00	14.45
52	1456.81	-2141.44	3016.74	4642.17	19279.00	113500.00	107.00	-100.00	14.45
53	1512.77	-2223.71	3040.66	4744.50	19704.00	113500.00	107.00	-100.00	14.45
54	1567.02	-2303.45	3065.87	4844.19	20118.00	113500.00	107.00	-100.00	14.45
55	1619.59	-2380.73	3092.84	4941.47	20522.00	113500.00	107.00	-100.00	14.45
56	1670.00	-2454.83	3121.66	5035.62	20913.00	113500.00	107.00	-100.00	14.45
57	1718.38	-2525.94	3152.90	5127.12	21293.00	113500.00	107.00	-100.00	14.45
58	1764.19	-2593.28	3186.58	5215.25	21659.00	113500.00	107.00	-100.00	14.45
59	1807.49	-2656.93	3223.17	5300.50	22013.00	113500.00	107.00	-100.00	14.45
60	1847.93	-2716.37	3262.82	5382.62	22354.00	113500.00	107.00	-100.00	14.45
61	1885.35	-2771.38	3305.82	5461.85	22683.00	113500.00	107.00	-100.00	14.45
62	1919.65	-2821.80	3352.50	5538.68	23002.00	113500.00	107.00	-100.00	14.45
63	1950.56	-2867.24	3402.98	5613.34	23312.00	113500.00	107.00	-100.00	14.45

64	1977.97	-2907.52	3457.58	5686.56	23616.00	113500.00	107.00	-100.00	14.45
65	2001.64	-2942.32	3516.55	5759.06	23917.00	113500.00	107.00	-100.00	14.45
66	2021.42	-2971.40	3580.43	5832.04	24220.00	113500.00	107.00	-100.00	14.45
67	2037.04	-2994.36	3649.42	5906.47	24529.00	113500.00	107.00	-100.00	14.45
68	2048.27	-3010.86	3724.06	5983.79	24850.00	113500.00	107.00	-100.00	14.45
69	2054.83	-3020.51	3804.33	6064.96	25187.00	113500.00	107.00	12.04	14.45
70	2057.06	-3023.79	3890.64	6151.41	25546.00	113500.00	107.00	12.04	14.45
71	2057.31	-3024.16	3940.72	6201.49	25754.00	113500.00	107.00	12.04	14.45
72	2057.52	-3024.46	3990.56	6251.33	25961.00	113500.00	107.00	-100.00	14.45
73	2057.69	-3024.72	4040.64	6301.41	26169.00	113500.00	107.00	-100.00	14.45
74	2057.84	-3024.93	4090.72	6351.50	26377.00	113500.00	107.00	-100.00	14.45
75	2057.96	-3025.10	4140.56	6401.34	26584.00	113500.00	107.00	12.04	14.45
76	2058.06	-3025.25	4190.64	6451.42	26792.00	113500.00	107.00	12.04	14.45
77	2058.14	-3025.38	4240.72	6501.50	27000.00	113500.00	107.00	12.04	14.45
78	2058.21	-3025.48	4290.56	6551.34	27207.00	113500.00	107.00	12.04	14.45
79	2058.27	-3025.57	4340.64	6601.42	27415.00	113500.00	107.00	12.04	14.45
80	2058.32	-3025.64	4390.72	6651.50	27623.00	113500.00	107.00	12.04	14.45
81	2058.36	-3025.70	4440.56	6701.34	27830.00	113500.00	107.00	12.04	14.45
82	2058.39	-3025.75	4490.64	6751.42	28038.00	113500.00	107.00	12.04	14.45
83	2058.42	-3025.79	4540.72	6801.50	28246.00	113500.00	107.00	12.04	14.45
84	2058.45	-3025.83	4590.56	6851.34	28453.00	113500.00	107.00	12.04	14.45
85	2058.47	-3025.85	4640.64	6901.42	28661.00	113500.00	107.00	12.04	14.45
86	2058.48	-3025.88	4690.72	6951.50	28869.00	113500.00	107.00	12.04	14.45
87	2058.50	-3025.90	4740.56	7001.34	29076.00	113500.00	107.00	12.04	14.45
88	2058.51	-3025.92	4790.64	7051.42	29284.00	113500.00	107.00	12.04	14.45
89	2058.52	-3025.93	4840.72	7101.50	29492.00	113500.00	107.00	12.04	14.45
90	2058.53	-3025.94	4890.56	7151.34	29699.00	113500.00	107.00	12.04	14.45
91	2058.53	-3025.95	4940.64	7201.42	29907.00	113500.00	107.00	12.04	14.45
92	2058.54	-3025.96	4990.72	7251.50	30115.00	113500.00	107.00	12.04	14.45
93	2058.54	-3025.97	5040.56	7301.34	30322.00	113500.00	107.00	12.04	14.45
94	2058.55	-3025.97	5090.64	7351.42	30530.00	113500.00	107.00	12.04	14.45
95	2058.55	-3025.98	5140.73	7401.50	30738.00	113500.00	107.00	12.04	14.45
96	2058.55	-3025.98	5190.56	7451.34	30945.00	113500.00	107.00	12.04	14.45
97	2058.56	-3025.99	5240.65	7501.42	31153.00	113500.00	107.00	12.04	14.45
98	2058.56	-3025.99	5290.73	7551.51	31361.00	113500.00	107.00	12.04	14.45
99	2058.56	-3025.99	5340.57	7601.35	31568.00	113500.00	107.00	12.04	14.45
100	2058.56	-3025.99	5390.65	7651.43	31776.00	113500.00	107.00	12.04	14.45
101	2058.56	-3026.00	5440.73	7701.51	31984.00	113500.00	107.00	12.04	14.45
102	2058.56	-3026.00	5490.57	7751.35	32191.00				

Simulation Results of S Shape Well with Trained DQN Agent

Index	N[m]	E[m]	V[m]	MD[m]	T[min]	WOB[N]	RPM	Reward	ROP[m/hr]
0	0.00	0.00	0.00	0.00	0.00	167500.00	94.00	15.72	18.86
1	0.00	0.00	50.30	50.30	160.00	167500.00	94.00	15.72	18.86
2	0.00	0.00	100.29	100.29	319.00	167500.00	94.00	15.72	18.86
3	0.00	0.00	150.28	150.28	478.00	167500.00	94.00	15.72	18.86
4	0.00	0.00	200.27	200.27	637.00	167500.00	94.00	15.72	18.86
5	0.00	0.00	250.26	250.26	796.00	167500.00	94.00	15.72	18.86
6	0.00	0.00	300.25	300.25	955.00	174000.00	178.00	30.95	37.14
7	0.00	0.00	350.39	350.39	1036.00	174000.00	178.00	30.95	37.14
8	0.00	0.00	400.53	400.53	1117.00	174000.00	178.00	30.95	37.14
9	0.00	0.00	450.05	450.05	1197.00	174000.00	178.00	30.95	37.14
10	0.00	0.00	500.19	500.19	1278.00	174000.00	178.00	30.95	37.14
11	0.00	0.00	550.33	550.33	1359.00	170500.00	180.00	30.65	36.78
12	0.00	0.00	600.60	600.60	1441.00	170500.00	180.00	30.65	36.78
13	0.00	0.00	650.26	650.26	1522.00	170500.00	180.00	30.65	36.78
14	0.00	0.00	700.53	700.53	1604.00	170500.00	180.00	30.65	36.78
15	0.00	0.00	750.19	750.19	1685.00	170500.00	180.00	30.65	36.78
16	0.00	0.00	800.46	800.46	1767.00	170500.00	180.00	30.65	36.78
17	0.00	0.00	850.12	850.12	1848.00	170500.00	180.00	30.65	36.78
18	0.00	0.00	900.39	900.39	1930.00	170500.00	180.00	30.65	36.78
19	0.00	0.00	950.05	950.05	2011.00	170500.00	180.00	30.65	36.78
20	0.00	0.00	1000.32	1000.32	2093.00	170500.00	180.00	30.66	36.79
21	2.84	-4.17	1152.28	1152.38	2341.00	167500.00	94.00	15.72	18.87
22	10.73	-15.77	1295.58	1296.39	2799.00	167500.00	94.00	15.72	18.87
23	23.06	-33.89	1429.92	1432.54	3232.00	167500.00	94.00	15.72	18.87
24	39.65	-58.29	1556.35	1562.40	3645.00	167500.00	94.00	15.72	18.87
25	60.25	-88.56	1674.67	1686.29	4039.00	167500.00	94.00	15.72	18.87
26	84.65	-124.43	1785.29	1805.15	4417.00	167500.00	94.00	15.72	18.87
27	112.70	-165.66	1888.62	1919.92	4782.00	167500.00	94.00	15.72	18.87
28	144.24	-212.03	1985.10	2031.55	5137.00	167500.00	94.00	15.72	18.87
29	179.17	-263.37	2075.16	2140.97	5485.00	167500.00	94.00	15.72	18.87
30	217.07	-319.08	2158.52	2248.20	5826.00	167500.00	94.00	15.72	18.87
31	257.98	-379.22	2235.98	2354.48	6164.00	167500.00	94.00	15.72	18.87
32	301.61	-443.36	2307.66	2460.13	6500.00	167500.00	94.00	15.72	18.87
33	347.72	-511.13	2373.79	2565.47	6835.00	167500.00	94.00	15.72	18.87
34	396.35	-582.61	2435.02	2671.44	7172.00	167500.00	94.00	15.72	18.87
35	447.03	-657.12	2491.34	2777.71	7510.00	167500.00	94.00	15.72	18.87
36	499.62	-734.42	2543.16	2884.62	7850.00	167500.00	94.00	15.72	18.87
37	554.01	-814.37	2590.89	2992.47	8193.00	167500.00	94.00	15.72	18.87
38	609.98	-896.64	2634.85	3101.26	8539.00	167500.00	94.00	15.72	18.87
39	667.17	-980.71	2675.25	3210.68	8887.00	167500.00	94.00	15.72	18.87

40	725.76	-1066.83	2712.67	3321.35	9239.00	167500.00	94.00	15.72	18.86
41	785.09	-1154.05	2747.17	3432.34	9592.00	167500.00	94.00	15.72	18.86
42	845.23	-1242.45	2779.19	3543.96	9947.00	167500.00	94.00	15.72	18.86
43	906.08	-1331.89	2809.15	3656.20	10304.00	167500.00	94.00	15.72	18.86
44	967.20	-1421.75	2837.23	3768.45	10661.00	167500.00	94.00	15.72	18.86
45	1028.37	-1511.66	2863.73	3880.38	11017.00	167500.00	94.00	15.72	18.86
46	1089.69	-1601.80	2889.10	3992.31	11373.00	167500.00	94.00	15.72	18.86
47	1150.76	-1691.57	2913.58	4103.61	11727.00	167500.00	94.00	15.72	18.86
48	1211.53	-1780.89	2937.57	4214.27	12079.00	167500.00	94.00	15.72	18.86
49	1271.62	-1869.22	2961.18	4323.69	12427.00	167500.00	94.00	15.72	18.86
50	1330.86	-1956.30	2984.39	4431.53	12770.00	167500.00	94.00	15.72	18.86
51	1389.23	-2042.11	3007.24	4537.79	13108.00	167500.00	94.00	15.72	18.86
52	1446.53	-2126.34	3029.99	4642.17	13440.00	167500.00	94.00	15.72	18.86
53	1502.44	-2208.51	3053.71	4744.36	13765.00	167500.00	94.00	15.72	18.86
54	1556.87	-2288.53	3078.82	4844.34	14083.00	167500.00	94.00	15.72	18.87
55	1609.41	-2365.77	3105.51	4941.50	14392.00	167500.00	94.00	15.72	18.87
56	1659.97	-2440.08	3134.11	5035.82	14692.00	167500.00	94.00	15.72	18.87
57	1708.26	-2511.06	3164.83	5127.01	14982.00	167500.00	94.00	15.72	18.87
58	1754.30	-2578.74	3198.07	5215.36	15263.00	167500.00	94.00	15.72	18.87
59	1797.76	-2642.63	3233.96	5300.58	15534.00	167500.00	94.00	15.72	18.87
60	1838.45	-2702.44	3272.69	5382.65	15795.00	167500.00	94.00	15.72	18.87
61	1876.28	-2758.05	3314.55	5461.89	16047.00	167500.00	94.00	15.72	18.87
62	1911.13	-2809.28	3359.77	5538.62	16291.00	167500.00	94.00	15.72	18.87
63	1942.94	-2856.04	3408.77	5613.47	16529.00	167500.00	94.00	15.72	18.87
64	1971.71	-2898.32	3461.21	5686.74	16762.00	167500.00	94.00	15.72	18.87
65	1997.61	-2936.40	3516.96	5759.07	16992.00	167500.00	94.00	-100.00	18.87
66	2021.05	-2970.85	3576.82	5832.02	17224.00	167500.00	94.00	-100.00	18.87
67	2042.04	-3001.70	3641.31	5906.55	17461.00	167500.00	94.00	-100.00	18.87
68	2060.44	-3028.75	3711.04	5983.60	17706.00	167500.00	94.00	-100.00	18.87
69	2076.09	-3051.76	3787.55	6065.05	17965.00	167500.00	94.00	-100.00	18.87
70	2088.97	-3070.70	3870.92	6151.52	18240.00	167500.00	94.00	-100.00	18.87
71	2094.93	-3079.45	3919.77	6201.51	18399.00	167500.00	94.00	-100.00	18.87
72	2099.78	-3086.59	3969.02	6251.51	18558.00	167500.00	94.00	-100.00	18.87
73	2103.52	-3092.09	4018.56	6301.51	18717.00	167500.00	94.00	-100.00	18.87
74	2106.15	-3095.94	4068.34	6351.50	18876.00	167500.00	94.00	-100.00	18.87
75	2107.65	-3098.15	4118.26	6401.50	19035.00	167500.00	94.00	-100.00	18.87
76	2108.13	-3098.86	4168.24	6451.49	19194.00	167500.00	94.00	-100.00	18.86
77	2108.42	-3099.29	4218.23	6501.48	19353.00	167500.00	94.00	-100.00	18.86
78	2108.69	-3099.68	4268.22	6551.47	19512.00	167500.00	94.00	-100.00	18.86
79	2108.93	-3100.04	4318.21	6601.46	19671.00	167500.00	94.00	-100.00	18.86
80	2109.16	-3100.37	4368.19	6651.45	19830.00	167500.00	94.00	-100.00	18.86
81	2109.36	-3100.67	4418.18	6701.44	19989.00	167500.00	94.00	-100.00	18.86
82	2109.55	-3100.95	4468.17	6751.43	20148.00	167500.00	94.00	-100.00	18.86

83	2109.73	-3101.21	4518.16	6801.42	20307.00	167500.00	94.00	-100.00	18.86
84	2109.89	-3101.45	4568.15	6851.41	20466.00	167500.00	94.00	-100.00	18.86
85	2110.04	-3101.66	4618.14	6901.40	20625.00	167500.00	94.00	-100.00	18.86
86	2110.17	-3101.86	4668.13	6951.39	20784.00	167500.00	94.00	-100.00	18.86
87	2110.30	-3102.04	4718.12	7001.38	20943.00	167500.00	94.00	-100.00	18.86
88	2110.41	-3102.21	4768.11	7051.37	21102.00	167500.00	94.00	-100.00	18.86
89	2110.52	-3102.37	4818.09	7101.36	21261.00	167500.00	94.00	-100.00	18.86
90	2110.61	-3102.51	4868.08	7151.35	21420.00	167500.00	94.00	-100.00	18.86
91	2110.70	-3102.64	4918.07	7201.34	21579.00	167500.00	94.00	-100.00	18.86
92	2110.78	-3102.76	4968.06	7251.33	21738.00	167500.00	94.00	-100.00	18.86
93	2110.86	-3102.87	5018.05	7301.31	21897.00	167500.00	94.00	-100.00	18.86
94	2110.93	-3102.97	5068.04	7351.30	22056.00	167500.00	94.00	-100.00	18.86
95	2110.99	-3103.06	5118.03	7401.29	22215.00	167500.00	94.00	-100.00	18.86
96	2111.05	-3103.15	5168.34	7451.60	22375.00	167500.00	94.00	-100.00	18.86
97	2111.10	-3103.23	5218.33	7501.59	22534.00	167500.00	94.00	-100.00	18.86
98	2111.15	-3103.30	5268.32	7551.58	22693.00	167500.00	94.00	-100.00	18.86
99	2111.20	-3103.36	5318.31	7601.57	22852.00	167500.00	94.00	-100.00	18.86
100	2111.24	-3103.43	5368.30	7651.56	23011.00	167500.00	94.00	-100.00	18.86
101	2111.28	-3103.48	5418.28	7701.55	23170.00	167500.00	94.00	-100.00	18.86
102	2111.31	-3103.53	5468.27	7751.54	23329.00				

Simulation Results of Complex Shape Well with Trained PPO Agent

Index	N[m]	E[m]	V[m]	MD[m]	T[min]	WOB[N]	RPM	Reward	ROP[m/hr]
0	0.00	0.00	0.00	0.00	0.00	113500.00	107.00	12.04	14.45
1	0.00	0.00	50.08	50.08	208.00	113500.00	107.00	12.04	14.45
2	0.00	0.00	100.16	100.16	416.00	113500.00	107.00	12.04	14.45
3	0.00	0.00	150.00	150.00	623.00	113500.00	107.00	12.04	14.45
4	0.00	0.00	200.08	200.08	831.00	113500.00	107.00	12.04	14.45
5	0.00	0.00	250.16	250.16	1039.00	113500.00	107.00	12.04	14.45
6	0.00	0.00	300.00	300.00	1246.00	113500.00	107.00	12.04	14.45
7	0.00	0.00	350.08	350.08	1454.00	113500.00	107.00	12.04	14.45
8	0.00	0.00	400.16	400.16	1662.00	113500.00	107.00	12.04	14.45
9	0.00	0.00	450.00	450.00	1869.00	113500.00	107.00	12.04	14.45
10	0.00	0.00	500.08	500.08	2077.00	113500.00	107.00	12.04	14.45
11	0.00	0.00	550.17	550.17	2285.00	113500.00	107.00	12.04	14.45
12	0.00	0.00	600.01	600.01	2492.00	113500.00	107.00	12.04	14.45
13	0.00	0.00	650.09	650.09	2700.00	113500.00	107.00	12.04	14.45
14	0.00	0.00	700.17	700.17	2908.00	113500.00	107.00	12.04	14.45
15	0.00	0.00	750.01	750.01	3115.00	113500.00	107.00	12.04	14.45
16	0.00	0.00	800.09	800.09	3323.00	113500.00	107.00	12.04	14.45
17	0.76	0.23	827.05	827.07	3435.00	113500.00	107.00	12.01	14.45
18	2.77	0.85	853.70	853.80	3546.00	113500.00	107.00	11.93	14.45

19	6.15	1.89	879.96	880.30	3656.00	113500.00	107.00	11.80	14.45
20	10.87	3.35	905.99	906.80	3766.00	113500.00	107.00	11.70	14.45
21	16.85	5.23	931.73	933.30	3876.00	113500.00	107.00	11.61	14.45
22	24.04	7.52	957.12	959.80	3986.00	113500.00	107.00	11.51	14.45
23	32.46	10.26	982.35	986.53	4097.00	113500.00	107.00	11.41	14.45
24	41.93	13.38	1007.15	1013.27	4208.00	113500.00	107.00	11.30	14.45
25	52.47	16.93	1031.73	1040.25	4320.00	113500.00	107.00	11.19	14.45
26	64.03	20.89	1056.04	1067.46	4433.00	113500.00	107.00	11.08	14.45
27	76.54	25.26	1080.09	1094.92	4547.00	113500.00	107.00	10.95	14.45
28	89.93	30.03	1103.86	1122.62	4662.00	113500.00	107.00	10.88	14.45
29	104.13	35.20	1127.35	1150.55	4778.00	113500.00	107.00	10.75	14.45
30	119.11	40.76	1150.56	1178.73	4895.00	113500.00	107.00	10.67	14.45
31	134.65	46.65	1173.31	1206.91	5012.00	113500.00	107.00	10.57	14.45
32	150.99	52.99	1195.98	1235.57	5131.00	113500.00	107.00	10.50	14.45
33	167.79	59.65	1218.22	1264.23	5250.00	113500.00	107.00	10.45	14.45
34	185.28	66.76	1240.41	1293.36	5371.00	113500.00	107.00	10.48	14.45
35	203.00	74.14	1262.01	1322.26	5491.00	113500.00	107.00	10.43	14.45
36	221.34	81.96	1283.59	1351.64	5613.00	113500.00	107.00	10.60	14.45
37	239.94	90.12	1304.81	1381.02	5735.00	113500.00	107.00	10.87	14.45
38	258.78	98.60	1325.69	1410.40	5857.00	113500.00	107.00	11.02	14.45
39	277.98	107.49	1346.42	1440.02	5980.00	113500.00	107.00	11.13	14.45
40	297.33	116.72	1366.86	1469.63	6103.00	113500.00	107.00	11.63	14.45
41	316.64	126.21	1386.85	1499.01	6225.00	113500.00	107.00	11.95	14.45
42	336.20	136.13	1406.76	1528.63	6348.00	113500.00	107.00	11.35	14.45
43	355.64	146.33	1426.28	1558.01	6470.00	113500.00	107.00	10.83	14.45
44	375.09	156.89	1445.59	1587.39	6592.00	113500.00	107.00	10.37	14.45
45	394.52	167.83	1464.71	1616.76	6714.00	113500.00	107.00	9.77	14.45
46	413.74	179.07	1483.51	1645.90	6835.00	113500.00	107.00	9.28	14.45
47	432.54	190.50	1501.85	1674.56	6954.00	113500.00	107.00	8.50	14.45
48	451.22	202.34	1520.08	1703.21	7073.00	113500.00	107.00	8.39	14.45
49	469.57	214.50	1538.04	1731.63	7191.00	113500.00	107.00	7.86	14.45
50	487.55	226.98	1555.77	1759.80	7308.00	113500.00	107.00	7.57	14.45
51	505.13	239.79	1573.28	1787.74	7424.00	113500.00	107.00	7.63	14.45
52	522.13	252.84	1590.44	1815.19	7538.00	113500.00	107.00	7.56	14.45
53	538.50	266.12	1607.26	1842.16	7650.00	113500.00	107.00	7.50	14.45
54	554.35	279.75	1623.91	1868.89	7761.00	113500.00	107.00	7.91	14.45
55	569.50	293.62	1640.24	1895.14	7870.00	113500.00	107.00	8.46	14.45
56	583.92	307.73	1656.25	1920.91	7977.00	113500.00	107.00	9.05	14.45
57	597.70	322.23	1672.10	1946.44	8083.00	113500.00	107.00	9.68	14.45
58	610.55	336.83	1687.49	1971.25	8186.00	113500.00	107.00	10.33	14.45
59	622.67	351.81	1702.72	1995.81	8288.00	113500.00	107.00	10.93	14.45
60	633.97	366.96	1717.64	2019.90	8388.00	113500.00	107.00	-38.02	14.45
61	644.34	382.07	1732.10	2043.26	8485.00	113500.00	107.00	11.67	14.45

62	654.13	397.58	1746.56	2066.62	8582.00	113500.00	107.00	11.83	14.45
63	663.04	412.97	1760.57	2089.26	8676.00	113500.00	107.00	11.96	14.45
64	671.29	428.51	1774.41	2111.66	8769.00	113500.00	107.00	10.73	14.45
65	678.91	444.21	1788.05	2133.81	8861.00	113500.00	107.00	6.72	14.45
66	685.89	459.92	1801.25	2155.49	8951.00	113500.00	107.00	11.99	14.45
67	699.90	497.18	1831.63	2205.59	9159.00	113500.00	107.00	-100.00	14.45
68	710.75	535.32	1861.80	2255.44	9366.00	113500.00	107.00	-100.00	14.45
69	719.08	574.33	1892.08	2305.53	9574.00	113500.00	107.00	-100.00	14.45
70	727.14	613.43	1922.32	2355.61	9782.00	113500.00	107.00	-100.00	14.45
71	735.13	652.36	1952.39	2405.45	9989.00	113500.00	107.00	-100.00	14.45
72	743.14	691.50	1982.59	2455.53	10197.00	113500.00	107.00	-100.00	14.45
73	751.12	730.67	2012.76	2505.61	10405.00	113500.00	107.00	-100.00	14.45
74	759.04	769.66	2042.77	2555.45	10612.00	113500.00	107.00	-100.00	14.45
75	766.98	808.86	2072.92	2605.53	10820.00	113500.00	107.00	-100.00	14.45
76	774.90	848.07	2103.04	2655.61	11028.00	113500.00	107.00	-100.00	14.45
77	782.76	887.11	2133.01	2705.45	11235.00	113500.00	107.00	-100.00	14.45
78	790.65	926.35	2163.12	2755.53	11443.00	113500.00	107.00	-100.00	14.45
79	798.52	965.60	2193.21	2805.61	11651.00	113500.00	107.00	-100.00	14.45
80	806.34	1004.66	2223.16	2855.45	11858.00	113500.00	107.00	-100.00	14.45
81	814.19	1043.93	2253.24	2905.53	12066.00	113500.00	107.00	-100.00	14.45
82	822.03	1083.20	2283.31	2955.61	12274.00	113500.00	107.00	-100.00	14.45
83	829.81	1122.29	2313.23	3005.45	12481.00	113500.00	107.00	-100.00	14.45
84	837.63	1161.58	2343.29	3055.53	12689.00	113500.00	107.00	-100.00	14.45
85	845.43	1200.87	2373.35	3105.61	12897.00	113500.00	107.00	-100.00	14.45
86	853.19	1239.97	2403.26	3155.45	13104.00	113500.00	107.00	-100.00	14.45
87	860.98	1279.27	2433.31	3205.53	13312.00	113500.00	107.00	-100.00	14.45
88	868.77	1318.57	2463.35	3255.61	13520.00	113500.00	107.00	-100.00	14.45
89	876.51	1357.69	2493.25	3305.45	13727.00	113500.00	107.00	-100.00	14.45
90	884.32	1397.19	2523.44	3355.78	13936.00	113500.00	107.00	-100.00	14.45
91	886.64	1409.57	2533.13	3371.67	14002.00	113500.00	107.00	-100.00	14.45
92	888.71	1421.96	2543.26	3387.81	14069.00	113500.00	107.00	-100.00	14.45
93	890.50	1434.13	2553.71	3403.95	14136.00	113500.00	107.00	-100.00	14.45
94	892.05	1446.43	2564.76	3420.57	14205.00	113500.00	107.00	-100.00	14.45
95	893.31	1458.55	2576.06	3437.19	14274.00	113500.00	107.00	-100.00	14.45
96	894.30	1470.84	2587.90	3454.29	14345.00	113500.00	107.00	-100.00	14.45
97	894.98	1482.99	2599.92	3471.39	14416.00	113500.00	107.00	-100.00	14.45
98	895.36	1495.34	2612.42	3488.97	14489.00	113500.00	107.00	-100.00	14.45
99	895.40	1507.58	2625.03	3506.56	14562.00	113500.00	107.00	-100.00	14.45
100	895.09	1520.05	2638.09	3524.62	14637.00	113500.00	107.00	-100.00	14.45
101	894.43	1532.44	2651.21	3542.68	14712.00	113500.00	107.00	-100.00	14.45
102	893.40	1544.91	2664.56	3560.99	14788.00	113500.00	107.00	-100.00	14.45
103	891.96	1557.50	2678.10	3579.53	14865.00	113500.00	107.00	-100.00	14.45
104	890.13	1570.02	2691.65	3598.08	14942.00	113500.00	107.00	-100.00	14.45

105	887.89	1582.63	2705.38	3616.86	15020.00	113500.00	107.00	-100.00	14.45
106	885.21	1595.31	2719.30	3635.89	15099.00	113500.00	107.00	-100.00	14.45
107	882.09	1608.06	2733.40	3655.16	15179.00	113500.00	107.00	-100.00	14.45
108	878.61	1620.55	2747.32	3674.18	15258.00	113500.00	107.00	-100.00	14.45
109	874.62	1633.23	2761.59	3693.69	15339.00	113500.00	107.00	-100.00	14.45
110	870.28	1645.67	2775.64	3712.96	15419.00	113500.00	107.00	-100.00	14.45
111	865.46	1658.22	2789.77	3732.47	15500.00	113500.00	107.00	-100.00	14.45
112	860.21	1670.72	2803.78	3751.98	15581.00	113500.00	107.00	-100.00	14.45
113	854.53	1683.18	2817.67	3771.49	15662.00	113500.00	107.00	-100.00	14.45
114	848.44	1695.61	2831.42	3790.99	15743.00	113500.00	107.00	-100.00	14.45
115	842.00	1708.22	2845.17	3810.74	15825.00	113500.00	107.00	-100.00	14.45
116	835.43	1720.77	2858.58	3830.25	15906.00	113500.00	107.00	-100.00	14.45
117	828.66	1733.41	2871.80	3849.75	15987.00	113500.00	107.00	-100.00	14.45
118	821.78	1746.01	2884.65	3869.02	16067.00	113500.00	107.00	-100.00	14.45
119	814.64	1758.90	2897.43	3888.52	16148.00	113500.00	107.00	-100.00	14.45
120	807.40	1771.78	2909.80	3907.79	16228.00	113500.00	107.00	-100.00	14.45
121	800.00	1784.81	2921.90	3927.06	16308.00	113500.00	107.00	-100.00	14.45
122	792.52	1797.85	2933.56	3946.08	16387.00	113500.00	107.00	-100.00	14.45
123	784.99	1810.91	2944.77	3964.87	16465.00	113500.00	107.00	-100.00	14.45
124	777.22	1824.34	2955.78	3983.89	16544.00	113500.00	107.00	-100.00	14.45
125	769.50	1837.64	2966.15	4002.44	16621.00	113500.00	107.00	-100.00	14.45
126	761.66	1851.15	2976.13	4020.98	16698.00	113500.00	107.00	-100.00	14.45
127	753.78	1864.71	2985.58	4039.29	16774.00	113500.00	107.00	-100.00	14.45
128	745.77	1878.48	2994.59	4057.60	16850.00	113500.00	107.00	-100.00	14.45
129	737.74	1892.30	3003.02	4075.66	16925.00	113500.00	107.00	-100.00	14.45
130	729.57	1906.33	3010.94	4093.73	17000.00	113500.00	107.00	-100.00	14.45
131	721.50	1920.20	3018.13	4111.31	17073.00	113500.00	107.00	-100.00	14.45
132	713.20	1934.47	3024.84	4129.14	17147.00	113500.00	107.00	-100.00	14.45
133	705.05	1948.57	3030.80	4146.48	17219.00	113500.00	107.00	-100.00	14.45
134	696.76	1963.10	3036.23	4164.07	17292.00	113500.00	107.00	-100.00	14.45
135	688.70	1977.44	3040.90	4181.17	17363.00	113500.00	107.00	-100.00	14.45
136	680.56	1992.19	3045.01	4198.52	17435.00	113500.00	107.00	-100.00	14.45
137	672.58	2006.92	3048.46	4215.62	17506.00	113500.00	107.00	-100.00	14.45
138	664.58	2022.03	3051.35	4232.97	17578.00	113500.00	107.00	-100.00	14.45
139	656.78	2037.09	3053.59	4250.07	17649.00	113500.00	107.00	-100.00	14.45
140	649.00	2052.50	3055.26	4267.41	17721.00	113500.00	107.00	-100.00	14.45
141	626.69	2097.05	3056.72	4317.27	17928.00	113500.00	107.00	-100.00	14.45
142	604.27	2141.83	3057.24	4367.35	18136.00	113500.00	107.00	-100.00	14.45
143	581.85	2186.61	3057.76	4417.43	18344.00	113500.00	107.00	-100.00	14.45
144	559.54	2231.17	3058.28	4467.27	18551.00	113500.00	107.00	-100.00	14.45
145	537.12	2275.95	3058.81	4517.35	18759.00	113500.00	107.00	-100.00	14.45
146	514.71	2320.73	3059.33	4567.43	18967.00	113500.00	107.00	-100.00	14.45
147	492.40	2365.29	3059.85	4617.27	19174.00	113500.00	107.00	-100.00	14.45

148	469.98	2410.07	3060.37	4667.35	19382.00	113500.00	107.00	-100.00	14.45
149	447.56	2454.85	3060.89	4717.44	19590.00	113500.00	107.00	-100.00	14.45
150	425.25	2499.42	3061.41	4767.28	19797.00	113500.00	107.00	-100.00	14.45
151	402.83	2544.20	3061.93	4817.36	20005.00	113500.00	107.00	-100.00	14.45
152	380.41	2588.98	3062.45	4867.44	20213.00	113500.00	107.00	-100.00	14.45
153	358.10	2633.54	3062.97	4917.28	20420.00	113500.00	107.00	-100.00	14.45
154	335.69	2678.32	3063.49	4967.36	20628.00	113500.00	107.00	-100.00	14.45
155	313.27	2723.10	3064.01	5017.44	20836.00	113500.00	107.00	-100.00	14.45
156	290.96	2767.67	3064.53	5067.28	21043.00	113500.00	107.00	-100.00	14.45
157	268.54	2812.45	3065.05	5117.36	21251.00	113500.00	107.00	-100.00	14.45
158	246.13	2857.23	3065.57	5167.44	21459.00	113500.00	107.00	-100.00	14.45
159	223.82	2901.79	3066.09	5217.28	21666.00	113500.00	107.00	-100.00	14.45
160	201.40	2946.57	3066.61	5267.36	21874.00	113500.00	107.00	-100.00	14.45
161	178.98	2991.36	3067.13	5317.44	22082.00	113500.00	107.00	-100.00	14.45
162	156.67	3035.92	3067.64	5367.28	22289.00	113500.00	107.00	-100.00	14.45
163	134.26	3080.70	3068.16	5417.36	22497.00	113500.00	107.00	-100.00	14.45
164	111.95	3125.27	3068.68	5467.20	22704.00				

Simulation Results of Complex Shape Well with Trained DQN Agent

Index	N[m]	E[m]	V[m]	MD[m]	T[min]	WOB[N]	RPM	Reward	ROP[m/hr]
0	0.00	0.00	0.00	0.00	0.00	167500.00	94.00	15.72	18.86
1	0.00	0.00	50.30	50.30	160.00	167500.00	94.00	15.72	18.86
2	0.00	0.00	100.29	100.29	319.00	167500.00	94.00	15.72	18.86
3	0.00	0.00	150.28	150.28	478.00	167500.00	94.00	15.72	18.86
4	0.00	0.00	200.27	200.27	637.00	167500.00	94.00	15.72	18.86
5	0.00	0.00	250.26	250.26	796.00	167500.00	94.00	15.72	18.86
6	0.00	0.00	300.25	300.25	955.00	174000.00	178.00	30.95	37.14
7	0.00	0.00	350.39	350.39	1036.00	174000.00	178.00	30.95	37.14
8	0.00	0.00	400.53	400.53	1117.00	174000.00	178.00	30.95	37.14
9	0.00	0.00	450.05	450.05	1197.00	174000.00	178.00	30.95	37.14
10	0.00	0.00	500.19	500.19	1278.00	174000.00	178.00	30.95	37.14
11	0.00	0.00	550.33	550.33	1359.00	170500.00	180.00	30.65	36.78
12	0.00	0.00	600.60	600.60	1441.00	170500.00	180.00	30.65	36.78
13	0.00	0.00	650.26	650.26	1522.00	170500.00	180.00	30.65	36.78
14	0.00	0.00	700.53	700.53	1604.00	170500.00	180.00	30.65	36.78
15	0.00	0.00	750.19	750.19	1685.00	170500.00	180.00	30.65	36.78
16	0.00	0.00	800.46	800.46	1767.00	170500.00	180.00	30.66	36.79
17	0.18	0.06	827.44	827.44	1811.00	170500.00	180.00	30.64	36.79
18	0.72	0.22	853.80	853.81	1854.00	170500.00	180.00	30.61	36.79
19	1.61	0.49	880.15	880.17	1897.00	174000.00	178.00	-100.00	37.15
20	2.84	0.87	906.74	906.80	1940.00	167500.00	94.00	-100.00	18.87
21	4.56	1.41	933.09	933.21	2024.00	167500.00	94.00	-100.00	18.87

22	7.01	2.19	959.70	959.94	2109.00	167500.00	94.00	-100.00	18.87
23	10.15	3.21	986.22	986.67	2194.00	167500.00	94.00	-100.00	18.87
24	14.00	4.48	1012.64	1013.40	2279.00	167500.00	94.00	-100.00	18.87
25	18.59	6.02	1039.25	1040.45	2365.00	167500.00	94.00	-100.00	18.87
26	23.88	7.83	1065.71	1067.49	2451.00	167500.00	94.00	-100.00	18.87
27	30.00	9.97	1092.61	1095.16	2539.00	167500.00	94.00	-100.00	18.87
28	36.74	12.37	1119.01	1122.52	2626.00	167500.00	94.00	-100.00	18.87
29	44.34	15.12	1145.80	1150.51	2715.00	167500.00	94.00	-100.00	18.87
30	52.73	18.23	1172.65	1178.81	2805.00	167500.00	94.00	-100.00	18.87
31	61.82	21.67	1199.23	1207.11	2895.00	167500.00	94.00	-100.00	18.87
32	71.70	25.49	1225.82	1235.73	2986.00	167500.00	94.00	-100.00	18.87
33	82.25	29.67	1252.08	1264.35	3077.00	167500.00	94.00	-100.00	18.87
34	93.59	34.26	1278.30	1293.28	3169.00	167500.00	94.00	-100.00	18.87
35	105.71	39.29	1304.43	1322.52	3262.00	167500.00	94.00	-100.00	18.87
36	118.47	44.72	1330.18	1351.77	3355.00	167500.00	94.00	-100.00	18.87
37	131.84	50.56	1355.52	1381.02	3448.00	167500.00	94.00	-100.00	18.87
38	145.96	56.90	1380.70	1410.58	3542.00	167500.00	94.00	-100.00	18.87
39	160.65	63.67	1405.44	1440.14	3636.00	167500.00	94.00	-100.00	18.87
40	175.89	70.90	1429.72	1469.69	3730.00	167500.00	94.00	-100.00	18.87
41	191.63	78.60	1453.52	1499.25	3824.00	167500.00	94.00	-100.00	18.87
42	207.67	86.70	1476.59	1528.50	3917.00	167500.00	94.00	-100.00	18.87
43	224.32	95.38	1499.42	1558.06	4011.00	167500.00	94.00	-100.00	18.87
44	241.37	104.57	1521.74	1587.62	4105.00	167500.00	94.00	-100.00	18.87
45	258.60	114.18	1543.33	1616.86	4198.00	167500.00	94.00	-100.00	18.87
46	275.94	124.22	1564.19	1645.79	4290.00	167500.00	94.00	-100.00	18.87
47	293.54	134.80	1584.56	1674.72	4382.00	167500.00	94.00	-100.00	18.87
48	311.16	145.83	1604.23	1703.34	4473.00	167500.00	94.00	-100.00	18.87
49	328.74	157.28	1623.22	1731.64	4563.00	167500.00	94.00	-100.00	18.87
50	346.47	169.28	1641.72	1759.94	4653.00	167500.00	94.00	-100.00	18.87
51	363.92	181.56	1659.34	1787.62	4741.00	167500.00	94.00	-100.00	18.87
52	381.32	194.33	1676.65	1815.29	4829.00	167500.00	94.00	-100.00	18.87
53	398.05	207.23	1693.52	1842.33	4915.00	167500.00	94.00	-100.00	18.87
54	414.10	220.23	1709.98	1868.74	4999.00	167500.00	94.00	-100.00	18.87
55	429.84	233.61	1726.43	1895.16	5083.00	167500.00	94.00	-100.00	18.87
56	444.90	247.04	1742.48	1920.94	5165.00	167500.00	94.00	-100.00	18.87
57	459.48	260.64	1758.33	1946.41	5246.00	167500.00	94.00	-100.00	18.87
58	473.40	274.22	1773.77	1971.25	5325.00	167500.00	94.00	-100.00	18.87
59	486.84	287.94	1789.02	1995.78	5403.00	167500.00	94.00	-100.00	18.87
60	499.82	301.77	1804.06	2019.99	5480.00	167500.00	94.00	-100.00	18.87
61	512.02	315.32	1818.51	2043.26	5554.00	167500.00	94.00	-100.00	18.87
62	523.93	329.13	1832.96	2066.53	5628.00	167500.00	94.00	-100.00	18.87
63	535.24	342.81	1847.01	2089.17	5700.00	167500.00	94.00	-100.00	18.87
64	546.27	356.71	1861.06	2111.81	5772.00	167500.00	94.00	-100.00	18.87

65	556.79	370.48	1874.64	2133.82	5842.00	167500.00	94.00	-100.00	18.87
66	566.99	384.31	1887.88	2155.52	5911.00	167500.00	94.00	-100.00	18.87
67	589.54	416.98	1918.26	2205.51	6070.00	167500.00	94.00	-100.00	18.87
68	610.63	450.64	1948.60	2255.51	6229.00	167500.00	94.00	-100.00	18.87
69	630.21	485.23	1978.91	2305.51	6388.00	167500.00	94.00	-100.00	18.87
70	648.23	520.68	2009.19	2355.51	6547.00	167500.00	94.00	-100.00	18.87
71	664.67	556.92	2039.45	2405.50	6706.00	167500.00	94.00	-100.00	18.87
72	679.47	593.87	2069.69	2455.50	6865.00	167500.00	94.00	-100.00	18.87
73	692.62	631.46	2099.90	2505.50	7024.00	167500.00	94.00	-100.00	18.87
74	704.08	669.62	2130.09	2555.49	7183.00	167500.00	94.00	-100.00	18.87
75	713.83	708.26	2160.26	2605.49	7342.00	167500.00	94.00	-100.00	18.87
76	722.10	747.26	2190.42	2655.48	7501.00	167500.00	94.00	-100.00	18.86
77	730.17	786.31	2220.57	2705.47	7660.00	167500.00	94.00	-100.00	18.86
78	738.23	825.38	2250.70	2755.46	7819.00	167500.00	94.00	-100.00	18.86
79	746.27	864.45	2280.83	2805.45	7978.00	167500.00	94.00	-100.00	18.86
80	754.29	903.53	2310.95	2855.44	8137.00	167500.00	94.00	-100.00	18.86
81	762.30	942.62	2341.06	2905.43	8296.00	167500.00	94.00	-100.00	18.86
82	770.29	981.73	2371.16	2955.42	8455.00	167500.00	94.00	-100.00	18.86
83	778.33	1021.08	2401.44	3005.73	8615.00	82500.00	94.00	-100.00	9.19
84	786.25	1060.04	2431.38	3055.49	8940.00	82500.00	94.00	-100.00	9.19
85	794.18	1099.26	2461.47	3105.56	9267.00	82500.00	94.00	-100.00	9.19
86	802.06	1138.39	2491.44	3155.48	9593.00	82500.00	94.00	-100.00	9.19
87	809.94	1177.66	2521.49	3205.55	9920.00	82500.00	94.00	-100.00	9.19
88	817.77	1216.82	2551.44	3255.46	10246.00	82500.00	94.00	-100.00	9.19
89	825.61	1256.11	2581.47	3305.53	10573.00	82500.00	94.00	-100.00	9.19
90	833.45	1295.52	2611.60	3355.76	10901.00	82500.00	94.00	-100.00	9.19
91	835.63	1307.75	2621.32	3371.54	11004.00	82500.00	94.00	-100.00	9.19
92	837.38	1320.03	2631.56	3387.62	11109.00	82500.00	94.00	-100.00	9.19
93	838.63	1332.33	2642.31	3404.02	11216.00	82500.00	94.00	-100.00	9.19
94	839.37	1344.45	2653.31	3420.41	11323.00	82500.00	94.00	-100.00	9.19
95	839.65	1356.71	2664.86	3437.26	11433.00	82500.00	94.00	-100.00	9.19
96	839.45	1368.89	2676.71	3454.26	11544.00	82500.00	94.00	-100.00	9.19
97	838.80	1381.02	2688.83	3471.42	11656.00	82500.00	94.00	-100.00	9.19
98	837.71	1393.19	2701.29	3488.88	11770.00	82500.00	94.00	-100.00	9.19
99	836.18	1405.43	2714.07	3506.65	11886.00	82500.00	94.00	-100.00	9.19
100	834.24	1417.62	2727.06	3524.57	12003.00	82500.00	94.00	-100.00	9.19
101	831.90	1429.79	2740.20	3542.64	12121.00	82500.00	94.00	-100.00	9.19
102	829.19	1441.95	2753.50	3560.87	12240.00	82500.00	94.00	-100.00	9.19
103	826.08	1454.21	2767.04	3579.40	12361.00	82500.00	94.00	-100.00	9.19
104	822.61	1466.46	2780.71	3598.08	12483.00	82500.00	94.00	-100.00	9.19
105	818.80	1478.71	2794.50	3616.92	12606.00	82500.00	94.00	-100.00	9.19
106	814.67	1490.96	2808.40	3635.91	12730.00	82500.00	94.00	-100.00	9.19
107	810.24	1503.20	2822.43	3655.05	12855.00	82500.00	94.00	-100.00	9.19

108	805.55	1515.35	2836.45	3674.20	12980.00	82500.00	94.00	-100.00	9.19
109	800.54	1527.62	2850.69	3693.64	13107.00	82500.00	94.00	-100.00	9.19
110	795.32	1539.77	2864.74	3712.94	13233.00	82500.00	94.00	-100.00	9.19
111	789.82	1552.04	2878.79	3732.39	13360.00	82500.00	94.00	-100.00	9.19
112	784.04	1564.43	2892.83	3751.99	13488.00	82500.00	94.00	-100.00	9.19
113	778.07	1576.76	2906.63	3771.44	13615.00	82500.00	94.00	-100.00	9.19
114	771.84	1589.26	2920.39	3791.04	13743.00	82500.00	94.00	-100.00	9.19
115	765.40	1601.82	2933.98	3810.64	13871.00	82500.00	94.00	-100.00	9.19
116	758.80	1614.38	2947.29	3830.09	13998.00	82500.00	94.00	-100.00	9.19
117	751.95	1627.14	2960.49	3849.70	14126.00	82500.00	94.00	-100.00	9.19
118	745.02	1639.81	2973.28	3868.99	14252.00	82500.00	94.00	-100.00	9.19
119	737.84	1652.73	2985.93	3888.44	14379.00	82500.00	94.00	-100.00	9.19
120	730.54	1665.69	2998.22	3907.74	14505.00	82500.00	94.00	-100.00	9.19
121	723.14	1678.71	3010.14	3926.88	14630.00	82500.00	94.00	-100.00	9.19
122	715.57	1691.91	3021.76	3946.02	14755.00	82500.00	94.00	-100.00	9.19
123	707.97	1705.08	3032.88	3964.86	14878.00	82500.00	94.00	-100.00	9.19
124	700.23	1718.46	3043.64	3983.70	15001.00	82500.00	94.00	-100.00	9.19
125	692.40	1731.94	3053.95	4002.39	15123.00	82500.00	94.00	-100.00	9.19
126	684.51	1745.52	3063.78	4020.92	15244.00	82500.00	94.00	-100.00	9.19
127	676.54	1759.21	3073.10	4039.30	15364.00	82500.00	94.00	-100.00	9.19
128	668.50	1773.01	3081.89	4057.53	15483.00	82500.00	94.00	-100.00	9.19
129	660.40	1786.91	3090.12	4075.60	15601.00	82500.00	94.00	-100.00	9.19
130	652.16	1801.03	3097.83	4093.68	15719.00	82500.00	94.00	-100.00	9.19
131	643.94	1815.13	3104.85	4111.45	15835.00	82500.00	94.00	-100.00	9.19
132	635.68	1829.32	3111.23	4129.06	15950.00	82500.00	94.00	-100.00	9.19
133	627.42	1843.61	3116.95	4146.53	16064.00	82500.00	94.00	-100.00	9.19
134	619.14	1858.12	3122.02	4163.99	16178.00	82500.00	94.00	-100.00	9.19
135	610.94	1872.74	3126.36	4181.30	16291.00	82500.00	94.00	-100.00	9.19
136	602.84	1887.43	3129.94	4198.46	16403.00	82500.00	94.00	-100.00	9.19
137	594.80	1902.32	3132.76	4215.63	16515.00	82500.00	94.00	-100.00	9.19
138	586.84	1917.39	3134.78	4232.79	16627.00	82500.00	94.00	-100.00	9.19
139	578.92	1932.73	3135.98	4250.10	16740.00	82500.00	94.00	-100.00	9.19
140	571.20	1948.05	3136.33	4267.26	16852.00	82500.00	94.00	-100.00	9.19
141	548.78	1992.82	3136.48	4317.33	17179.00	82500.00	94.00	-100.00	9.19
142	526.45	2037.47	3136.61	4367.25	17505.00	82500.00	94.00	-100.00	9.19
143	504.09	2082.27	3136.72	4417.32	17832.00	82500.00	94.00	-100.00	9.19
144	481.83	2126.95	3136.80	4467.24	18158.00	82500.00	94.00	-100.00	9.19
145	459.54	2171.78	3136.87	4517.31	18485.00	82500.00	94.00	-100.00	9.19
146	437.34	2216.49	3136.93	4567.22	18811.00	82500.00	94.00	-100.00	9.19
147	415.10	2261.35	3136.97	4617.29	19138.00	82500.00	94.00	-100.00	9.19
148	392.96	2306.09	3137.00	4667.21	19464.00	82500.00	94.00	-100.00	9.19
149	370.77	2350.97	3137.03	4717.28	19791.00	82500.00	94.00	-100.00	9.19
150	348.60	2395.87	3137.05	4767.35	20118.00	82500.00	94.00	-100.00	9.19

151	326.52	2440.64	3137.07	4817.27	20444.00	82500.00	94.00	-100.00	9.19
152	304.40	2485.55	3137.08	4867.34	20771.00	82500.00	94.00	-100.00	9.19
153	282.35	2530.34	3137.09	4917.26	21097.00	82500.00	94.00	-100.00	9.19
154	260.26	2575.27	3137.09	4967.33	21424.00	82500.00	94.00	-100.00	9.19
155	238.25	2620.07	3137.10	5017.24	21750.00	82500.00	94.00	-100.00	9.19
156	216.18	2665.02	3137.10	5067.31	22077.00	82500.00	94.00	-100.00	9.19
157	194.19	2709.83	3137.11	5117.23	22403.00	82500.00	94.00	-100.00	9.19
158	172.15	2754.79	3137.11	5167.30	22730.00	82500.00	94.00	-100.00	9.19
159	150.18	2799.61	3137.11	5217.22	23056.00	82500.00	94.00	-100.00	9.19
160	128.15	2844.57	3137.11	5267.29	23383.00	82500.00	94.00	-100.00	9.19
161	106.13	2889.54	3137.11	5317.36	23710.00	82500.00	94.00	-100.00	9.19
162	84.19	2934.38	3137.12	5367.27	24036.00	82500.00	94.00	-100.00	9.19
163	62.18	2979.35	3137.12	5417.34	24363.00	82500.00	94.00	-100.00	9.19
164	40.25	3024.19	3137.12	5467.26	24689.00				